# ADDIS ABABA UNIVERSITY

## ADDIS ABABA INSTITUTE OF TECHNOLGY

## School of Mechanical and Industrial Engineering

### Graduate program Railway Mechanical Engineering

# Shape Optimization of AALRT Wheel Profile

A thesis submitted to the school of Graduate Studies of Addis Ababa University in Partial fulfillment of the degree of Master of Rolling Stock

By : **Tesfaye Atalay**

Advisor: **Tsegaye Feleke (M.sc)**

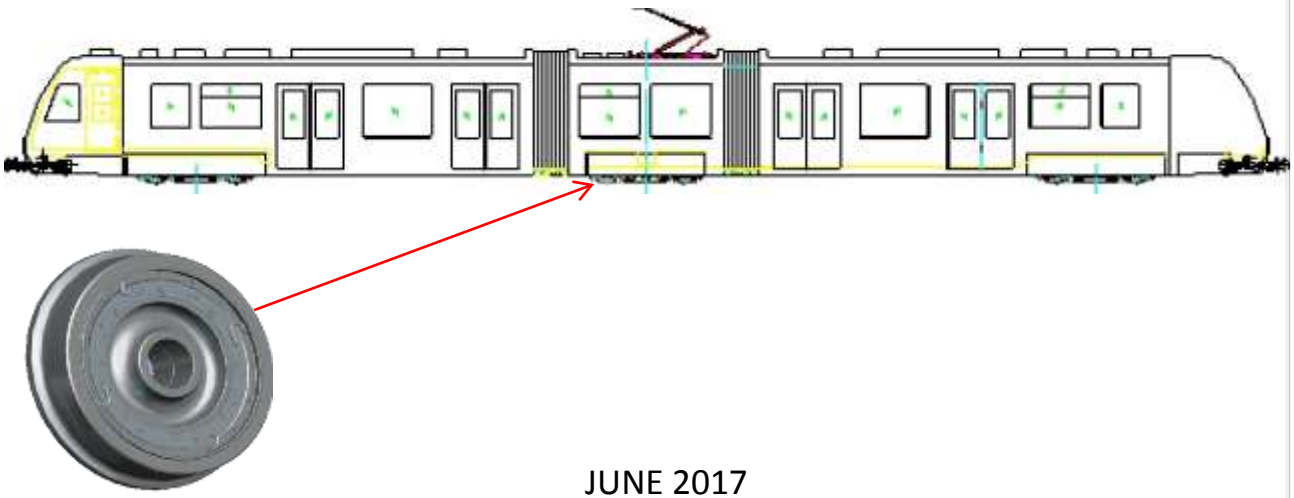

JUNE 2017

ADDIS ABABA UNIVERSITY

SCHOOL OF GRADUATE STUDIES

ADDIS ABABA INSTITUTE OF TECHNOLOGY

SCHOOL OF MECHANICAL AND INDUSTRIAL ENGINEERING

# Shape Optimization of AALRT Wheel Profile

By

**Tesfaye Atalay**

June 2017

**Approval by Board of Examining:**

| | | |
|---|---|---|
| Daniel Tilahun (Dr.) | _____ | _____ |
| Head, Railway center, | Signature | Date |
| Tsegaye Feleke (Msc.) | _____ | _____ |
| Name of Advisor | Signature | Date |
| Habtamu Tkubet (MSc.) | _____ | _____ |
| Name of Internal Examiner | Signature | Date |
| Tollosa Dreibsa (MSc) | _____ | _____ |
| Name of External Examiner | Signature | Date |

# DECLARATION

I declare that this piece of work is my own and all sources of materials used for this thesis work have been accordingly acknowledged. The thesis has been submitted in partial fulfillment of the requirements for the degree of Master of Science at Addis Ababa University and is reserved at the University Library to be made available to users. I truly declare that this thesis work is not submitted to any other institution anywhere for the award of any academic degree, diploma, or certificate. With accurate acknowledgment of the source, users are free to use this thesis without special permission.

Tesfaye Atalay Muluye _____ _____

By Signature Date

As thesis research advisor, I hereby approve that I have read and evaluated this thesis prepared, under my guidance, by Tesfaye Atalay, entitled "Shape Optimization of AALRT Wheel Profile". I recommend it be submitted as fulfilling the thesis requirement.

Tsegaye Feleke (MSc.) _____ _____

Name of advisor Signature Date

# ACKNOWLEDGMENTS

Conducting this thesis research from thesis proposal preparation, data collection, and to the final write up of the thesis could have not been fruitful if it was not for a generous assistance of individuals, institutions and numerous researchers who have made contributions to the literatures in this field.

This thesis author is extremely thankful to advisor and teacher *Mr.**Tsegaye Feleke*** for his willingness to advise the research, for his encouragement, guidance and valuable comments.

Thank you my family and all friends who helps me in many aspects.

# ABSTRACT

AALRT is the first modern light rail transit for Ethiopia; it was warmly welcomed by the public and after 1 ½ year still it doesn't answer publics need of transport. However during this short period the trains suffer with fast wheel wear problem and ERC loses money for maintenance costs when changing and re-profiling wheels.

This study aims to reduce wheel rail wear by optimizing wheel profile and check dynamic performance analysis of used and new optimized wheel profile.

The methodology of this paper starts using two basics 1. If the shape of the Rolling Radius Difference function is defined by the wheel and rail profiles, then the opposite is also valid 2) When the same type of rolling stock is running on the same track and no influence of other type railway vehicles then there is a possibility to design or optimize a new wheel profile, which matches an existing rail profile. Then the obtained profile checked regarding to dynamic performances (tested for stability, wear and safety requirements) using SIMPACK computer package.

After optimization and performance analysis the result of this paper shows optimized wheel profile has wear index of 1900N, 420N and 56N on R50curve, R150 curve and on straight track respectively. Which is optimized by 1100N, 120N and 22N wear index compared to currently used AALRT wheel profile.

As Conclusion compared to AALRT wheel profile the optimized profile has less wear rate, better dynamic performance, and the same safety requirements. Therefore wheel profile optimization has great impact on wheel Rail wear and AALRT have to work on it for better result.

**Key words**: wear index, RRD function, Profile optimization, Dynamic Performance, SIMPACK.

# TABLE OF CONTENTS

# LIST OF FIGURE

# LIST OF TABLE

# LIST OF ACRONYMS AND ABBREVIATIONS

AALRT: Addis Ababa Light Rail Train

CRECG: China Railway Group

ERC: Ethiopian Railway Corporation

LFLRV: Low floor Light Rail Vehicle

RCF: Rolling contact fatigue

RRD: Rolling Radius Difference

S1002: Europian Standard wheel profile

UIC: International Union of Railways

UIC60: 60kg Rail profile

MARS: Multipoint Approximation based on Response Surface fitting

APTA: American Public Transport Association

SIMPACK: Multi body dynamic analysis Software

R150m: Rail line Curve with 150m radius

L/V Ratio: Derailment coefficient

RET: Rotterdam metro network

Y/Q: Sum of Lateral load over Vertical load

Fx= longitudinal creep force

ξ= longitudinal creepage

Fy= lateral creep force

**η**= lateral creepage

$L_{k=}$ wavelength

***r*** = wheel radius

***S:*** contact points

*f:* frequency

*Y:* lateral displacement

Ψ: yaw angle

**γ:** wheelset conicity

$\gamma_e$ : equivalent conicity

V: Vehicle Speed

$y_0$: Amplitude of wheelset

r1 and r2: Rolling radius

y – Δr= Rolling radius difference functions

$\Delta r = r_1 - r_2$: Rolling Radius difference

$y$ : Lateral displacement$\Delta r$ ( $y$)

2b: distance between contact points

$y_w$. $O_{zw}$: Wheel set coordinate System

$\gamma_i$: angle between y-axis of wheelset

i and i+l: constraint point number

Ys: wheelset lateral displacement on straight

Yc: wheelset lateral displacement on curve

$Y_{fw}$: wheelset lateral displacement where flange width measured

$Y_{max}$: Maximum wheelset lateral displacement

$Y_{fh}$: wheelset lateral displacement where top of flange is measured

Δrfh: Rolling radius difference at top of flange

$\Delta r_{fw}$:Rolling radius difference at flange width measured

W:wear index

# CHAPTER ONE

# INTRODUCTION

## 1.1. Background

Rail transportation is one of the most important transportation modes to transport passengers and goods from one place to another. Compared to other transportation mode electrified railway transportation mode is cost effective, for the reason that the railway vehicle wheels have lower moving resistance caused by the rolling of the wheels on the tracks determine an incomparable lower consumption of energy per ton than other means of transport. In addition to this, self- guidance ability gives railway vehicles the possibility of moving in a demanded speed totally safe and independent of atmospheric conditions. As both wheels and rails are metallic, vehicles have the capability to carry loads extreme greater than other land transport systems. This skill, united with that of self-guidance, makes the possibility of forming heavy convoys of vehicles (trains), which offer the wheel-rail system the benefit of a huge transport capacity.[23]

Railway lines construction in Ethiopia was first started in October 1897.The first commercial service began in July 1901, from Djibouti to Dire Dawa. By 1917 the line reached Addis Ababa. It was passenger and freight transport to the Eastern Ethiopia. Now it is 100 years old diesel railway (781 km) and due to the age it is deteriorating and malfunctioning. The new standard gauge Railway line from Djibouti to Ethiopia starts to work in 2017. Also 34 km standard gauge Addis Ababa Light Rail Transit starts in 2016 [25].

Electrified railway system has most important environmental advantages which are more and more becoming significant as concern about climate change grows. Shifting freight traffic from the less efficient highway system to the more efficient rail system reduces both carbon emission and transport cost.

Rail vehicles are exposed to a wide variety of dynamical phenomena such as static and dynamic instabilities, lateral guidance problems on curved track and ride quality.

External inputs such as rail irregularities, sudden disturbances like switch, braking or accelerating and other failures, all affect the dynamic behavior of a railway vehicle. This

problem can be studied by dynamic response analysis of rail vehicle. Problems take place due to these unwanted inputs while railway vehicle begin to move indifferent directions as pitch, vertical, roll, yaw and lateral directions. These movements cause vibrations and damage in railway components with uncomfortable ride passenger. Lateral displacements happen due to defects and irregularities in the track which cause different undesirable motions like roll, yaw, and pitch. Lateral forces occur in the wheel-rail contact patch plane owing to interactions between the wheel and the rail which force wheelsets to move laterally and may climb the rail. [1]

During the last decades substantial progress has been made in the design of railway vehicles and running gear. Tilting trains, high speed trains, active steering wheelsets and other sophisticated solutions have been introduced. In spite of this progress, the mechanics of a railway wheelset remains unchanged and an inappropriate combination of wheel and rail profiles can easily deteriorate all these technological advances.

### 1.1.1. Problems in Railway Transport

Current problems in railway transport associated with wheel/rail contact: [7]

- Environmental (noise and poor ride quality)
- .Safety (derailment due to wheel climb or broken rail);
- Economic (excessive wear, rolling contact fatigue);

**Environmental problems:** Railways and mass transit systems represent one of the most air pollution caring modes of transportation. However, two problems remain: noise and poor ride quality. Noise originates from rough wheel and rail surfaces, corrugation-induced vibrations, or stick-slip–induced squeal. Corrugated wheels produce noise at frequencies dependent on train-speed. As the train accelerates and decelerates between stations high sound is produced. Although the lateral dynamic instability known as hunting is now well understood, it remains a common problem on many mass transit and heavy haul systems, as the conformal wear of wheel to rail often results in hunting.

**Safety problems:** Derailments from broken rail or wheels, and wheel climb derailments represent the most serious safety hazards. Although many factors contribute to wheel climb, contact angle and the magnitude of friction coefficient are the most important. Yet, both friction

coefficient, and the contact angle between the worn wheel-flange and the gauge of the worn rail are difficult to control in practice.

Ethiopia experiences the worst train disaster in the history of Africa and one of top 10 Deadliest Train Accident in the world. The accident took place in the town of Awash in Ethiopia in 1985 because of the derailment of an express train. Train derailed after the engineer failed to reduce speed at the curving bridge and eventually plunged into a ravine on the Awash River. **[6]**

**Economic problems:** Wear is a problem that is well understood and that can be solved; however, it can occur unexpectedly on new lines. There, measures must be taken to control it.

On wheels, the most common problem is flange wear. Substantial metal removal from the wheel tread is required to restore the thickness of the flange. Wear, therefore, now requires as much or more attention than it did 100 years ago.

RCF is first established by numerous micro-cracks and, if left untreated, results in the development of flaking or spalling, with cracks growing to a depth of 5 mm or more. This is a very costly problem. Both rails and wheels are affected. It was initially thought to be a problem associated only with heavy haul lines. It is a great economic challenge for railway companies to grind off RCF and other rail surface damage without wasting valuable, undamaged metal. [7]

Vehicle-track interaction includes ride comfort and safety, vehicle stability, wheel-rail forces, wheel-rail corrugation, wheel out of-roundness, noise propagation, etc., and is influenced by a variety of factors. [1]

Safety is the most important attribute of quality of service and operation for railways. The condition of wheels and rails has a great impact on railway safety. Wheel profiles have a significant effect on wheel/rail contact and overall vehicle and track dynamic performance. Therefore, having railway vehicles and especially wheels in an acceptable condition is a major concern for both railway operators and infrastructure owners.

Dynamic performance, safety and maintenance cost of which strongly depend on the wheel set dynamics and particularly on how good is design of wheel and rail profiles.

Some parameters have an influence on the wheel wear at different levels:

- Vehicle characteristics**:** (Axle load, Primary suspension stiffness and geometry, Car body/ Bogie rotational stiffness, Motor or trailer axle, Traction / Braking forces & characteristics)
- Wheel / Rail contact**:** (Wheel & Rail Profiles and rail cant, Wheel/Rail friction coefficient, lubricator device, Wheel material)
- Operating conditions: Curve radius and track cant in curve distribution, Mission profile.[4]

The geometrical characteristics of contact between wheel and rail it is possible to judge on the dynamic behavior of the wheel set and dynamic properties (like stability) of the vehicle.

The wheel and rail cross-sectional shapes define not only the kinematical and dynamical properties of the wheel set but also the physical properties such as contact stresses, creep and wear. Therefore, an ill-designed combination of wheel and rail profiles can be a source of various railway problems such as high wear rate of the wheels, instability (hunting) of a wheel set as well as rolling contact fatigue defects of the rails. These problems on their turn lead to cost inefficiency and unsafely in exploitation. [5]

To increase revenue for train operators and decrease cost for railway infrastructure owners, there is a need to monitor the conditions of the assets. A major cost-driver for operators is the production loss due to wheels, especially from maintenance costs when changing and re-profiling wheels. [2]

It is possible to find an optimal combination of wheel and rail profile when dealing with closed railway system, i.e. when the same type of rolling stock is running on the same track and no influence of other type railway vehicles presents. Example of such systems includes heavy haul and tramlines like Addis Ababa light rail train. Due to the fact that a rail costs much more than a wheel and wheels are more often re-profiled, it looks attractive to design a new wheel profile, which matches an existing rail profile. [3]

The objectives of optimum wheel and rail profiles are to provide: Stable performance over the range of normal train speeds Safety from derailment under adverse but realistic operating conditions Maximized wheel and rail life.

### 1.1.2. Wheel/rail interface development

A transport system consisting of a vehicle moving along a prepared track that provides guidance and support for the vehicle has been known for more than 400 years. As with many mechanical systems, it has developed over the course of centuries and is still developing.

'***Wagon ways'*** were developed in Germany in the 1550s, and the use of these tracks, consisting of wooden (usually edged) rails for horse-drawn wagons, spread across Europe. At first confined to mines, they were in use in Britain for surface transport by the early 1600s.

Such railways existed in a number of areas, and in most cases their function was to facilitate the transport of coal from the pits to a stair on a riverbank, from where it could continue by water. Because rails were smoother than roads, a greater quantity could be carried, and without damage to highways.

In the late 1760s, the Coalbrookdale Company began to ***fix plates of cast iron*** to the wooden rails. These (and earlier railways) had flanged wheels as on modern railways, but Coalbrookdale introduced another system, in which un-flanged wheels ran on L-shaped metal plates; these became known as ***plate ways***.

John Curr, a Sheffield colliery manager, invented this flanged rail, though the exact date of this is disputed. William Jessop, a civil engineer, used this design in 1789.

On July 26, 1803, Jessop opened the Surrey Iron Railway in south London – arguably, the world's first public railway, albeit a horse-drawn one.

The first steam locomotive was built by *Richard Trevithick*, an English engineer, in 1804.

In 1813, *George Stephenson* persuaded the manager of the colliery where he worked to allow him to build a steam-powered machine. He built the Blucher, *the first successful flanged wheel* adhesion locomotive. The flanges enabled the trains to run on top of the rails rather than in sunken tracks. This greatly simplified construction of switches and rails, and opened the path to the modern railway.

The conventional railway wheelset, which consists of two wheels mounted on a common axle, has a long history and evolved empirically.

In the early days of the railways, speeds were low, and the design objectives were the reduction of rolling resistance and solving problems of strength and wear. The flanges were positioned on the inside, the outside, or even on both sides of the wheels.

Flange positioning was debated all the way through the 1820s. Wheels were normally fixed to the axle, although freely rotating wheels were sometimes used in order to reduce friction in curves. From the beginning, the play allowed between wheel flange and rail was minimal.

*Coning was* introduced partly to reduce the rubbing of the flange against the rail, and partly to ease the motion of the vehicle around curves.

Moreover, by the time wheels were made of cast iron, taper had already become normal foundry practice.

Beginning in the early 1830s, ***flange way clearance*** was opened up to reduce the lateral forces between wheel and rail such that, in current practice, typically 7 to 10 mm of lateral displacement is allowed before flange contact.

Figure 1.1 the wheel rolling on a steel rail is the basis of almost all railway systems (Source AALRT).

Wheel/rail interface advances in tandem with the development of the railways. First, cylindrical free-rotating wheels running on flanged rails were replaced by rigidly mounted on axle conical wheels with flanges (see Figure 1.1).

This design was successfully used until the 1970s, when increased axle load, travel speed, and maintenance demands placed new requirements on wheel/rail interface.

Extensive research on in-service wheel and rail profiles reveals that *worn profiles* have curvilinear shapes, in contrast to the quasi-linear shape of the conical wheel.

It was discovered that the *worn shape* of the wheel is more stable, i.e. less changes with the mileage and wear. Another advantage of the worn shape was that it is already ground-in to the existing rail; therefore, the initial high wear rate typical of new wheels was significantly reduced. Ever since, many railways have adopted the curvilinear wheel profiles as a standard. (See Figure 1.2)

Although great progress has been made in railway transportation systems of all kinds (intercity transport, mass transit systems, and heavy haul), some wheel/rail interface problems persist and, moreover, new problems continue to emerge. [3]

These safety, economic, and environmental problems can be greatly reduced or brought under control through modification and optimization of wheel/rail interface.

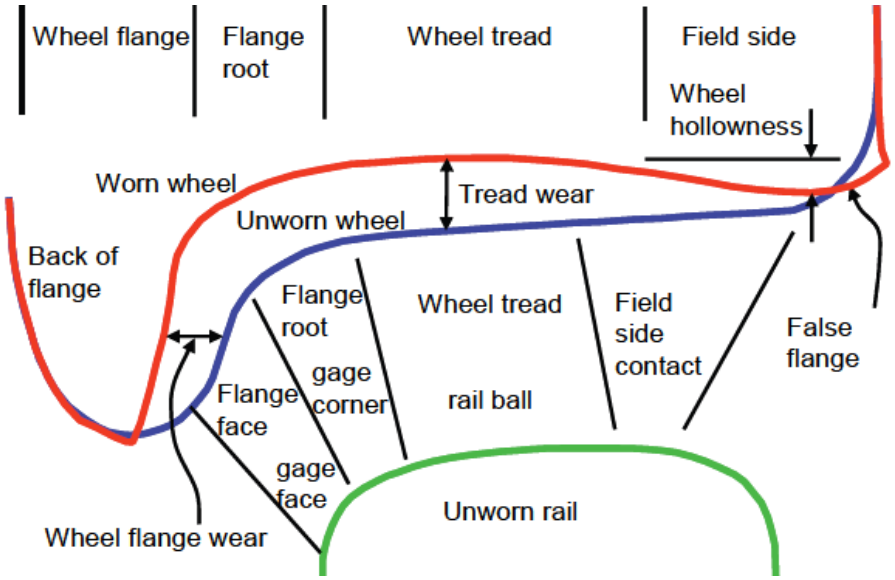


Figure 1.2 Worn and unworn wheels with unworn rail.

### 1.1.3. Criteria's in wheel profile design

Optimizing wheel/rail interface requires a focus on four areas: contact mechanics, wheel/rail dynamics, metallurgy, and friction management. [8]

Xinggao Shu describes Wheel and rail profile design is a matter of optimizing several criteria. Some criteria must be satisfied, but some can be compromised to achieve an overall optimum solution. The following criteria are usually used to design a wheel profile:

- ✓ Lateral Stability — should be achieved for normal operating speeds in the empty and loaded conditions; hunting performance depends on the nonlinear conicity function
- ✓ Maximum Contact Angle — should be greater than 72 degrees to avoid flange climbing derailments; APTA recommends at least 72 degree (suggested tolerance +3° and -2°) angle for commuter cars (APTA SS-M-015-06 2007)
- ✓ L/V Ratio —should be less than 0.8 to avoid flange climbing derailments
- ✓ Wear Index — should be as low as possible to avoid wear on wheels and rail in curves

- ✓ Contact Stress — should be as low as possible; high contact stress contributes to rolling contact fatigue and metal flow
- ✓ Contact Position — should be widely spread to avoid concentrated wear; should not be too far toward the field side of the rail to avoid rail rollover moments
- ✓ Rolling Resistance —should be as low as possible to reduce power consumption and draft forces

Wheels and rails gradually wear and change their profiles in service; therefore, their contact geometry properties can never keep constant.

Three of these performance indices, car lateral stability, wheel/rail contact position, and stress, are significantly affected by wheel/rail wear. The effects of wear on these criteria are mostly negative, leading to car instability, deteriorated ride quality, and damage to wheels and rails. [9]

Ivan Y. Shevtsov,2008 in his PhD thesis widely describes that Wheel/rail contact physically occupies an area the size of a small coin, and such contact transfers the load from a vehicle ranging from 3.5 t (28 t lightweight passenger coach) to 17.5 t (heavy freight car of 140 t) per wheel.

The material in and around the contact area is therefore highly stressed. High rates of wear might be expected from such contact but, because the load is applied and removed many times during the passage of each train, there is the added possibility of fatigue of the rail surface. The ideal material, which would have zero wear and suffer zero fatigue, and which would nevertheless be economically viable, is yet to be found.

The selection of railway wheel and rail profiles is a challenge that has faced engineers since the dawn of the railway age. From the first cylindrical wheels running on flat plates, wheels were made conical to produce better guidance, and flanges were added for safety.

Modern wheels often have complex profiles based on the shape of worn wheels in an attempt to increase their life. Rails also now have complex profiles with different radii on the rail head where the wheel tread makes contact, and on the corner, where the flange contacts.

A *high level of wheelset conicity* allows good curving behavior even in the tightest curve, without flange contact. This can however, lead to a relatively low critical speed and possibly dangerous hunting instability. A *low level of wheelset conicity* on the other hand, allows stable operation at high speeds, but flange way clearance will quickly be used up in curves, resulting in flange contact and possible flange climb derailment.

Flange angle and root radius are also variables that can have a significant effect on the potential for derailment. In addition to vehicle behavior, engineers must consider stresses on both the wheel and rail. These have a major influence on the development of RCF, which can have expensive and sometimes dangerous consequences. [10]

**Figure 1.3 Addis Ababa Light Rail Train, stadium station (to Kality and Hayat junction)**

## 1.2. Statement of the problem

To increase revenue for train operators and decrease cost for railway infrastructure owners, there is a need to monitor the conditions of the assets. A major cost-driver for operators is the production loss due to wheels, especially from maintenance costs when changing and re-profiling wheels. Even if it's been a year and two months since Addis Ababa Light rail train starts, the AALR train suffers with fast wheel/rail wear.so if it is not assessed and studied carefully this problem will cost the country in terms of operation or money.

### 1.2.1. Problems observed in Addis Ababa LRT

a. Burn on wheel thread

b. Flat spot on wheel thread

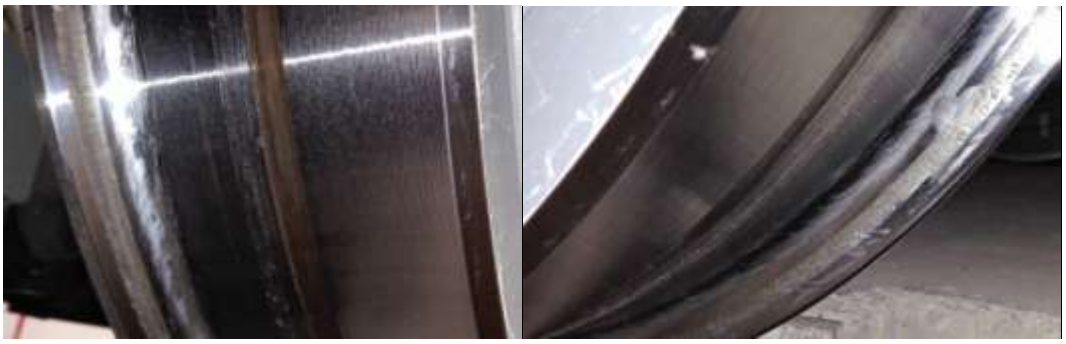

c. Wheel thread scratch and flange thickness

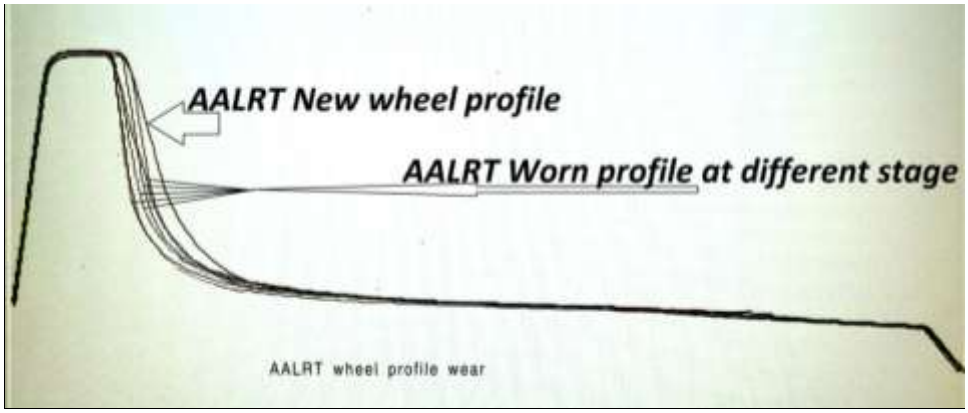


d. New and worn wheel profile of AALRT (data taken from under flour Lath Machine)

**Figure 1.4** a-d **Problems observed on Addis Ababa LRT wheel**

## 1.3. Objective

### 1.3.1. General Objectives:

The main objective of this paper is to study the possibility of reducing wheel rail wear by optimizing wheel profile and check dynamic performance analysis for optimized wheel profile.

### 1.3.2. Specific objectives:

- Study wheel profile of AALRT
- Study wheel rail contact and its influence on wheel wear.
- Study wheel profile shape optimization methods and generate optimized wheel profile
- Model AALRT Wheel profile and Vehicle (articulated three bogie passenger train) in SIMPACK software package
- Test the optimized profile dynamic performance analysis for stability, wear and dynamic contact stresses with the SIMPACK computer package.

## 1.4. Methodology

The wheel profile design procedure: The first step is an analysis of the current wheel/rail profiles. Profile measurements with under flour lath machine are used to analyze the wheelset contact properties to design a target rolling radius difference (RRD) function.

The second step is the definition of an optimum (target) RRD function. The problem of finding a wheel profile corresponding to the target RRD function was formulated as an optimization problem.

The optimized profile is tested for stability, wear and dynamic contact stresses with the SIMPACK computer package. If the dynamic performance of a vehicle with the obtained wheel profile does not satisfy the imposed requirements, the RRD function should be adjusted and the optimization should be performed again in an iterative process.

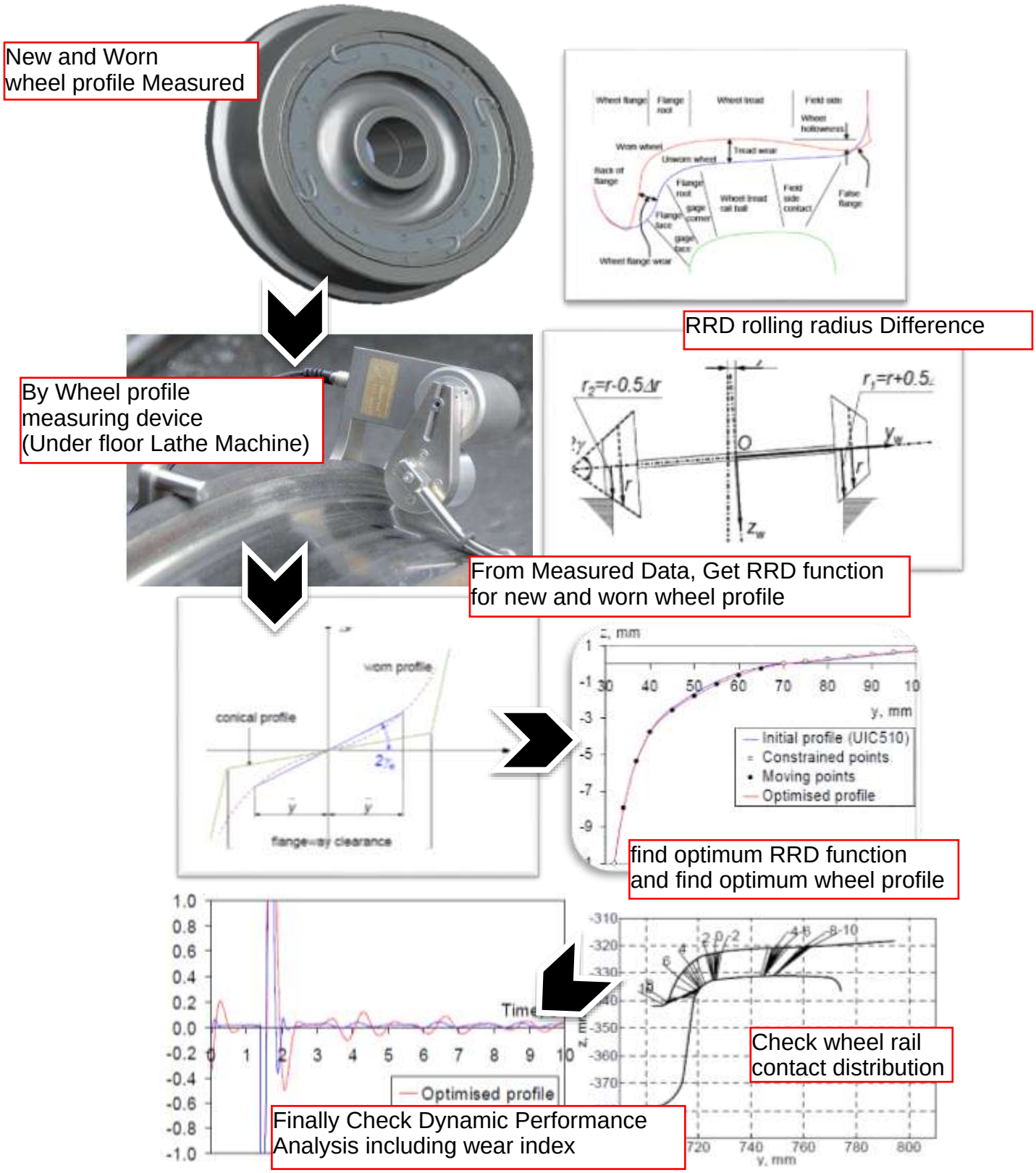


Fig1-5 wheel profile optimization methodology steps

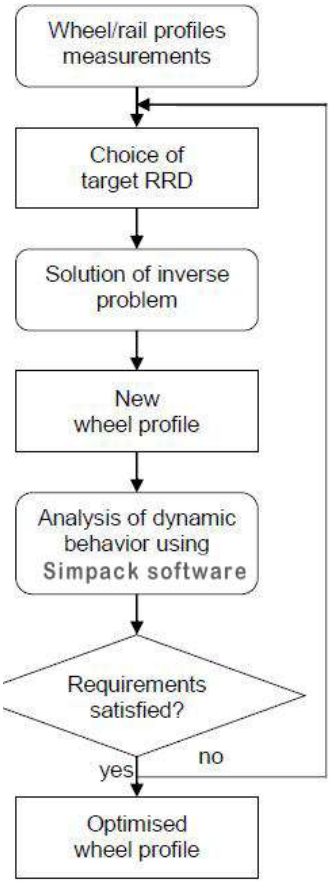


Fig1-6 pictorial flow of Methodology steps (**source**: Research center of Railway Engineering, TU Delft)

## 1.5. Scope and Limitation of the Paper

### 1.5.1. Scope

The scope of this research will be study the causes of wear, study history of wheel profile optimization, taking data of wheel profile measurements from AALRT current used trains, by find out the rolling radius difference of measured wheel profiles find average optimum wheel profile, modeling wheel and full train structure and make analysis in SIMPACK software package, simulating dynamic performance and drawing conclusions based on both the analysis and simulation results. Optimization of rail profile is not considered in the study.

Machining the wheel based on the new optimized wheel profile is beyond this study

### 1.5.2. Limitation

- limitations of the current study are:
  - The rail vehicle model used in the simulation study comprises a rigid car body, i.e. car body flexibility was not considered in the current study but it does influence rail vehicle dynamics and it is another engineering problem which needs to be solved

- Track flexibility and mass were not considered in the current study but they do influence rail vehicle dynamics; therefore, the effect of such track parameters on rail vehicle dynamic behavior is another engineering problem which needs to be studied.
- Effect of wind, traction and braking were not considered in the current study but they do influence rail vehicle dynamics so incorporating traction and braking in rail vehicle dynamics analysis results in better simulation results.
- All wheel profiles were considered identical from left to right on a given axle and from axle to axle and all wheels remains in contact with the rails as well as no wheel flats was considered but in practice all wheel profiles are not identical, there are wheel lifts and wheel flats which influence ride dynamics; hence, consideration of such things will give better result.

- This research is intended to study and optimize the shape of wheel profile for Addis Ababa Light Rail Train by measuring currently used new and worn profile. To get an optimum (target) RRD function it will need carful measurement and measuring device, and because of lacking measuring device, Under floor Wheel lathe machine is used as measuring device instead of mini prof profile measuring device.
- There will be also a limitation of Machining and Practical testing the new optimized wheel profile.

## 1.6. Significance of the study

The main focus area of the study is optimizing Addis Ababa Light Rail Train to reduce wheel rail wear. but to get the target solution this study asses different vast portions starting from study the parameters that will affect AALRT wheel wear, study the behavior of wheel profile and the vehicle of AALRT by itself, Study wheel rail contact geometry , model wheel and real simulation of articulated three bogie vehicle using SIMPACK software. Also dynamic performance analysis is checked by this software. So this study will be significant for further study of new rail trains that Ethiopia starts to use and planned to use.

As a Railway research academy that Addis Ababa University planned to open in 2018, this study will help for candidates to focus on problems of AALRT and the way of approach for solution as well.

## 1.7. Organization of The Paper

The thesis report comprises 5 chapters and the remainder of the thesis is organized as follows. **Chapter 1** describes the general introduction about rail transportation, problems in railway transportation, history of wheel rail interface development, statement of the problem, objective, scope and limitations.

**Chapter 2** presents review of related research works done and theoretical literatures relevant for the study such as Wheel rail wear; Wheel profile optimization methods; Multi body system dynamics, rail vehicle dynamics modeling and simulation and ride behavior of rail vehicles

In **chapter 3**, the research methodology such as wheel rail contact geometry, wheel profile optimization methods and simulation condition are presented. **Chapter 4** presents results of the analysis and discussion of the analysis results. Moreover, the study is summarized in **chapter 5** by presenting conclusions, recommendations and future work directions. Finally, the detail of the data used for the study such as rail vehicle design data; track design data and wheel rail data as well as analysis results are presented in the **appendix** section.

# CHAPTER TWO

# LITERATURE REVIEW

In order to study wheel rail contact and the shape optimization of wheel profile of Addis Ababa Light Train, the literature related to wheel rail contact, wheel rail wear and optimization of wheel rail profile has been reviewed.

## 2.1. General Reviews of wheel rail contact and wear in Railways

Some parameters have an influence on the wheel wear at different levels:

- Vehicle characteristics (Axle load, Primary suspension stiffness and geometry, Carboy / Bogie rotational stiffness, Motor or trailer axle, Traction / Braking forces & characteristics)
- Wheel / Rail contact (Wheel & Rail Profiles and rail cant, Wheel/Rail friction coefficient, lubricator device, Wheel material)
- Operating conditions: Curve radius and track cant in curve distribution, Mission profile

**Problem Reports of Light Rail Train Used Transits:**

Many factors influence the type of wheel profile that an operator may choose to use on their trains. These include the curvature of the infrastructure, the design speed and the type of rail. Generally, for light rail applications, coned wheels are used in order to navigate tight curves.

Coned wheels connected by a rigid axle allow rail vehicles to steer around curves by creating a differential in rolling radius. When in a curve, the inside wheel rotates with a smaller radius, and travels a shorter distance, than the outside wheel. This differential reduces friction and flange contact, reducing wear on the wheels and the rails.

Light rail vehicles that contain double-articulation using a short center trailer. To achieve a low-floor design in the middle of the train, the axle is removed, allowing the wheels to turn independently from one another.

Without an axle, the self-steering mechanism that stabilizes the vehicle is removed. Coned or not, the wheels are free to rotate independently of one another, which means it no longer self-steers towards the center of the track.

As a result, flange contact becomes more common with IRW systems. In some situations, such as tight curves, turnouts or even when travelling at higher speeds on straight tracks with unevenness, the trailer may be guided by the flanges of the wheels rather than the rolling radius differential. This contact increases friction, wear and sometimes noise.

***NJ Transit reported*** "higher wheel wear on the center trucks of its LFLRV fleet than on the wheels of the motor trucks" and "very high rail wear on sharp curves."

***Portland Trimet*** came to a similar conclusion, reporting that "Portland MAX has experienced higher LFLRV wheel flange wear on the center truck than on the motor trucks."

At its worst, the forces generated through this increased flange contact may be high enough to let the wheel climb over the tracks and cause a derailment, and the report notes:

As with any engineering issue, there are methods for mitigation, including modification of infrastructure for better wheel-rail interfaces and maintenance. Wear and noise can be mitigated using several methods, including lubrication, which Sound Transit has done. Additional protection through curves could also be provided by restraining rails. Operationally, the report also suggests that curves should be taken at constant speeds, with acceleration only after the curve has passed. Finally, improved vehicle and infrastructure design can also reduce these negative effects.

However, the need for these mitigation measures demonstrates that for light rail, "track standards have to be tighter than might be acceptable with more conventional vehicles. It is also generally recognized that the management of the wheel/rail interface is even more critical."

Generally, this means that it is more difficult for light rail to achieve the same performance (speed, acceleration, curving capabilities, etc.) compared to a conventional train.

## 2.2. Related Literatures about the stated problem

During the last several decades, a number of efforts have been made to use numerical methods in the wheel and rail design process.

***Magel and Kalousek [2002]*** describe Optimization of the rail grinding process, and the factors affecting the selection of the one- or two-point contact profiles. one of the ways in which railways have traditionally maintained the shape of the rail is through rail profile grinding.

Over the years, researchers, railways, and rail grinding contractors have developed a series of patterns that are used to impose a specific profile upon the rail. These profiles have been characterized as 'one-point' and 'two-point' contact profiles.

***Grohmann and Schoech [2002]*** describe a long-term experiment launched by the German Railways (Deutsche Bahn) to specify a target profile with appropriate grinding.Optimal rail maintenance policy can be developed to balance wear and surface fatigue through grinding. The objective is to maximize rail service life, and to consequently optimise the life cycle costs of rails.

***Sato [1990]*** describes Design of the rail head profiles for the Tokaido Shinkansen line in Japan. To improve rail conditions on this line, studies of worn rail profiles and rail damage were carried out, and the causes of damage assessed. Then, the abrasion of rail corners on tangent track was studied. Through the study of contact points between wheel and rail, the fact that the lateral movement of bogies is accelerated by tilting of the rail was made clear. On the basis of these findings, new measures, such as limiting the displacement of contact points between wheel and rail, cutting off neighboring parts of the running fringe, having the rail head side conform to the tyre profile, and cutting off the gauge corner on curves with larger radius, and on tangent track, were proposed, and a new rail profile with full use of grinding was designed.

***Sato [1996]*** discussed use of heavy rail on heavy haul railways to reduce rail defects and track deterioration. The clear advantages of using heavy rail on high-speed railways. Since future railways should guarantee the dynamic stability of rolling stock and be free of rail defects, it is appropriate to consider modifying the wheel running band formed by rail grinding. A new 75 kg rail profile with full use of grinding was proposed. This profile was developed based on experience with rail profile design in Japan.

***Sato [2005]*** Mathematical equations were used to model the profile, instead of drawings. An historical review of wheel and rail profile development on the Shinkansen line in japan.

***Smallwood et al. [1990]*** use optimization techniques to minimize rail contact stresses. A modification to the transverse rail profile has been proposed which should result in reduction in contact stress. Contact stresses between wheel and rail are believed to be influential in the initiation and growth of RCF cracks, particularly on the high rails of curves on high speed lines. Theoretical methods have been used to investigate the effect of profile changes on contact stress and conicity. The predicted contact stresses for the modified profile are up to 50% lower than those for an unworn standard British Railways (BR) profile, while the conicity remains

within an acceptable range. The metal removal required to achieve this profile appears practical using the latest generation of more aggressive grinding trains.

**Casini and Tacci [1996]** describes about ORE C116 committee has endeavored to determine a standard European profile adapted for wear. An attempt to create a standard profile was made with the ORE S1002 wheel profile. The ORE S1002 profile was calculated on the basis of the DB II profile, by transforming the three arcs of the wheel into a higher degree polynomial curve. The ORE S1002 wheel profile is adapted for wear for rails inclined at 1:40.

***Smith and Kalousek [1990]*** developed a numerical procedure for design of a wheel profile, described by a series of arcs. Although the procedure was specifically developed for steered axle vehicles.

**Casini and Tacci [1996]** also use a series of arcs to develop a new wheel profile adapted for the Italian network.

***Leary et al. [1990]*** describes the process of designing a new wheel profile for North American railways, where in alternative profiles are derived through *two* techniques: *an average worn wheel profile,* and *profiles based on expansions of rail shapes*. Both methods provide good base designs for candidate profiles. However, the initial wheel shapes produced were modified to suit the specific concerns of the task involved. This was done through careful computer analysis of the dynamic and contact stress characteristics of each wheel.

***Shen et al. [2003],*** proposes procedure for design of a wheel profile using a numerical optimization technique. Wherein the contact angle function is used for the design of railway wheel profiles. Using the inverse method for known contact angles and rail profile, a corresponding wheel profile was found.

***Magel and Kalousek [2004]*** design a wheel profile to reduce RCF on rails, they suggest that creepage can be controlled and manipulated to minimize contact fatigue. Although creep forces are dramatically influenced by a range of operational conditions that include traction and braking demands, friction coefficient and suspension characteristics, the focus of the research was on wheel and rail profiles. Through quasi-static and dynamic modeling they show a modified wheel profile, by reducing both normal contact stress and traction, can play a significant role in mitigating RCF.

***Zakharov and Zharov [2000 and 2003]*** works a research on wheel/rail contact problems on Russian Railways. Serious problems of wheel and rail profile design arise particularly when combined freight and passenger traffic exists on the line. Profile selection policies and real practices applied on Russian Railways are described by Zakharov et al. [2006].

***Ushkalov et al. [2002]*** describes about a non-linear 'one-point' contact type wheel profile was developed to reduce wheel flange wear. This profile was implemented on an upgraded freight bogie. Running tests over three years (about 190000 km) have shown that this modernization resulted in an increase of the critical velocity of empty cars by 30–40 km/h, decrease in wheel flange wear by a factor of two, along with other benefits. Ukrainian Railways is now performing the above described modernization on several hundred freight cars.

## 2.3. Literature Review on wheel profile optimization methods

Researchers have adopted various methods with different targets and strategies to develop a new theoretical wheel profile, and the following are examples of profile design based on:

- Target RRD function (Smith and Kalousek 1991, Shevtsov et al. 2005)
- Target contact angle (Shen et al. 2003)
- Target conicity and wide contact range (Polach 2009)
- Using a Genetic Algorithm (Persson and Iwnicki 2004 and Novales et al. 2006)

Typically, a wheel profile was designed using a trial and error approach to reach design targets. Wheels cannot be designed without reference to rail profiles. Theoretical or measured rail and/or wheel profiles were usually selected as "seeds" or references during the design process.

[1] **Smith and Kalousek 1991:** developed a numerical procedure for design of a wheel profile described by a series of arcs. Although the procedure was specifically developed for steered axle rail transit vehicles, some important aspects of it can be applied to conventional rail transit systems as well.

[2] **Shevtsov et al. 2005:** proposed a procedure for design of a wheel profile that improves wheel and rail interaction by reducing wear while taking into account rolling contact fatigue. The procedure uses an optimality criteria based on a RRD function. The criteria accounts for stability of a wheelset, minimum wear and contact stresses of wheels and rails as well as safety requirements. Using the proposed procedure, Shevtsov et al. designed a new wheel profile and conducted simulations using ADAMS/Rail software.

[3] **Shen et al. 2003:** proposed a wheel profile design method using a target wheel/rail contact angle function and rail profile information. A computer program was developed to produce an independent wheelset profile for a rail transit car.

[4] **Polach 2009:** investigated the relationship between the equivalent conicity, contact angle, and location of the contact area in nominal position, the contact stress, and lateral contact spreading on worn rail profiles. New wheel profiles were created with target conicity and at the same time wide contact spreading.

[5] **Persson and Iwnicki 2004 and Novales et al. 2006**: used optimization procedures based on a genetic algorithm to design a wheel profile for railway vehicles. Two existing wheel profiles were chosen as "parents," and "genes" were formed to represent these profiles. These genes were mated to produce offspring genes and then reconstructed into profiles that had random combinations of the properties of the parents. Each of the offspring profiles were evaluated by running a computer simulation of the behavior of a vehicle fitted with these wheel profiles and calculating a penalty index. An inverted penalty index was used as the fitness value in the genetic algorithm. The method was used to produce optimized wheel profiles for two variants of a typical vehicle, one with a relatively soft primary suspension and the other with a relatively stiff primary suspension.

[6] **Coenraad Esveld, Valery L. Markine, and Ivan Y. Shevtsov,(*2006)*,** In this article they hardly note that By studying the geometrical characteristics of contact between wheel and rail it is possible to judge on the dynamic behavior of the wheelset and dynamic properties (like stability) of the vehicle. The wheel and rail cross-sectional shapes define not only the kinematical and dynamical properties of the wheelset but also the physical properties such as contact stresses, creep and wear.

Therefore, an ill-designed combination of wheel and rail profiles can be a source of various railway problems such as high wear rate of the wheels, instability (hunting) of a wheelset as well as rolling contact fatigue defects of the rails.

To solve this problem a numerical method for wheel profile design was discussed based on optimization of the Rolling Radius Difference function. Using this procedure the wheel profile design for the Rotterdam metro network (RET) metro train in Netherland has been improved. The results of the dynamical simulations have shown that the performance of railway vehicle is improved by improving the contact properties of wheel and rail. Double point contact between wheel and rail produces high wear and leads to hollow wear of wheels. The new wheel profile was implemented on the RET metro trains. Due to the optimized wheel profile the

instability of the metro trains has been eliminated and the lifetime of the wheels has been increased from 25,000 km to 114,000 km.

[7] **M. Ignesti, A. Innocenti, L. Marini, E. Meli n, A. Rindi, P. Toni** (*2012)* In this work the authors present two innovative wheel profiles, specifically designed with the aim of improving the wear and stability behavior of the standard ORE S1002 wheel profile matched with the UIC60 rail profile canted at 1/20 rad, which represents the wheel–rail combination adopted in Italian railway line.

They develop two wheel profiles, one wheel profile has been designed with the purpose of spreading the contact points in the flange zone on a larger area in order to reduce wear phenomena and having a constant equivalent conicity for small lateral displacements of the wheelset with respect to the centred position in the track.

The other wheel profile is instead designed in order to guarantee the same kinematic characteristics of the matching formed by ORE S1002 wheel profile and UIC60 rail profile with laying angle $\propto_p$ equal to 1/40 rad, characterized by good performances in both wear and kinematic behavior.

Wheel profiles evolution has been calculated through a wear model developed and validated by the authors with experimental data relative to the Italian Aosta-Pre Saint Didier railway line.

[8] **Oldrich Polach∗ (2010),** this article deals with design of new wheel tread profile. An interrelationship between the equivalent conicity, contact angle and location of contact area in nominal position, the contact stress and lateral contact spreading is explained and illustrated on examples of measured worn wheel profiles. This relationship has been considered in the proposed method for profile design applied to create new profiles with target conicity and at the same time wide contact spreading. The proposed profiles are suited for vehicles running on straight tracks and/or high power traction vehicles. The paper presents possible methods for a design of wheel profile with continuously changing curvature. The presented examples confirm an improvement using proposed profile design methodologies in comparison to an arc profile design created by trial and error.

For vehicles characterized by dominating tread wear, the wear distribution can be estimated based on the lateral position of the contact points on the profile shape. This simplified wear estimation can be used to select the optimum wear distribution of the contact points on the wheel profile which can then be applied to create the new wheel profile. The proposed

methodology of the wheel profile design based on simplified wear estimation can be combined with simulations of wear development under realistic conditions.

[9] **H.M. Tournay (July 2008),** This paper reviews current current developments in vehicle and track condition measurement and the role of wayside detection in controlling the size and position of the contact patch as well as the forces acting across this patch. The paper closes with a suggested challenge for the future: as flange and gage corner wear are increasingly controlled and as track tolerances improve, the wear of wheel and rail becomes increasingly concentrated on the wheel tread and the rail crown.

The paper suggested that, as a consequence, wheelset conicity and wheel and rail contact stress changes during the service life of the wheel may become greater than those under high flange wear conditions resulting in reduced vehicle stability and increased wheel and rail fatigue problems during the service life of the wheelset. Consequently, the prediction of wear and material flow patterns on wheel and rail becomes increasingly important in determining system performance as a function of system design parameters such as track gage, wheelset tolerances, and profile shapes for given track topology.

[10] **Joseph Kalousek∗ (2004)**, In this study, The wear that shapes wheel and rail profiles has a profound effect on curving performance and dynamic stability of bogies. Reducing the spread between worn and unworn profiles, and in particular reducing the concavity of worn wheels, can significantly improve curving and ride quality of bogies, decrease wheel/rail damage and increase wheel and rail lifespan.

In general, the design of a new wheel will be focused on five main problems in wheel/rail contact:

- Wear of contact surfaces;
- Rolling contact fatigue;
- Stability on a straight track;
- Stability on passing curves (minimization of *Y/Q* and track forces);
- Safety requirements.

These problems maintain a complex relationship with each other. For example, decreasing wear can lead to RCF problems, and increasing conicity to pass curves with larger rolling radius can lead to decreased critical speed of the vehicle, and vice versa. Depending on the type of

railway system, one of these five problems may be more pronounced; however, they all are present in the wheel/rail interface, and should be considered together.

Obviously, an optimum profile is a compromise between stability, curving, wear, and RCF. Magel and Kalousek [2002] formulated criteria for optimal wheel/rail contact. Optimized wheel and rail profiles from the aspect of contact mechanics should satisfy the following criteria:

- Avoid contact stresses greater than three times the strength of material in shear;
- Avoid closely conformal contact;
- Design appropriate steering capability;
- Ensure effective conicity that is within the conicity window of the truck;
- Arrange for as many contact points across the wheel tread as possible.

In the past, such a compromise would have been achieved by manually modifying the wheel shape to find satisfactory contact characteristics in relation to a given rail. However, this design approach is quite time consuming and expensive. Therefore, it would be advantageous to develop and use numerical methods for the design of the wheel and rail profiles.

## 2.4. Research Gap

As reviewed above researchers, journals, and text books studied the effect of wheel profile on wheel wear with two bogie railway vehicle. But the stated problem occurs on the line that uses three bogie vehicles. Wheel profile optimization is dependent on its own constructed rail line with its own rail profile. Even the problem is vital there is no body (as the author knows) tries to study the wheel and rail profiles of Addis Ababa Light Rail Transit. By using the visible problem, study and optimize Addis Ababa light rail transit wheel profile is the gap to solve the stated problem.

# CHAPTER THREE

# MODEL, OPTIMIZATION AND ANALYSIS OF AALRT WHEEL PROFILE

## 3.1. Geometric contact between track and wheelset

The conventional railway wheelset consists of two wheels rigidly mounted on a common axle. Normally, wheels have a coned or profiled tread with a flange on the inside edge. The tread cone angle is about 2º, while the flange cone angle is about 70º. The wheelset rests on two rails fixed to the sleepers (ties) or other support (e.g., embedded rail).

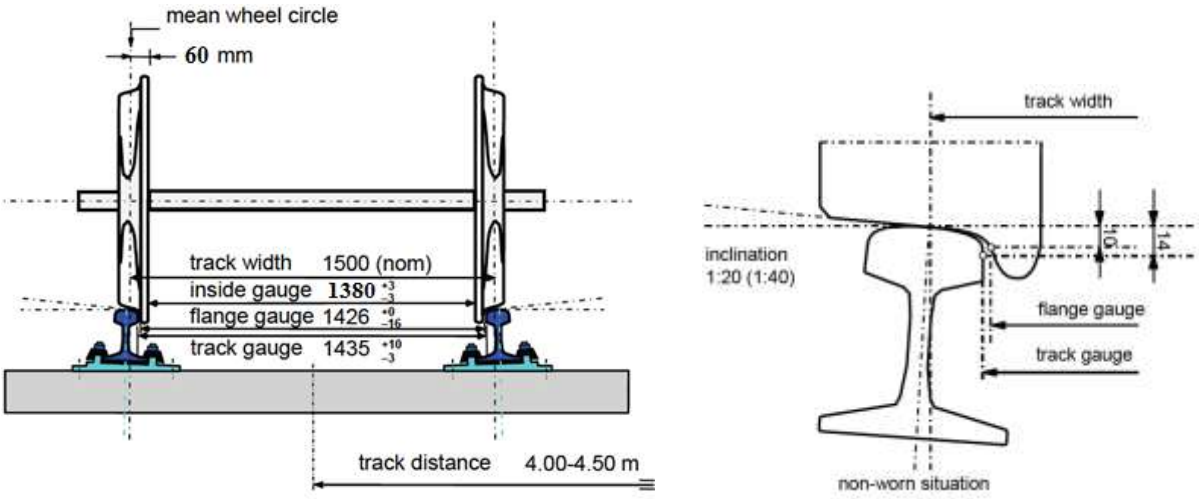


**Figure 3.1 a) A typical wheelset on rails and b) The shapes of wheel/rail surfaces**

A wheelset runs on rails normally inclined (canted) at **1 in 40** or (1 in 20). The gap between the flange of the wheel and the gauge side of the rail is such that it allows ***4–7*** mm lateral wheelset displacement before flange contact occurs.

The shapes of wheel/rail surfaces (tread, flange root and flange of the wheel, rail head, gauge corner, and gauge face of the rail) are important to vehicle stability, wheel/rail interaction forces, contact stresses, and wear characteristics.

Vehicle and track dynamics systems interact via wheel/rail interface, using output from one model as input for another, and vice-versa. For example, track irregularities can be used as an input for wheel/rail contact, causing disturbances in contact forces, which in turn will be used as an input for the vehicle model.

To determine forces in wheel/rail contact, values of creepage and spin are required, which can be obtained from analysis of geometric contact between wheelset and track.

## 3.2. Basics of wheelset and track interaction

### 3.2.1. Kinematics of a wheelset on straight track

The coned wheels are rigidly attached to a solid axle. If the track is considered to be rigid, then the railway wheelset has two main degrees of freedom:

- the lateral displacement $y$ , and
- the yaw angle $\psi$ .

If, as the wheelset is rolling along the track, it is displaced slightly to one side, the wheel on one side is running on a larger radius and the wheel on the other side is running on a smaller radius.

If pure rolling is maintained, the wheelset would move back into the centre of the track, and a steering action would be realized with the aid of coning. However, it will be found that following such a disturbance, the wheelset overshoots the centre of the track and traces out a more or less sinusoidal path as it proceeds down the track. This motion is referred to as kinematic oscillation. [15]:

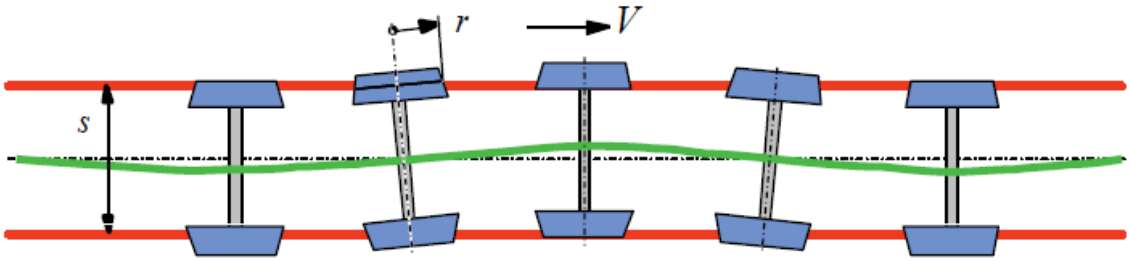


**Figure 3.2 the kinematic oscillation of a wheelset.**

Kinematic oscillation was first analysed mathematically for the case of purely coned wheels by Klingel in 1883, who showed that the frequency of oscillation is proportional to speed and to the square root of the cone angle. Klingel's description of wheelset oscillation assumes that pure rolling is maintained throughout the motion of the wheelset. In reality, this is not so because of the phenomenon of creep, first described in the present application by Carter in 1916, Wickens [2003].

### 3.2.1.1. *Klingel theory*

Freely rolling wheelsets perform a sinusoidal motion, as shown in above Figure. Klingel derived the relationship between the wavelength $L_k$ *and* the wheelset conicity $\gamma$ , wheel radius ***r***, and the lateral distance between contact points ***s*** as

$$L_k = 2\pi\sqrt{\frac{rs}{2\gamma}}.$$ Equation 1

Thus with Klingel, the linear, purely kinematic motion of a single wheelset is solved. Klingel's formula shows that as the speed is increased, so is the frequency of kinematic oscillation. If *V* represents vehicle speed, the time domain frequency of the Klingel movement is

$$f = \frac{V}{L_k}.$$ Equation 2

The Klingel movement is dependent only on track and wheelset geometric characteristics, and represents a global effect of wheel–rail interaction.

If the frequency *f* is close to one of the natural frequencies of the wheelset, the periodic movement could cause the vehicle instability**.** The lateral accelerations on the wheelset due to Klingel movement are described by the ratio

*V/ $L_k$*:

$$\ddot{y}_{\max} = 4\pi^2 y_0 \left(\frac{V}{L_k}\right)^2,$$ Equation 3

Where $y_0$ is the amplitude of wheelset lateral displacement.

At the same speed, a lower conicity $\gamma$ produces a movement with greater wavelength, but with lower lateral acceleration. Lateral oscillations caused by coning have been experienced since the early days of the railways.

Wheelset stability can be provided by the proper choice of the longitudinal stiffness of the primary suspension of the bogie.

### 3.2.1.2. *Rolling radius difference*

Let us continue with a simplified wheelset with a conical wheel profile. When the conical wheel runs on the circular rail without flange contact, there is only one contact point between the wheel and rail profiles, as shown in Figure 3.3. On the wheel profile, this point identifies the rolling radius.

In the central position of the wheelset, due to the symmetry of the wheelset/track system, the rolling radii $r$ and $r_1$, $r_2$ for the right and left wheels are equal, $r_1 = r_2 = r$ .

If the wheelset centre is displaced for quantity $\Delta y$ , then the rolling radii due to conicity of the wheels will be different for the right and left wheels, creating rolling radii difference (RRD) $\Delta r = r_1 - r_2$. An instantaneous difference between the rolling radius of the right and the left wheel can be defined as a function of lateral displacement ***y*** of a wheelset with respect to its central position (Figure **3.3**), according to:

$$\Delta r(y) \equiv r_1(y) - r_2(y) \,. \qquad \text{Equation 4}$$

Some examples of rolling radius difference functions (also known as a ' $y - \Delta r$ ' curve) for purely conical, and worn profiles, are given in Figure 3.4. Due to wear, a wheel profile changes (see Figure 1.2), and consequently so does its RRD function. As is evident, RRD function is dependent on wheel and rail shape; it is also included in the equations of wheelset motion, and therefore is a very important parameter for wheelset dynamics.

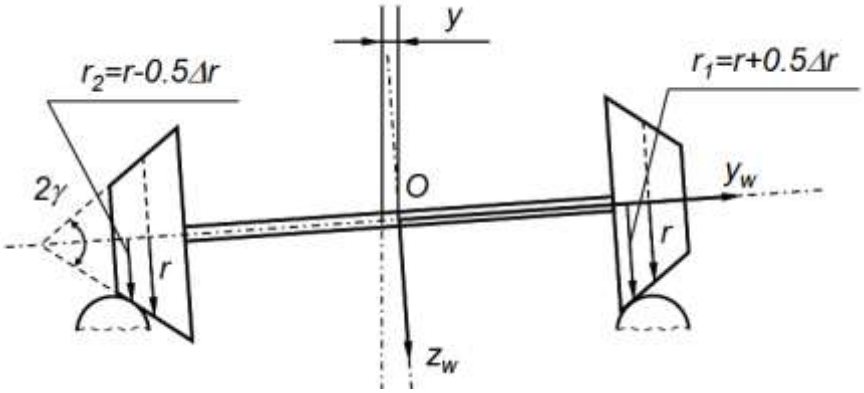


Figure 3.3 Rolling radius ($r_1$ and $r_2$) corresponding to wheelset displacement $y$ , wheels are conical, $\gamma$ is wheel conicity.

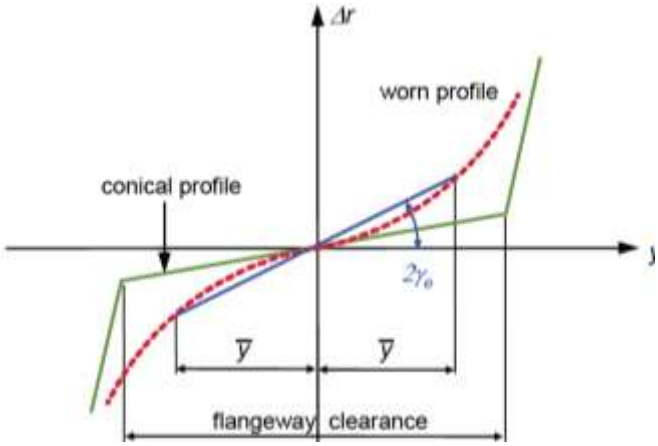


Figure 3.4 Rolling radius difference functions ('y − Δ*r*' curves).

### *3.2.1.3. Equivalent conicity*

In klingle's theory; its wavelength is independent from of vehicle speed and is a function of the angle $\gamma$ of the conical wheel profile.

So, wheel conicity $\gamma$ provides information about wheel–rail interaction:

- A high conicity value is suitable to counteract the centrifugal effects on curved track, but it generates a periodic movement on straight sections that can reduce riding comfort;
- Low conicity increases the ride quality, but on curved track it can cause the contact between the rail gauge and the wheel flange, producing excessive wear for both rail and wheel.

On a modern wheelset, the real wheel profile is not conical, but it has a curvilinear shape that matches the rail head profile, as shown in Figure 3.5.

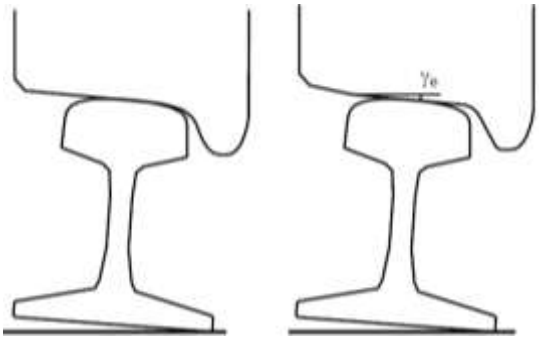


Figure 3.5 a) Real (left) and conical b) (right) wheel profiles on the rails.

To characterize wheel–rail interaction for a wheelset with real wheel profiles, a parameter, "equivalent conicity", is introduced. To identify the equivalent conicity, characteristics of the real wheelset/track pair are replaced with an "equivalent wheelset" with conical wheel tread surface. This replacement is valid for only one value of the wheelset lateral displacement.

Let's assume a lateral shift of the wheelset for quantity ***y*** from the central position. This shift is schematically shown in Figure **3.3**. The shift translates the contact points on the wheel profiles, leading to differences in the rolling radii $\Delta r = r_1 - r_2$ , Conicity $\gamma$ of the wheel tread can then be expressed as a function of wheelset rolling radii difference and wheelset lateral displacement:

$$\gamma = \frac{r_1 - r_2}{2y} = \frac{\Delta r}{2y}.$$

Equation 5

The equivalent conicity $\gamma_e$ is determined for a certain lateral displacement $y = \bar{y}$ . For the conical wheel profile $\Delta r\ (y)$ is a linear function, and the conicity $\gamma_e = \gamma$ is constant and independent from the displacement $y$ .

The equivalent conicity provides a quantitative measure of the influence of wheel/rail interaction on running quality. The threshold values for the equivalent conicity are defined in the UIC 518 fiche (UIC CODE 518 [2003]). The higher the vehicle speed, the lower should be the conicity of the wheel/rail pair to provide the required critical speed.

The equivalent conicity must be lower than 0.5 to ensure vehicle stability, though it must be higher than 0.1 to generate the appropriate restoring forces. For real-world wheelsets, equivalent conicity is maintained in the range of 0.2–0.3.

### 3.2.2. Kinematics of a wheelset on curved track

The action of a wheelset with coned wheels in a curve was understood intuitively early in the development of railways. Consider a conical wheelset on curved track of radius *R*, as shown in Figure 3.6. A simple geometric relationship between the outward movement of wheelset ***y***, the radius of the curve *R*, the wheel radius *r*, the distance between the contact points 2*b* and the conicity $\gamma$ of the wheels can be derived in order to obtain pure rolling:

$$\frac{r+\Delta r}{r-\Delta r}=\frac{R+b}{R-b} \qquad \text{Equation 6}$$

Therefore, the required rolling radii difference in wheelset for passing a curve without slippage can be calculated according to the formula

$$\Delta r=\frac{2br}{R}. \qquad \text{Equation 7}$$

Taking into account equation (5), the relationship between lateral displacement ***y*** of the wheelset and curve radius ***R*** can be derived as follows:

$$y=\frac{rb}{\gamma R}. \qquad \text{Equation 8}$$

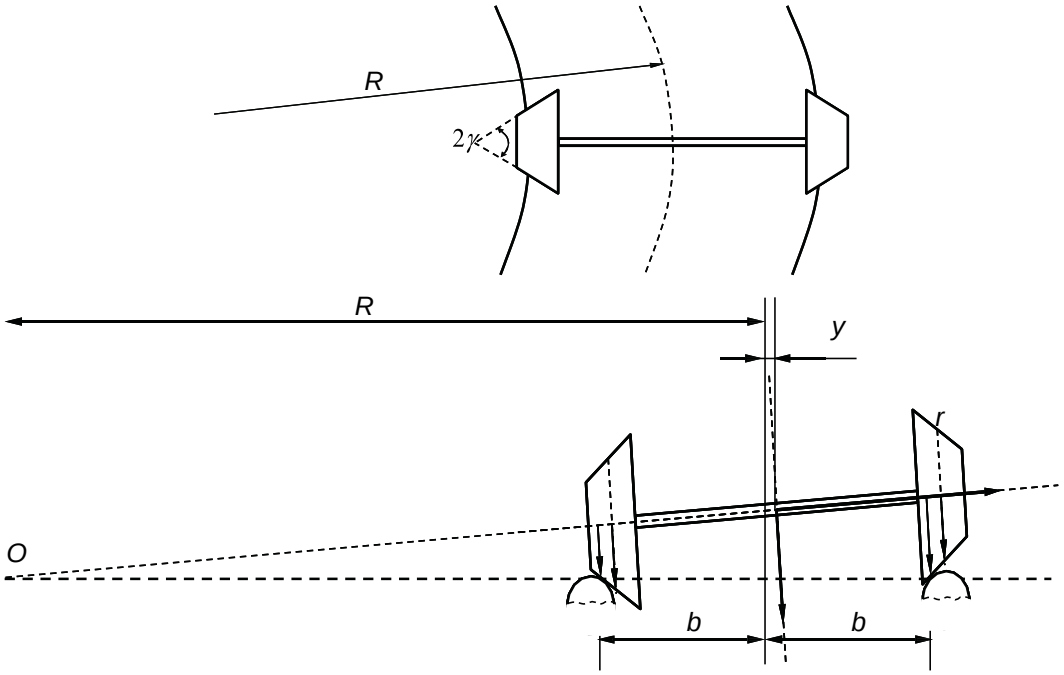


Figure 3.6 Rolling of a coned wheelset in a curve.

The application of Redenbacher's formula (equation 8) shows that a wheelset will be able to move outwards to achieve pure rolling only if either the radius of curvature or the flange way clearance is sufficiently large. Otherwise, a realistic consideration of curving requires analysis of the forces acting between the vehicle and the track.

Let us consider equation (7) assuming that flange way clearance is sufficient, and that the distance between the contact points $2b$ is equal to track width $2b = s = 1.5\ m$ . The required values of the RRD for passing curve with radius $R$ without slippage are presented in Table 1 (wheel radius $r$ is presented in brackets).

Table 1: Required RRD (Δr) for AALRT curves with radius R .

| $R$ , m | ***Δr, mm (r=0.330 m) AALRT*** | $\Delta r$ , mm (r=0.331 m) | $\Delta r$, mm (r=0.390 m) | $\Delta r$, mm (r=0.460 m) | $\Delta r$, mm (r=0.500 m) |
|---|---|---|---|---|---|
| 5000 | ***0.099*** | 0.0993 | 0.117 | 0.138 | 0.15 |
| 3000 | ***0.165*** | 0.166 | 0.195 | 0.230 | 0.250 |
| 2000 | ***0.2475*** | 0.248 | 0.293 | 0.345 | 0.375 |
| 1500 | ***0.33*** | 0.331 | 0.390 | 0.460 | 0.500 |
| 1000 | ***0.495*** | 0.4965 | 0.585 | 0.690 | 0.750 |
| 500 | ***0.99*** | 0.993 | 1.170 | 1.380 | 1.500 |
| 300 | ***1.65*** | 1.655 | 1.950 | 2.300 | 2.500 |

| | | | | | |
|---|---|---|---|---|---|
| 150 | ***3.3*** | 3.310 | 3.900 | 4.600 | 5.000 |
| 100 | ***4.95*** | 4.965 | 5.850 | 6.900 | 7.500 |
| ***50*** | ***9.9*** | 9.930 | 11.700 | 13.800 | 15.000 |
| ***30*** | ***16.5*** | 16.550 | 19.500 | 23.000 | 25.000 |

From equation (7) and Table 1, it is clear that the wheels with smaller radius require smaller RRD to pass curve in comparison with wheels of larger radius. Due to the fact that tram tracks feature great numbers of the sharp curves, tram vehicles use wheels with smaller radius to be able to produce the required RRD within given wheel/rail profile combinations.

## 3.3. Analysis of geometric wheel/rail contact

Analysis of wheel/rail contact is performed to study the effects of wheel/rail interaction on vehicle performance or wheel/rail wear. Depending on the objectives, the analysis can be geometric, static, or dynamic.

- Geometric analysis concerns *only* wheel and rail shapes and their relative positions, without regard to the vehicle or its motion. The results from geometric analysis are parameters of wheel/rail contact constraints.
- Static analysis gives normal contact stress under a specified loading condition.
- Dynamic assessment is usually performed using vehicle simulation software, which provides detailed information on vehicle dynamics and wheel/rail interaction, including normal forces, tangential forces, creepages, displacements, velocities, accelerations, and other dynamic parameters for wheel and rail contact patches. Contact parameters resulting from dynamic assessment are related not only to wheel/rail shapes and relative positions, but are also influenced by speed, vehicle/bogie characteristics, and track geometry.

In geometric wheel/rail contact software, any possible combination of wheel and rail profile contact situations can be analyzed for many wheelsets against a measured pair of rails, or many rails against a measured pair of wheels. This method provides a comprehensive view of wheel/rail contact at a system level.

For example, thousands of wheels with different profiles (due to different levels of wear or resulting from different truck performance) could contact a section of rail at different positions and, therefore, could produce different contact patterns and different levels of contact stress. The performance of the majority of wheel/rail pairs is therefore the focus of the assessment.

The distribution of contact parameters can be used to predict likely vehicle performance, wheel/rail wear, and contact fatigue.

For example, consider a group of measured wheels contacting a pair of rails measured on a curve. If the rails are judged to have unsuitable profiles due to resulting high contact stress and undesirable contact patterns, then appropriate action can be taken. If only a small number of wheels display unwanted wheel/rail interaction, then it might be best to remove such wheels from service. Alternatively, if many wheels cause problems, then it might be best to re-profile the rail by grinding.

## 3.4. Analysis of the problem and Wheel profile optimization

The kinematic properties of wheel–rail contact, such as rolling radius, contact angle and wheelset roll angle vary as the wheelset moves laterally, relative to the rails. The nature of the functional dependence between these geometrically constrained variables and the wheelset lateral position is defined by the cross-sectional shape of wheel and rail.

By studying the geometric characteristics of the contact between wheel and rail, it is possible to judge the dynamic behavior of the wheelset, as well as dynamic properties (like stability) of the vehicle.

The wheel and rail cross-sectional shapes define not only the kinematic and dynamic properties of the wheelset, but also such physical properties as contact stress, creep, and wear.

An important characteristic of contact between wheel and rail is the rolling radius of the wheel at the contact point. Consequently, the difference between the rolling radius of the right and the left wheel (rolling radius difference or RRD) as a function of the lateral displacement of a wheelset is one of the main characteristics of wheel/rail contact that defines the behavior of a wheelset on a track.

The rolling radii of the left and right wheels are present in the equations of wheelset motion (see Dukkipati [2000]). Therefore, the RRD function is important for the dynamic behaviour of a wheelset. From another viewpoint, the RRD function is defined by the wheel and rail cross-sectional profiles. Track and wheelset geometric parameters of course influence the RRD function as well, but they are considered to be given.

But if the shape of the RRD function is defined by the wheel and rail profiles, then the opposite is also valid; that is, the RRD function can define the shape of the wheel or rail profile. In computational modeling of railway vehicle, modification of the RRD function can change dynamic behavior of the wheelset helping to achieve the required performance. This modified

RRD function virtually corresponds to a new combination of wheel/rail profiles. For a given rail profile, one may solve the inverse problem in order to find a wheel profile to match the modified RRD function. The inverse problem can be solved using an optimization method. This idea was used as a strategic concept in the creation of the procedure for wheel profile design.

In the wheel profile design procedure, the optimization searches for an optimum wheel profile by minimizing the difference between targets (desired) and actual RRD functions. To solve the minimization problem, an optimization procedure based on Multipoint Approximations based on Response Surface fitting (MARS method) was used. Different constraints can be applied in the optimization procedure to reflect safety, construction, and other requirements for the designed profile.

Static analysis of geometric wheel/rail contact is used as a first step in the design of appropriate profiles. Analysis of railway vehicle dynamics is needed to verify that the designed profiles will perform well under given vehicle and track conditions.

### 3.4.1. AALRT Wheel Profile

#### 3.4.1.1. Modeling AALRT Wheel Profile

In order to optimize the wheel profile of AALRT wheel profile its shape and wheel rail contact has to be modeled and studied carefully. Addis Ababa Light Rail Transit uses a standard rail profile UIC 60 and rarely used wheel profile with nominal diameter of 660 mm. the figure below shows all the dimensions of AALRT.

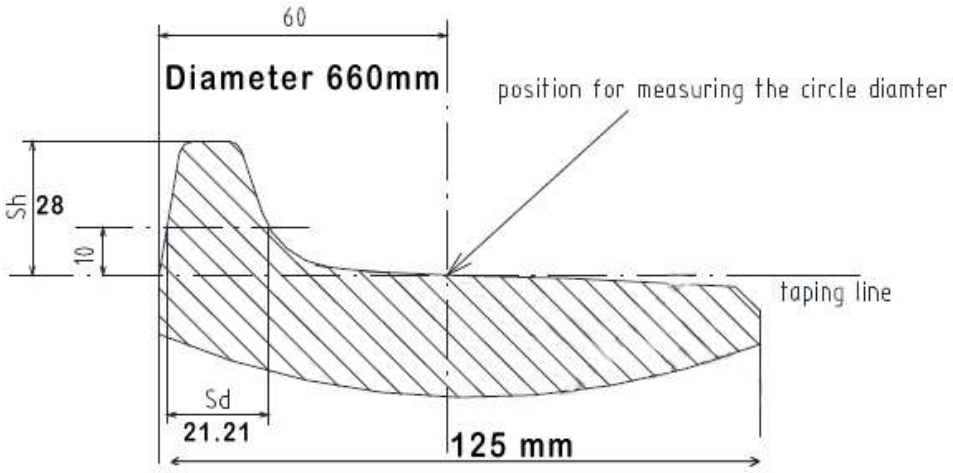


Figure 3.7 Dimensions of AALRT wheel profile (Source: AALRT Kality depot)

Modeling of AAALRT wheel profile is done starting from measuring profile gage and tracing its internal wheel profile shape on A4 paper to get real shape of the profile.


Figure 3.8 AALRT wheel profile Gage (Source: AALRT Kality depot)

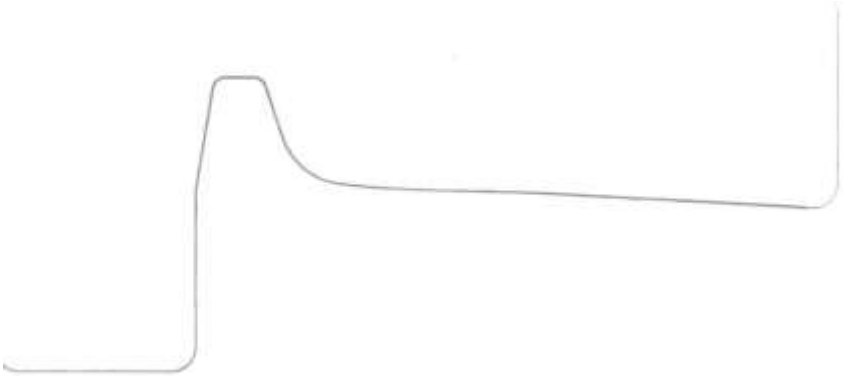

Figure 3.9 Trace of AALRT wheel profile on A4 paper

The traced shape of AALRT wheel profile image is converted to graph using **Image2Graph** Computer application.

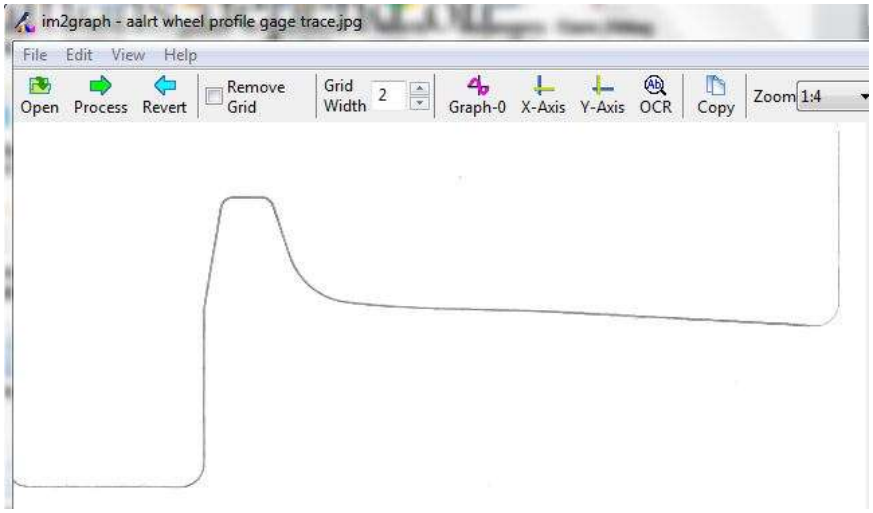


Figure 3.10 traced AALRT wheel profile imported to Image2Graph app

The traced image exported from Image2Graph application to excel file in the form of Cartesian coordinate system. See fig below

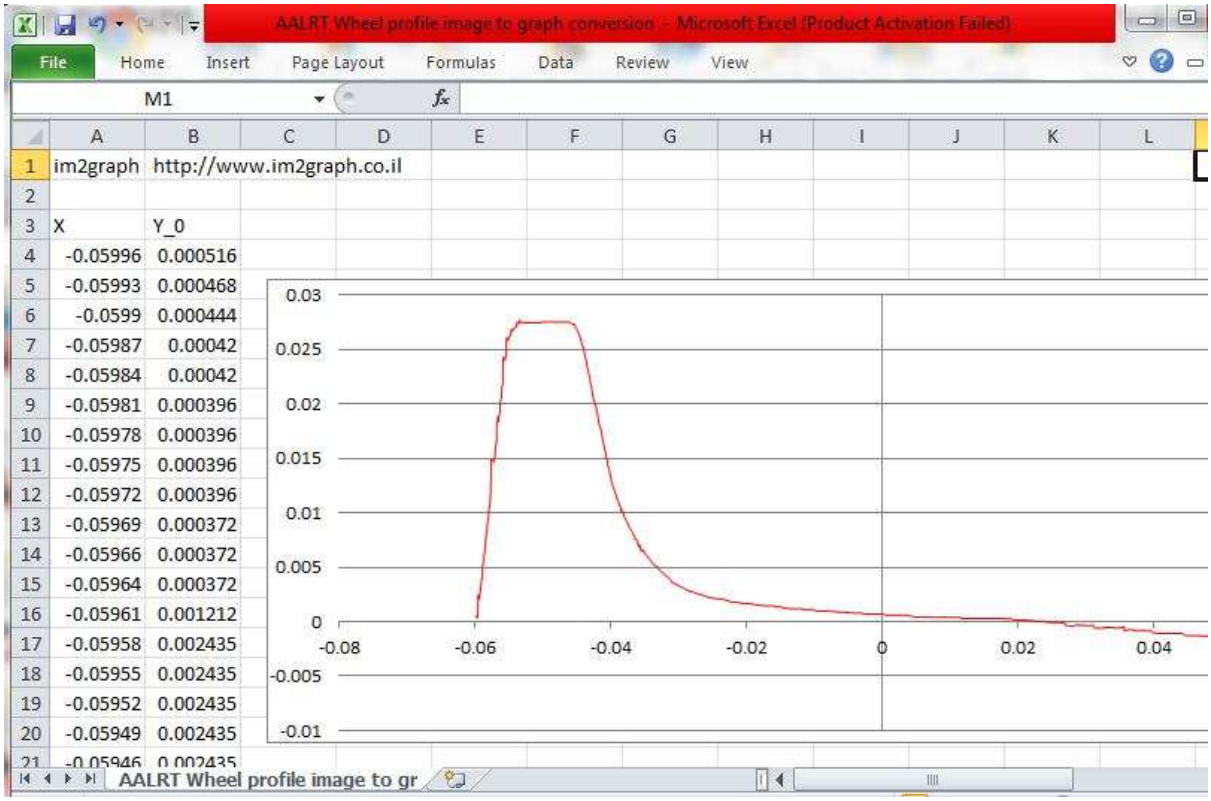


Figure 3.11 wheel profile excel file exported from image2graph application.

In order to see the real wheel rail contact condition the wheel profile is modeled to SIMPACK software. The Method of modeling wheel profile is presented in figures below.

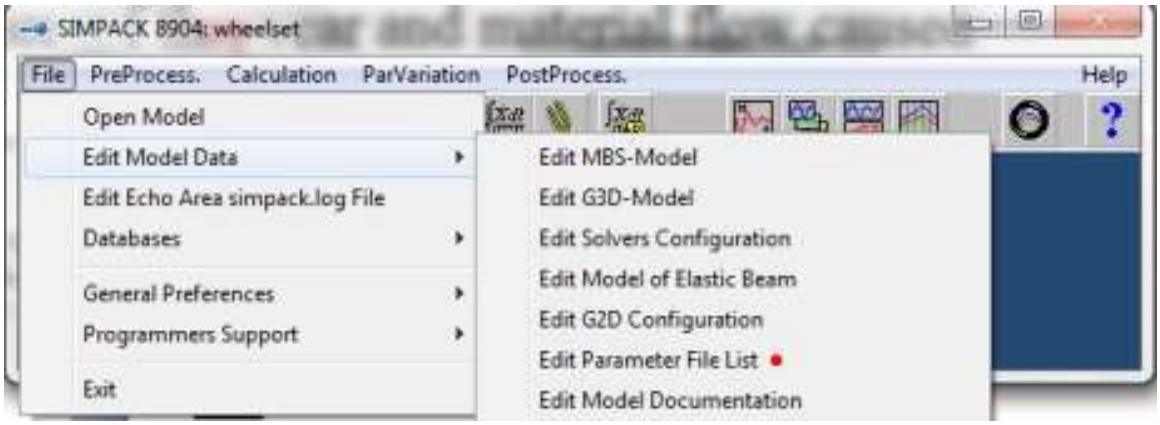


Figure 3.12 SIMPACK software to edit Model (Model in this case is the wheel) data.

Using the coordinate values exported from image2graph wheel profile data is edited.

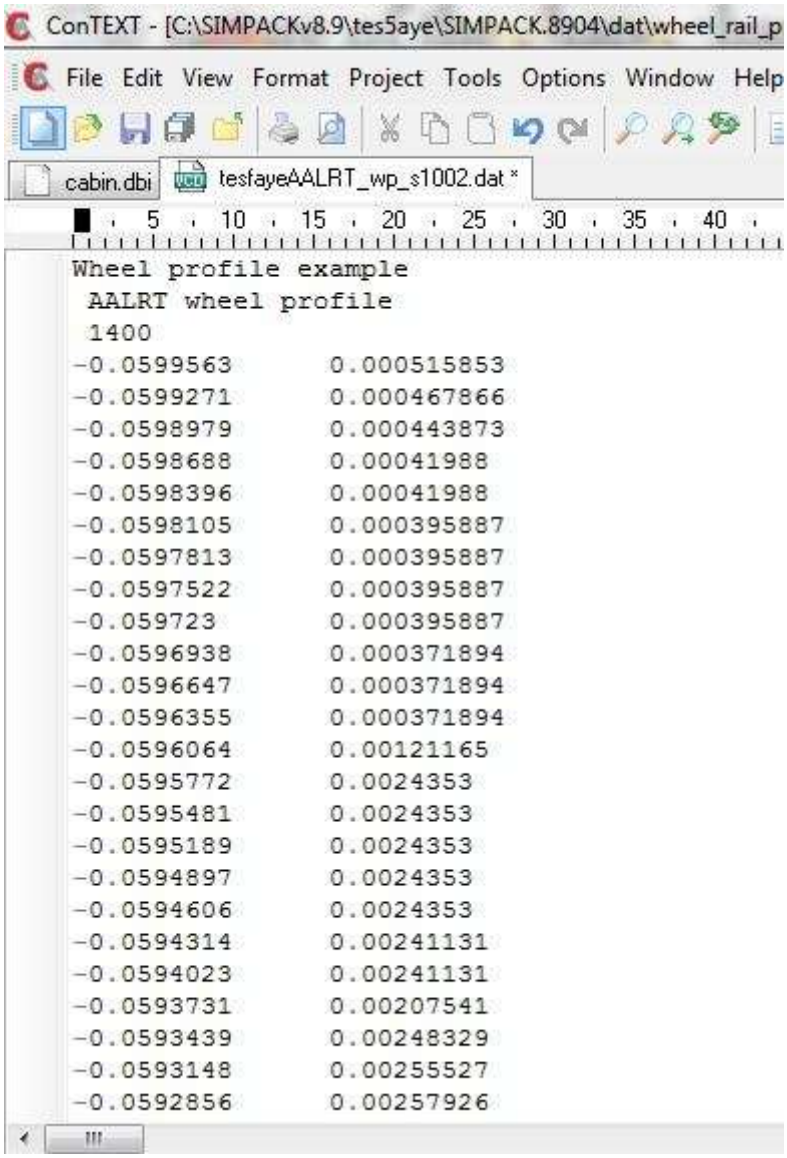


Figure 3.13 Edited AALRT Wheel profile in SIMPACK software data modeler

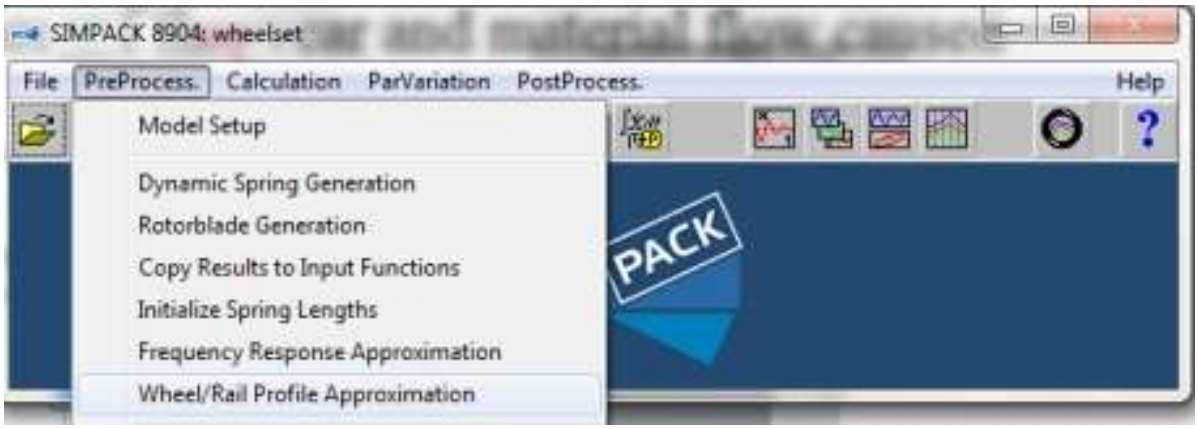


Figure 3.14 Wheel/Rail profile approximation

The Cartesian coordinates of AALRT wheel profile is saved to SIMPACK file database with the format that SIMPACK software can read (.dat) file. Then Using Wheel rail profile approximation tool (as shown by the fig above) the profile is approximated by multiple node approximation with optimum value. Finally approximated wheel profile is saved to wheel profile file (.wp) to SIMPACK database.

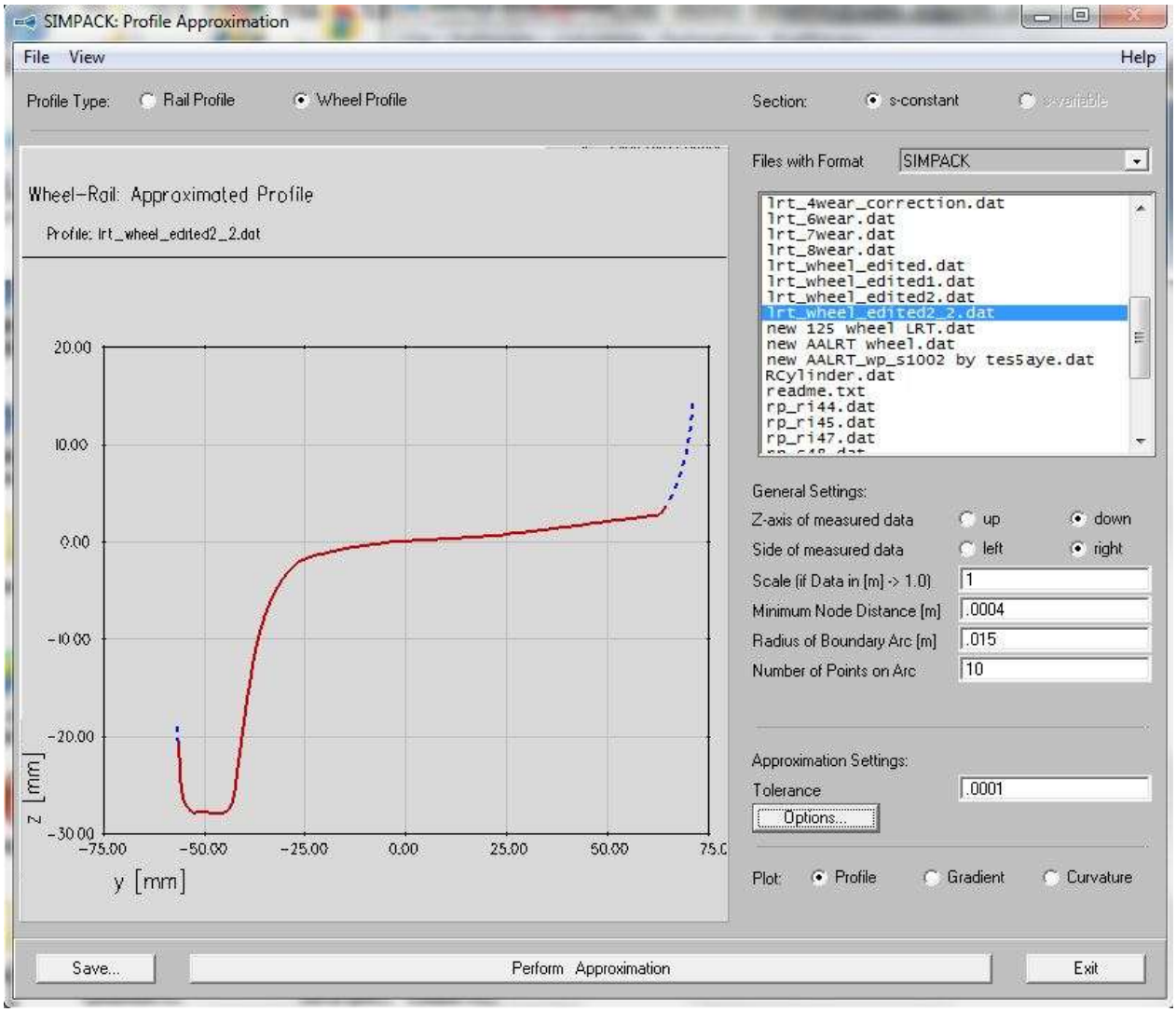


Figure 3.15 wheel profile Approximation using SIMPACK software

Then SIMPACK will generate the wheel profile as shown below. Wheel rail global values can be edited with required inputs. For AALRT the generated inputs of wheel profile with radius of 0.33m, track gauge 1.435m, rail cant 1:40, UIC60 rail profile and One point contact are considered. Generated Wheel model and wheel rail global values are shown in the figure below.

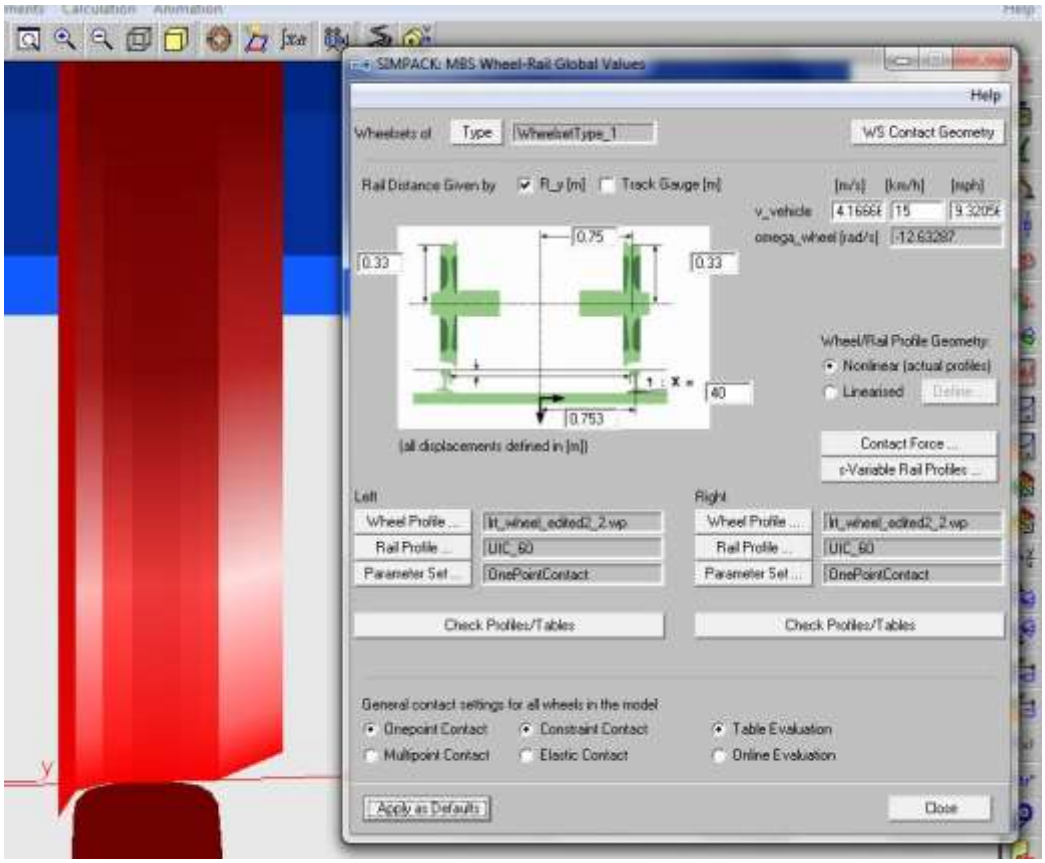


Figure 3.16 Modeled wheel and wheel/rail global values used for AALRT

Then SIMPACK can show the real wheel rail contact geometry from used UIC60 rail and AALRT wheel profile.

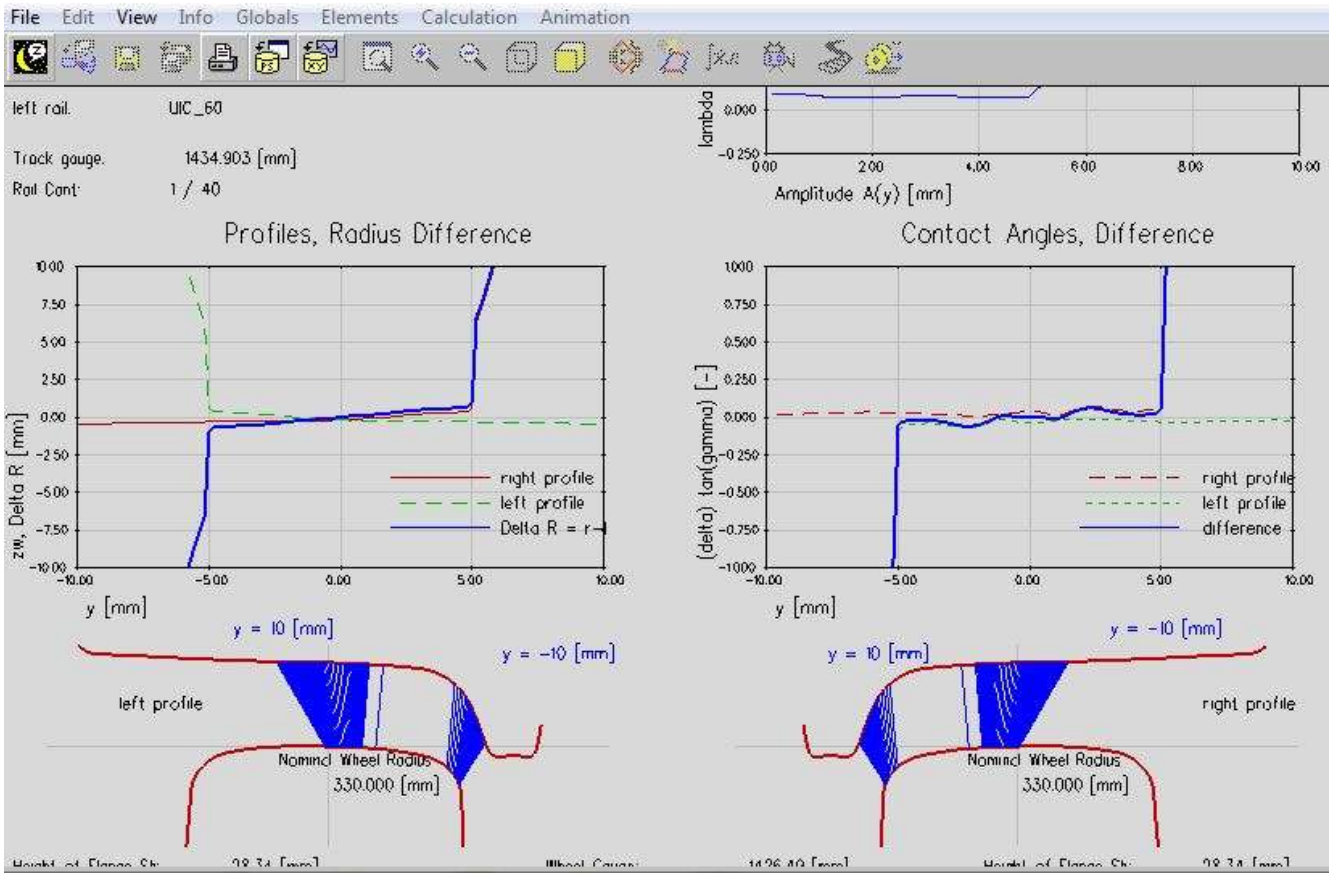


Figure 3.17 Generated wheel rail contact and profiles rolling radius difference (RRD)

For worn profiles similar method is used to see their wheel rail contact.

### 3.4.1.2. Worn profile of Addis Ababa LRT

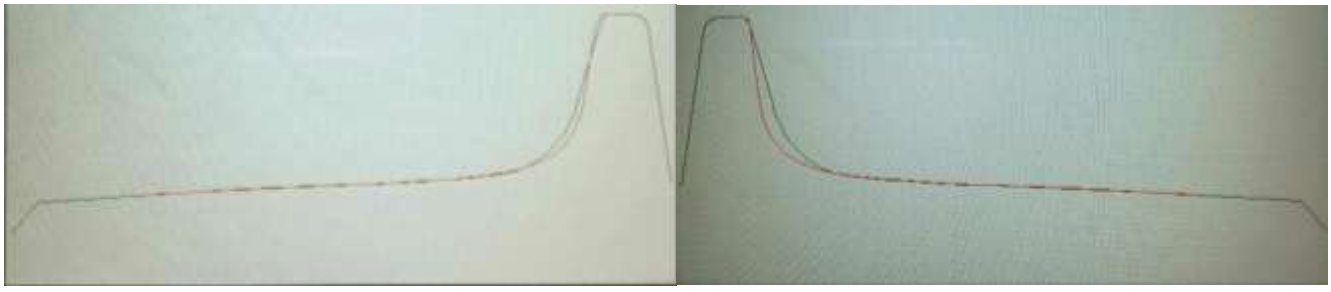

a.

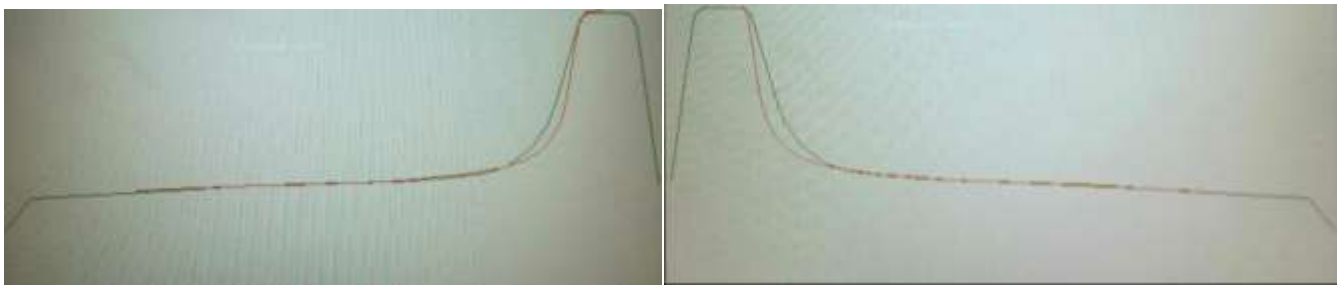

b.

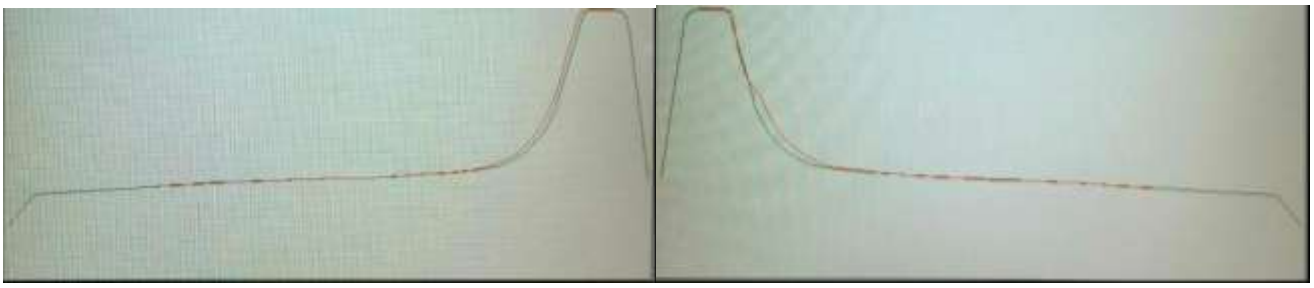

c.

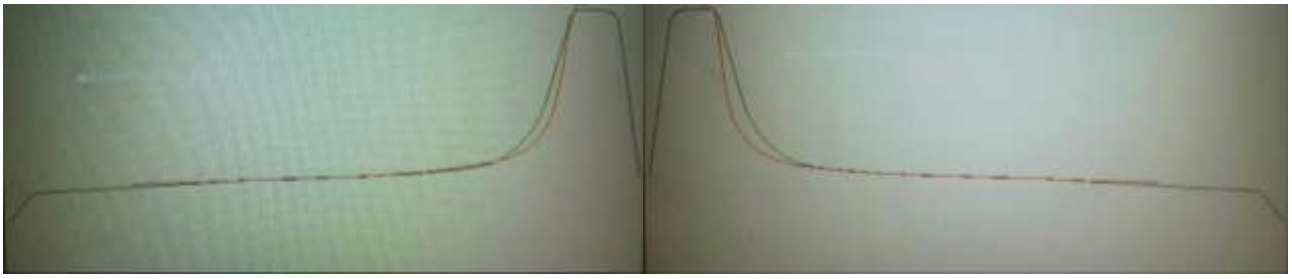

d.

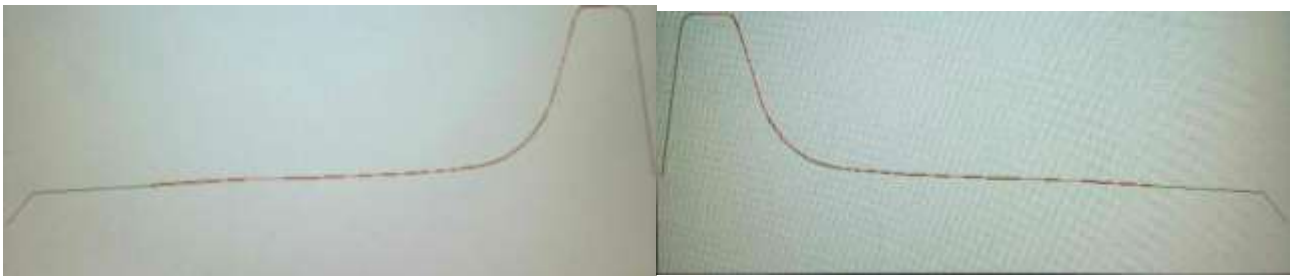

e.

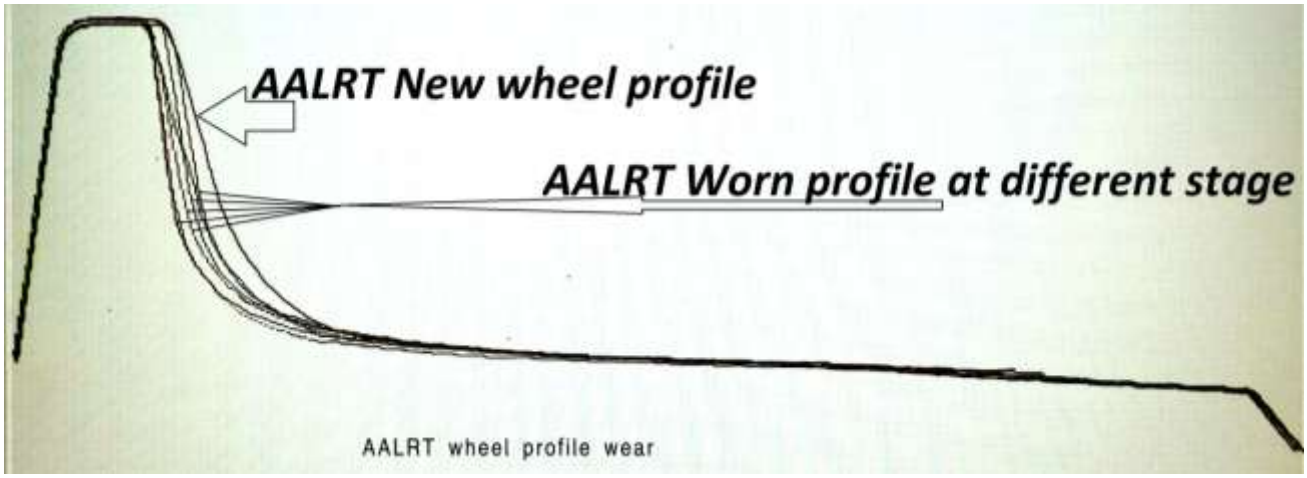


f.

Figure 3.18 a-f worn and new AALRT wheel profile measured by under flour Lath Machine

## 3.4.2. Overview of wheel/rail contact types

### 3.4.2.1. Types of wheel and rail profiles

At the present time, railways commonly use curvilinear wheel profiles as the standard wheel profile. However, until several decades ago, a conical wheel profile was widely used. Since Safety requirements are the same for different wheel profiles, which leads to the same flange shape.

The AALRT Wheel profile is derived from the S1002 profile; therefore, the S1002 profile is present in this study. For the analyses of geometric contact properties, the contact situation between the wheels and rails for various lateral displacements of the wheelset are considered. So S1002wheel profile is used for comparison, since it is standard wheel profile that many railway companies used. And Addis Ababa Light Rail Transit uses a rail UIC60 with inclination of 1:40.

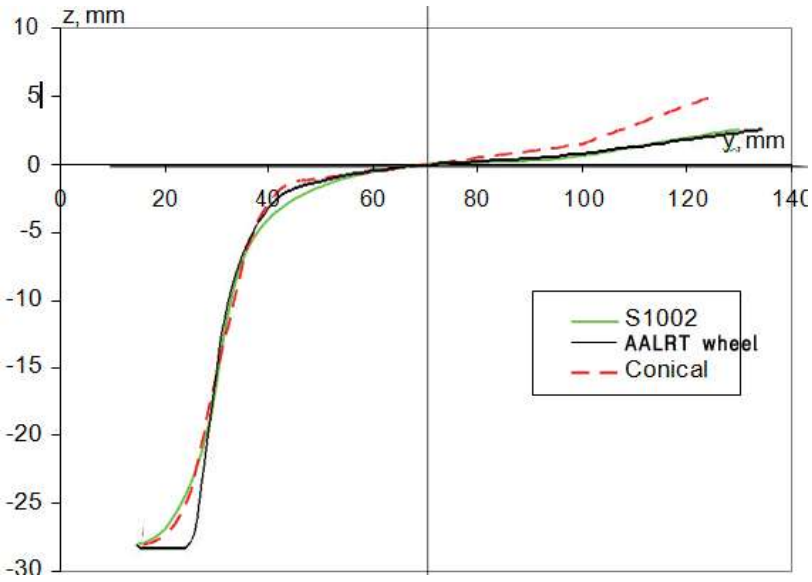


Figure 3.19 S1002, AALRT wheel and Conical wheel profiles.

After the geometry of wheel and rail profiles is known, the properties of geometric wheel/rail contact are studied. The rail gauge is 1435 mm, measured at 14 mm below the track top, the wheel radius is 330 mm, and the wheelset inner gauge is 1380 mm. Wheelset inner gauge and track gauge are taken as constants.

Wheel profiles can differ on many parameters, depending on the requirements imposed by the rolling stock on which they are used. For example, tram wheels usually have shorter flange height, thinner flange width, and shorter wheel tread.

While the number of standard wheel profiles is limited to one or two profiles per Railway Company or network, the number of the standard rail profiles is usually larger. This is a consequence of the use of rails of different weight per meter for the different types of lines.

The sizes of the rail heads differ in accordance with the weight of the rails and consequently rail profiles are different. Also, inclination of the rails plays a significant role in the actual shape of the rail profile.

### 3.4.2.2. Types of wheel/rail contact

As shown in Figure 3.20, in the general case for unworn wheel and rail profiles, four types of wheel/rail contact can take place:

1. wheel tread–rail head contact: occurs mainly on straight track and in large radius curves
2. wheel flange root–rail gauge corner: occurs in curves
3. Wheel flange–rail gauge corner: (flange contact) occurs only in sharp curves, or when the wheel attempts to roll over the rail head.
4. wheel field part of the tread–rail field side: occurs when the wheelset is shifting toward the one side of the track rail, introducing flange root or flange contact of the wheel on the other side, simultaneously the wheel on the opposite side will experience contact on the field side of the tread

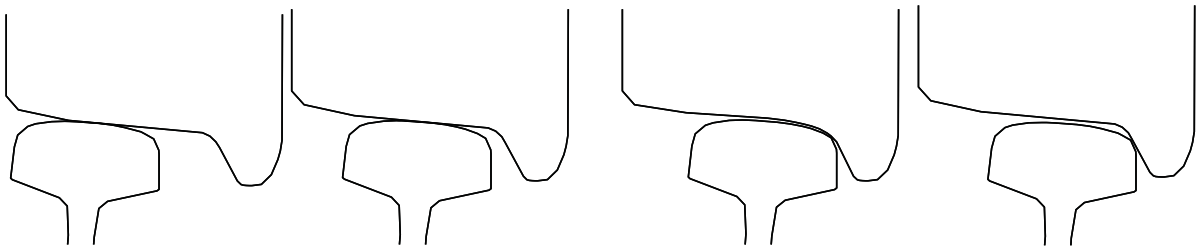

Field tread side-rail head (4) tread–rail head (1) flange root-gauge corner (2) flange-gauge corner (3)

Figure 3.20 Types of contact between wheel and rail profiles.

One or two contact points can exist between wheel and rail along with conformal contact. Let us consider contact between wheel flange root and rail gauge corner, as shown in Figure 3.21. If the wheel flange root radius is larger than the gauge corner radius of the rail, then single point contact between wheel and rail will occur. If the radii of the circular arcs of the flange root and the gauge corner are identical, then conformal flange root–gauge corner contact can occur. In the case where wheel flange root radius is smaller than rail gauge root radius, double point contact will occur. In general, the same is valid for the wheel tread and rail head curvatures, i.e., to achieve a single point contact between wheel tread and rail head, the curvature of the rail head must be larger than the curvature of the wheel tread.

Single-point, double-point, and conformal types of wheel/rail contact have significant influence on rolling contact behavior. Depending on the targets and requirements in wheel and rail profile design, one or another type of contact can be either desirable or unwanted.

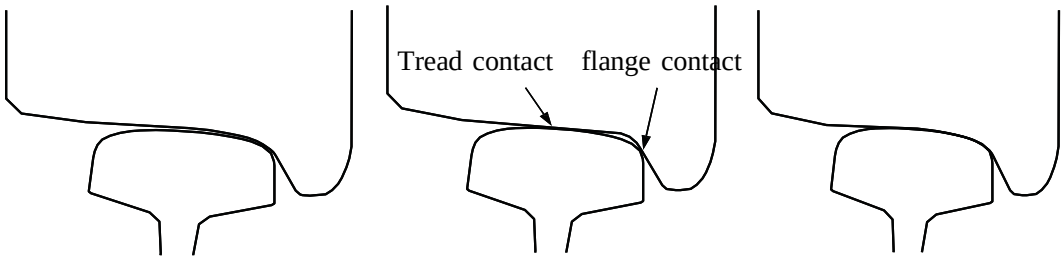


Figure 3.21 One and two point contact between wheel flange root and rail gauge corner.

### 3.4.3. Properties of geometric wheel/rail contact

Analysis of geometric wheel/rail contact can provide researchers with a number of parameters describing wheel/rail interface. In the present section, focus is made on the rolling radii difference function, and its relation with wheel and rail profiles.

#### 3.4.3.1. Three main parts of RRD function and their relation to wheel/rail contact

Wheel and rail contact can be roughly divided into three parts corresponding to track curvature:

1. Straight track: Contact occurs between the central region of the rail head and wheel tread for both sides

2. Large radius curves: Contact occurs between tread and flange root parts of the wheel and gauge side of the rail head. Wheel flange contact is rare. On the opposite side of the track, contact is moving to the field side of the wheel and rail

3. Small radius curves: Contact occurs between the wheel flange root and flange, and the gauge corner of the rail. On the opposite side of the track, the field side of the wheel contacts with the field side of the rail.

**Contact point distribution**

The contact point distribution of good wheel rail contact is expected to be uniformly distributed The contact point is limited to the regions highlighted in figure shown below.

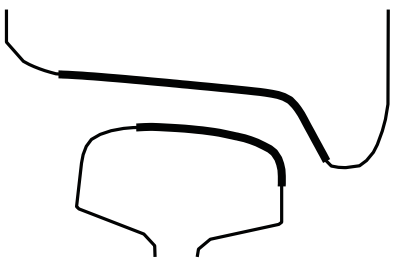

Figure 3.22: Potential contact on wheel and rail.

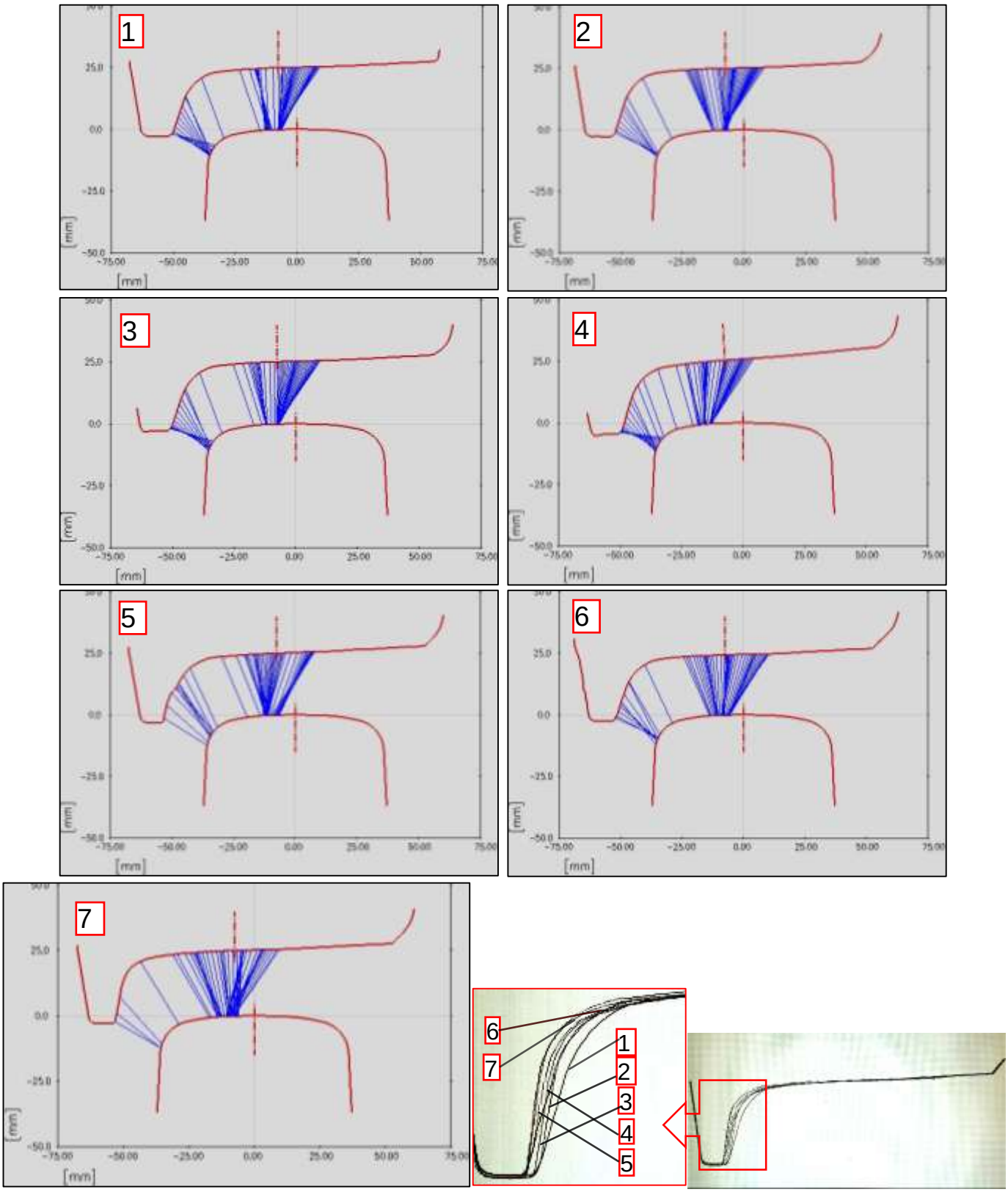


Figure 3.22 Wheel rail contact points for unworn wheel profile and different wear steps of AALRT wheel profile

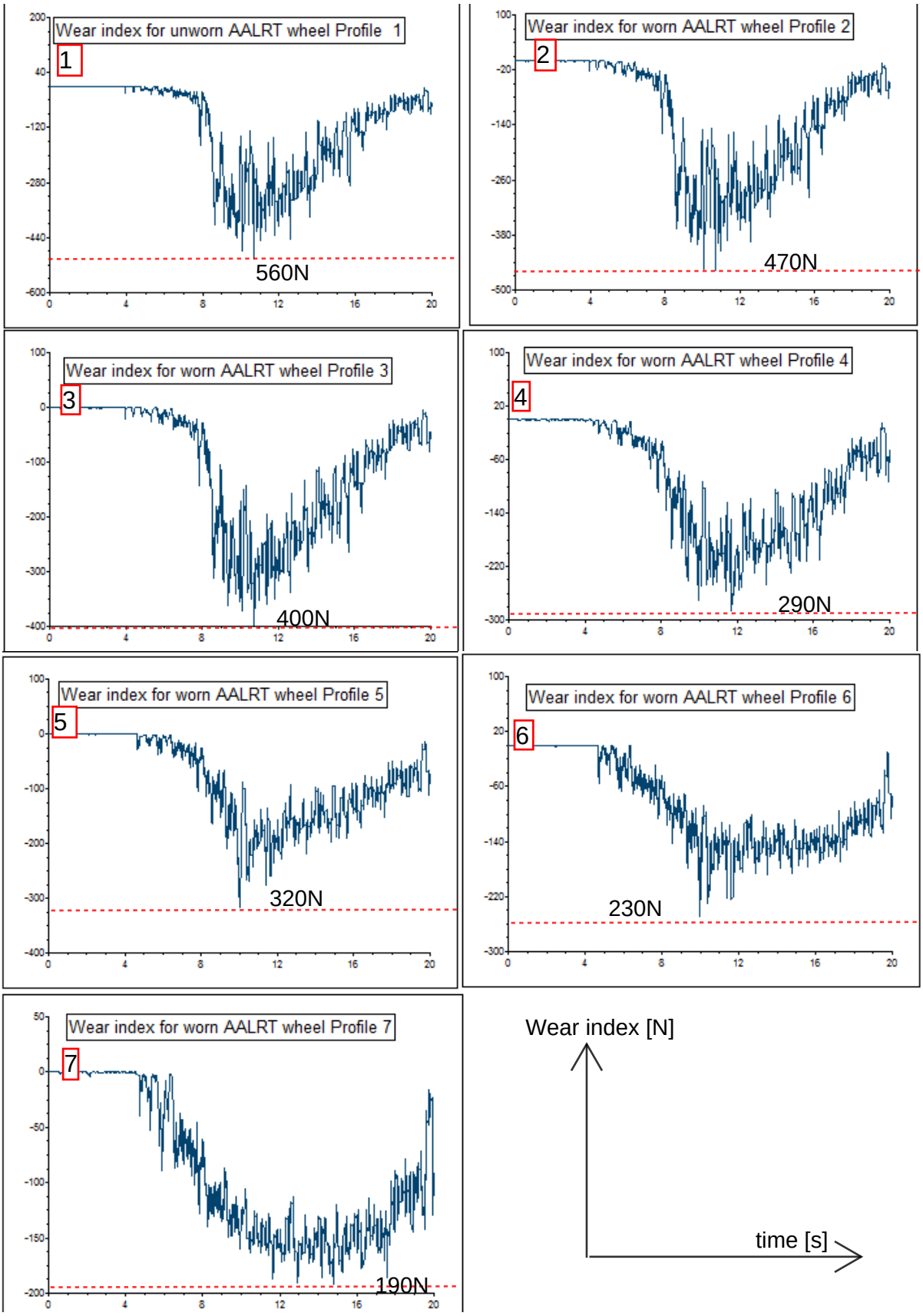


Figure 3.23 Wear index of unworn and different worn AALRT wheel profile (SIMPACK result: tested on 500m long, 150m radius curve track with a speed of 60Km/h)

Figure 3.22 Wheel rail distribution of unworn wheel profile shows wheel flange and rail gauge contact at sharp curves and wheel thread and rail head contact for straight track. Then for worn wheels wheel rail contact distribution lines get better for second, third and fourth worn steps then flange contact lines decreased for fifth and next wear steps.

Wear index result from SIMPACK software, modeled AALRT vehicle tested on 500m long, 150m radius curve track with a speed of 60Km/h for 20 seconds, showed in figure 3.23. Wear index value for unworn wheel profile is 560N and wear index for worn wheel profiles get decrease step by step.

To select optimum target profile, a wheel rail combination with better wheel rail contact distribution and minimum wear index as possible is selected from new and worn profiles in figure 3.22 and figure 3.23.

Wheel rail contact distribution is better on number 4 worn wheel profile as shown above figure 3.22. Minimum wear index is shown with number 6th and $7^{th}$ worn wheel profiles but even if their contact is good on straight track, its contact on sharp curves is poor.

So for optimization of RRD function average wheel profile is selected from measured worn wheel profiles that has better wheel rail contact distribution and lesser wear index when compared to new wheel profile.

But to get better wheel rail contact, in addition to selecting a profile from worn profiles of AALRT, contact points of unworn wheel profile is studied by comparing with mostly used standard S1002 wheel profile.

To illustrate this, the wheel/rail contact points of a new (unworn) wheel profile S1002 with an unworn UIC54 rail inclined 1:40 and new AALRT Wheel profile with unworn UIC60 rail inclined 1:40 are shown in Figure 3.24. In this figure the lines between the wheel and rail profiles connect the corresponding contact points, which were calculated for each 5 mm and 10 mm of lateral wheelset displacement respectively. Lateral wheelset displacements are shown above the wheel profile. The coordinate system in this figure is the wheelset coordinate system $y_w$ $O_{zw}$ with the origin in the center of the wheelset in neutral position. It should be noted that in this figure the wheel is shifted 10 mm vertically. Please, pay attention, that z - values are plotted with negative value to show graphs in convenient perception.

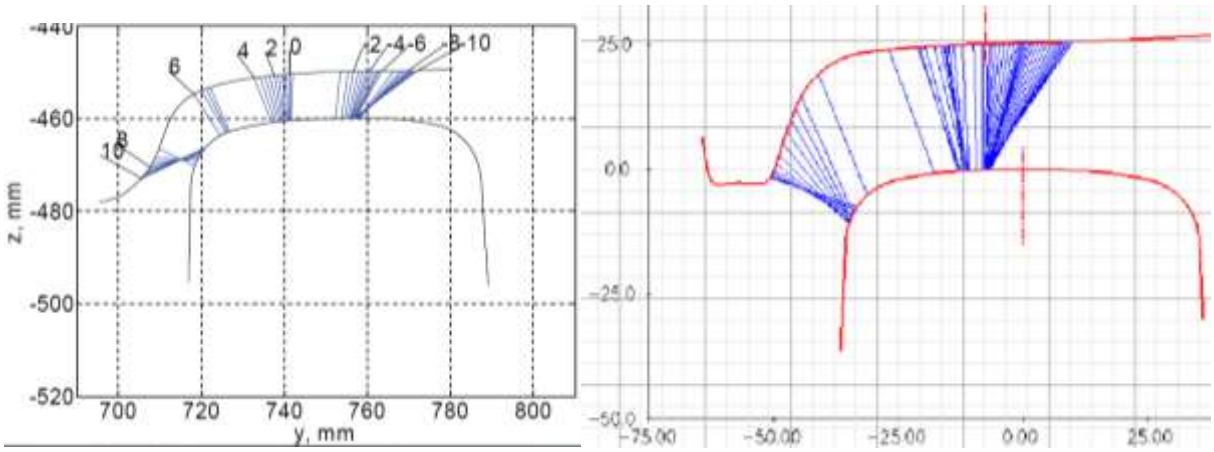


Figure 3.24Contact points of S1002 wheel on UIC54 (1:40) rail and AALRT Wheel on UIC60 rail.

The rolling radii difference versus lateral displacement of the wheelset for S1002 wheel and UIC54 rail profiles, and AALRT Wheel and UIC 60 rail profile is shown in Figure 3.25.

By comparing Figure 3.24 and Figure 3.25, one can find direct correlation between a discontinuity (a jump) in the position of the contact point between wheel and rail after 6, 4, and -0.5 mm of lateral displacement (for s1002) and discontinuity (a jump) in the position of the contact point between wheel and rail after 5.5,3, and -1 mm of lateral displacement(for AALRT wheel) see Figure 3.24. These discontinuities can be found directly in the rolling radii difference function.

In S1002 wheel rail profile connection, For 4 mm of lateral displacement, one can see a sharp increase in RRD, and for 6 mm of lateral displacement, the increase in RRD is even sharper. For the jump of contact point after -0.5 mm of lateral displacement, the changes in the RRD function are less visible, due to smaller changes; however, one can find variation in the tangent to the RRD function around ± 0.5 mm of lateral displacement.

In AALRT wheel rail profile connection, from -1 of lateral displacement, one can see sharp increase in RRD function and for 5.5 mm of lateral displacement, the increase in RRD even get sharper.

The wheel/rail combination S1002-UIC54 clearly indicates four areas of the contact. Starting from the field side, one can see contact between wheel tread and rail head top part. Such contact occurs when the wheelset is moving toward the opposite rail. Next, contact between wheel tread (closer to the flange root side) and the rail central region occurs for 0-4 mm of lateral displacement.

But Wheel/Rail combination AALRT Wheel-UIC60 clearly indicates three areas of contact. Wheel tread and rail head top part when the wheel set moves to opposite rail. Contact between wheel tread (closer to the flange root side) and the rail central region occurs for 0-5.5 mm of lateral displacement.

This typically corresponds to the motion of a wheelset on a straight track, and in large radius curves (in this particular case curves larger than R=500 m, see Table 3.1 for r=0.330 m). Further, in wheel/rail combination S1002-UIC54 for 4.5–6 mm of lateral displacement, contact occurs between the wheel flange root and the rail gauge corner parts, and in AALRT Wheel-UIC60 wheel rail combination only one contact occurs between the wheel flange root and the rail gauge corner parts corresponding to wheel/rail contact in smaller radius curves (smaller than R=500 m). Finally, for displacements larger than 5 mm, contact between wheel flange and rail gauge occurs for both wheel rail combinations.

The RRD function can provide significant information about wheel/rail contact properties. Undoubtedly, its shape and behavior are dependent on wheel radius, track and wheelset inner gauges and, of course, on wheel and rail shapes.

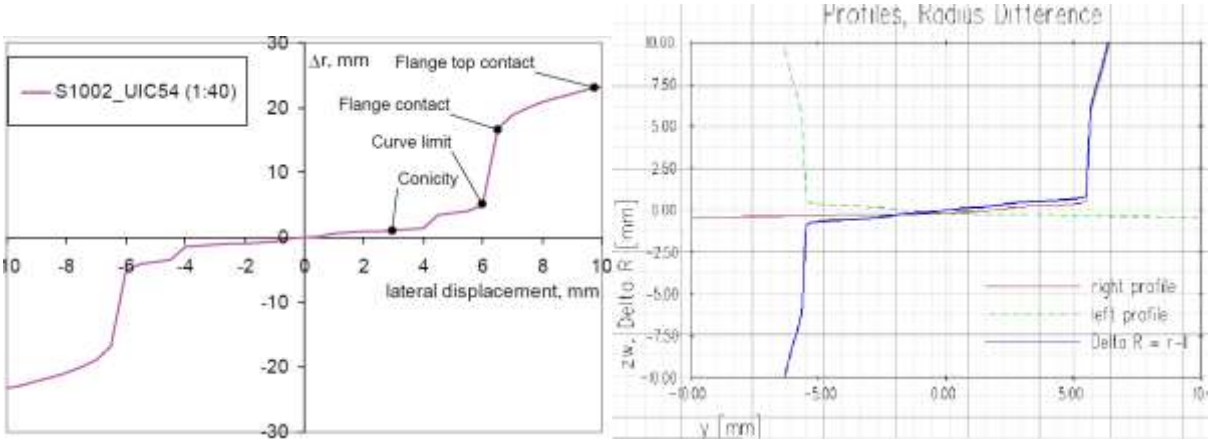


Figure 3.25 RRD function of S1002 wheel on UIC54 (1:40) rail and AALRT Wheel on UIC60 (1:40).

### 3.4.3.2. Dependence of RRD function properties on wheel profile

Let us consider geometric contact of AALRT wheel and S1002 wheel profiles (see Figure 3.26) with UIC60 (1:40).

The wheel/rail contact points for the AALRT wheel profile and S1002 wheel profile with the UIC60 rail, are shown in Figure 3.26a and Figure 3.26b.

Contact behaviour of wheel rail combination AALRT wheel profile/UIC60, Wheel tread–top rail contact exists up to 5 mm of wheelset lateral displacement. After 5 mm of lateral

displacement, the contact point jumps to the wheel flange–rail gauge corner. This indicates during curve negotiation it produces conformal contact, rather than double point contact. Both double point and conformal contact situations can produce a high wear rate. Situation between wheel tread–rail head and wheel flange–rail gauge corner is typical for AALRT wheel profiles. By comparing Figure 3.26a and Figure 3.26b corresponding to AALRT wheel profile and the S1002 wheel profile, one can observe on AALRT wheel rail contact there is a discontinuity (a jump).

But the wheel/rail combination S1002/UIC60 has more uniformly distributed contact points on a straight track and in curves. This wheel/rail combination produces a single contact point between flange root–rail gauge corner. As a result, the wear rate of the S1002 wheels on the UIC60 rails is much lower.

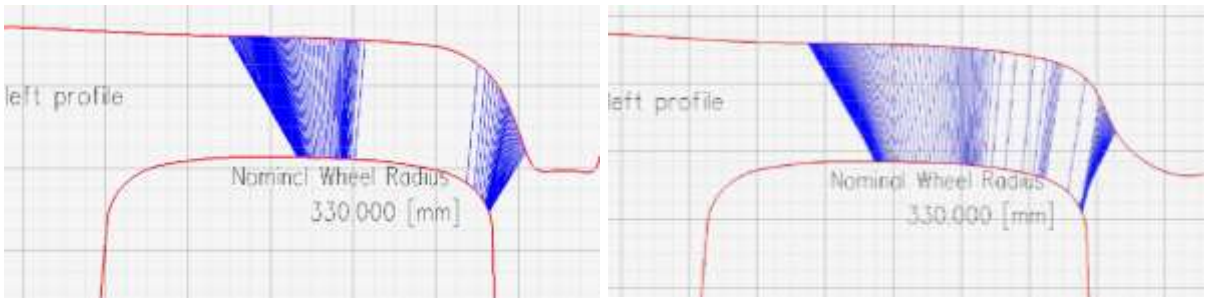


(a) (b)

Figure 3.26 (a) Contact points of AALRT wheel on UIC60 rail and (b) Contact points of S1002 wheel on UIC60 (1:40) rail.

As was mentioned earlier, rolling radius difference plays an important role in vehicle dynamics and is therefore investigated next.

The RRD functions of AALRT and S1002 wheel profiles on UIC60 rail are shown in Figure 3.27.This figure reveals that S1002/UIC60 wheel/rail combination has much higher inclination of RRD function compared to the AALRT wheel profile /UIC60 combination which means that the corresponding equivalent conicity is higher for the S1002/UIC60 than for the AALRT/UIC60 rail.

The higher conicity allows a vehicle to pass curves at the required RRD. However, due to stiff primary suspension, a hunting problem does not occur with the S1002/UIC60 wheel/rail profile combination at the operational speed.

As can be seen from Figure 3.27, both wheel and rail profiles define the shape of the RRD function. They are responsible for the absence or presence of the jumps of contact points and

consequently for the absence or presence of sharp bends in the corresponding RRD function. Also wheel and rail profiles define tangent (or equivalent conicity) of the RRD function.

For non-linear wheel profiles, conicity can be influenced by other parameters. These other parameters, namely wheel radius, track gauge, and wheelset inner gauge, define the distortion of the RRD function.

- Decrease or increase in wheel radius is responsible for corresponding stretching or shrinking of the RRD function in the vertical direction.
- Increase in track gauge (and/or decrease of wheelset inner gauge) leads to stretching of the RRD function in the lateral direction. And vice versa,
- Decrease of the track gauge (and/or increase of the wheelset inner gauge) leads to shrinking of the RRD function in the lateral direction

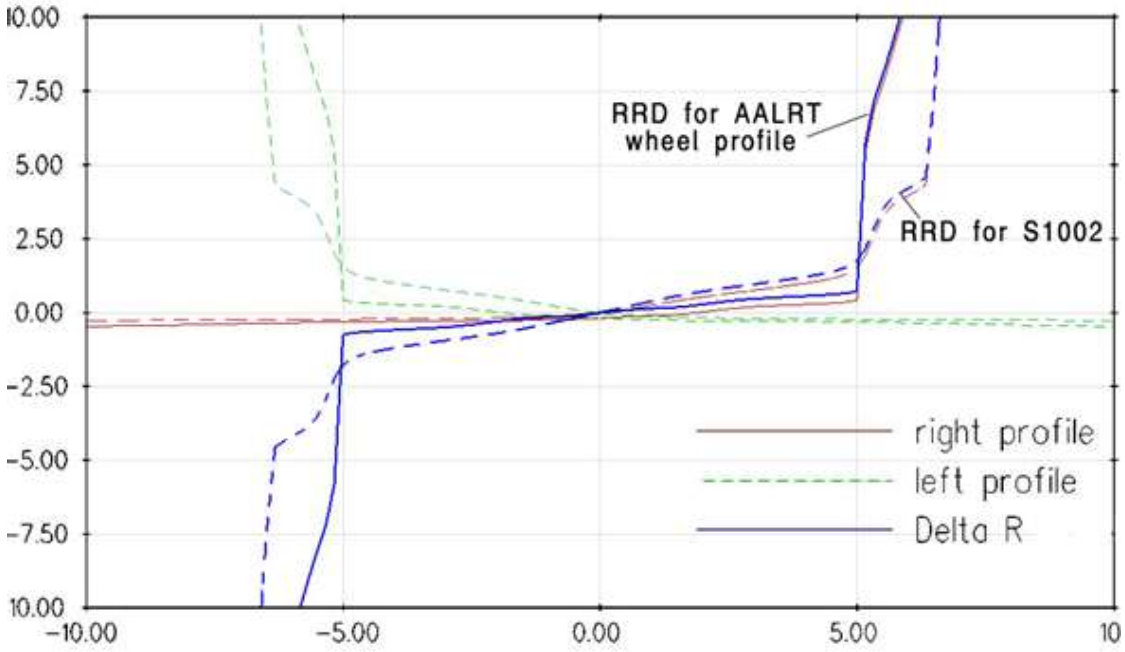


Figure 3.27 RRD functions of AALRT wheel and S1002wheels on UIC60 (1:40) rail.

From analysis of the RRD function, one can obtain important information about wheel/rail contact.

## 3.4.4. Wheel profile optimization

### 3.4.4.1. Applied limits

During profile design, a number of limits (or constraints) can be applied on a designed wheel profile. Two safety requirements are considered in this case.

The first is the requirement for wheel flange thickness, which is checked after optimization. The second is the requirement to avoid derailment of the vehicle, which is achieved through

restriction of the minimum flange angle. This requirement is checked for the optimized profile as well.

The unworn wheel flange width should be at least 16 mm for AALRT tram wheels. The wheel flange angle should be between 65 and 70 degrees for the considered trams.

Constraints on angles between the adjacent parts of a profile are introduced to avoid zigzags of wheel profile, and thus to exclude unrealistic wheel designs during optimization. Moving points are numbered from 1 to $N$, starting from the low left side to the upper right side of the profile (see Figure 3.29). Constraints for point number $i$ are written as

$$F_j \equiv 1 - \gamma_{i+1}/\gamma_i \geq 0, \quad j = 1, \ldots, k,$$

for the concave part of the profile. Accordingly for the convex part of the profile, these requirements read

$$F_j \equiv 1 - \gamma_i/\gamma_{i+1} \geq 0, \quad j = k+1, \ldots, N+1$$

$\gamma_i$ is the angle between the y-axis of wheelset and straight line connecting points i and i+l of the wheel profile.

### 3.4.4.2. Design of Limiting (Target) RRD function

A target rolling radii difference function can be obtained in several ways:

- It can be a modification of a RRD function for an existing wheel/rail profile combination, when a problem in wheel/rail contact can be clearly identified. (Shevtsov et al. [2004 ]).
- The designer can use the average RRD curve for worn wheels and rails; however, care must be taken on equivalent conicity to avoid the instability problem with the designed wheels. Shevtsov et al. [2003, 2005].
- The limiting RRD function can be built based on the RRD function of the successful wheel/rail profile combinations from a similar railway system can be used.

The target RRD function used for this paper is that, a profile with better wear index and contact distribution is identified from worn and unworn wheel profiles of AALRT listed in Figure 3.22 and figure 3.23 then by taking average RRD function with better contact, new limiting (Target) RRD function is built based on RRD function of wheel/rail profile combination (S1002 wheel profile) used in many railway systems.

The target RRD function is used in the optimization procedure for the design of a new light rail train wheel profile. The optimization of the wheel profile is performed for UIC60rail.

Two design cases are considered. In the first design of target RRD function, to improve

contact situation, not completely redesign wheel profile.it is decided to not apply many constraints on the shape of the function.

The S1002 wheel and UIC60 rail have good contact properties on the tread part of the wheel. However, the contact properties of AALRT flange contact are not as good for this wheel/rail combination. A big jump of contact point from the tread to the flange can be observed. A decision is made to use the S1002 profile as the starting profile in optimization, and to improve the flange contact of this profile because S1002 profile is standard wheel that has good combination with UIC60.

The modified RRD function of the S1002 wheel and UIC60 rail is used as a target function. As can be seen from Figure 3.28, from 0 to 5.0 mm of lateral displacement RRD function of the S1002/UIC60 combination is left without changes. After 5.0 mm to 6 mm of lateral displacement of the wheelset, target RRD function is smoothed to achieve smooth flange contact.

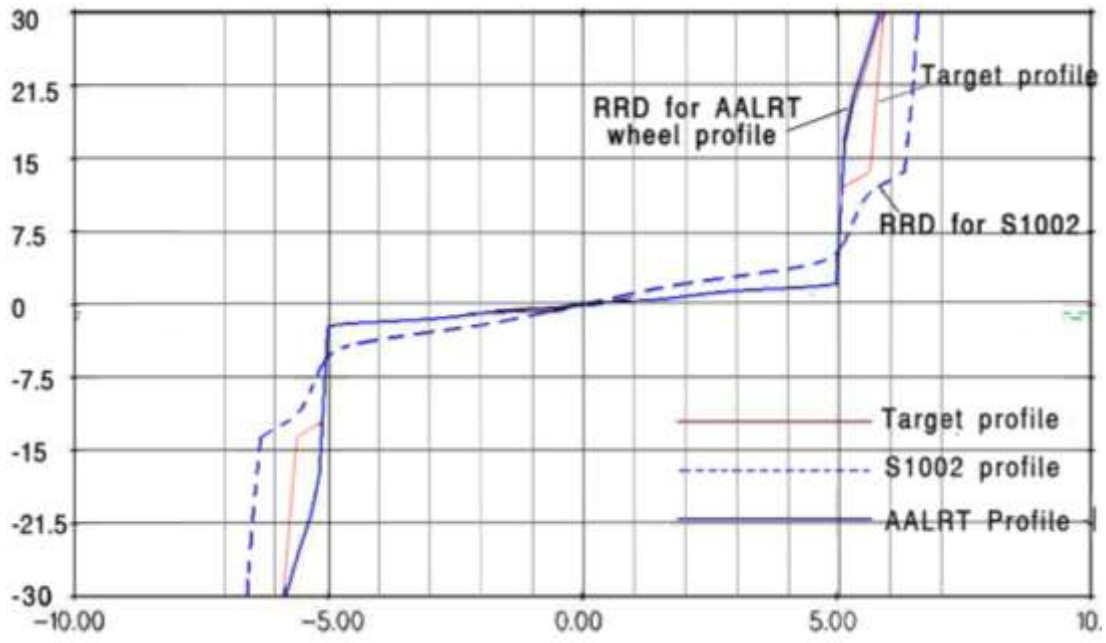


Figure 3.28 Generated RRD functions for the AALRT and S1002 wheel profiles on UIC60 rail and target RRD function

In this optimization problem, 21 mm flange height of tram wheels is used. Therefore, the RRD values should coincide for top flange contact of the wheels with the same flange height; see "Target" and "AALRT profile_UIC60" lines at 6 mm of lateral displacement.

The second design of the target RRD function, the target RRD function is designed based on

the procedure. Several additional requirements to the designed wheel profile are imposed. These requirements were added by observing problems of AALRT.

According to the standards, wheel flange width should be at least 16 mm, as in the AALRT wheel. The wheel flange angle should be between 65 and 70 degrees. The newly turned wheels have 70-degree flange angle, while the average angle of the worn AALRT wheel profiles is 65 degrees. Keeping the wheel flange angle within these limits guarantees safety against derailment.

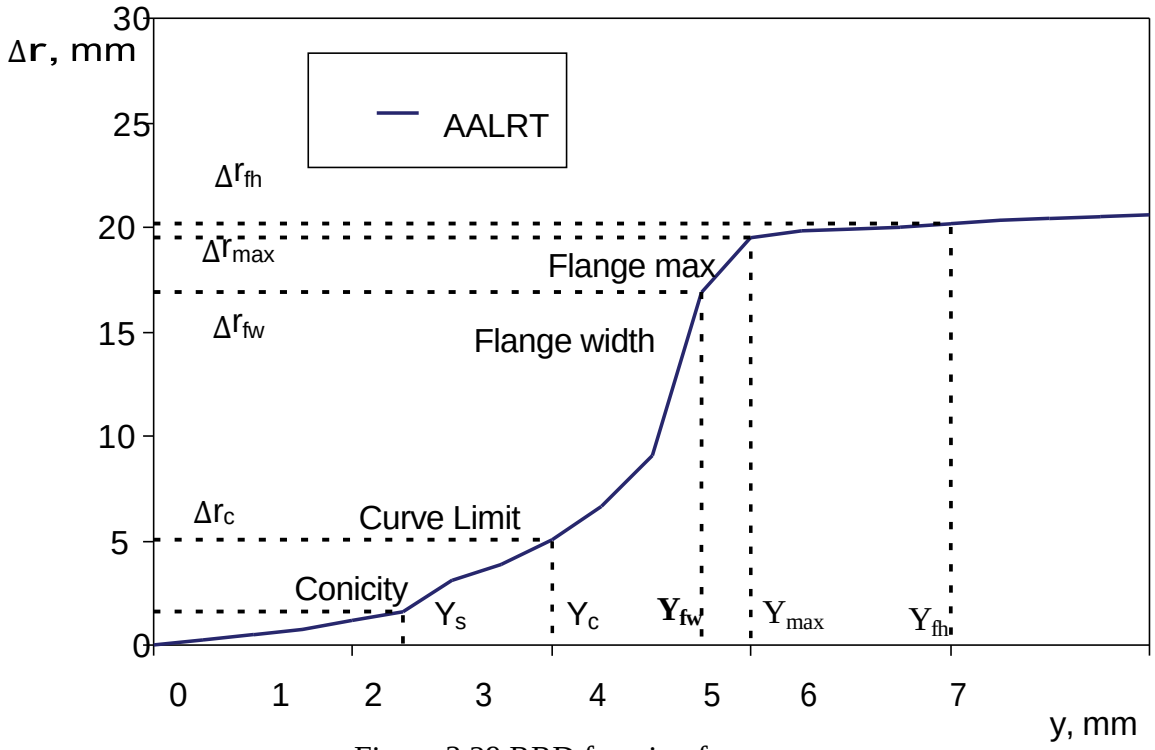


Figure 3.29 RRD function for tram system.

In fig 3.29 first point is Ys , corresponding to wheelset lateral displacement on a straight track. The next point is Yc , corresponding to the wheelset lateral displacement in curve. Between points Ys and Yc , RRD function must increase up to the maximum required (or available, if required RRD is too high) . For point $Y_{fw}$ , the value of wheelset lateral displacement corresponds to the wheel contact point where wheel flange width is measured. Maximum feasible wheelset lateral displacement is achieved at point $Y_{max}$ , above which the contact point moves to the top of the flange, and the wheelset can derail. Point $Y_{fh}$ corresponds to the area of top flange contact, which is easy to visualise for tram wheels due to the short wheel flange.

Using these five constraint points, $Y_s$ , $Y_c$ , $Y_{fw}$ , $Y_{max}$ and $Y_{fh}$ , with the corresponding Δr 's ,a designer can describe the shape of the desired RRD function. This five constraint points used in the description of RRD function $Y_s$ , $Y_{fw}$ and $Y_{max}$ , as well as (0,0), and the endpoint of RRD function, just skipping the $Y_c$ point. In this particular case, $Y_{fh}$ is not used, as top flange contact is reached at a wheelset lateral displacement far beyond our point of interest. Finaly Using cubic spline interpolation, one can obtain a new design of RRD function.

The Required RRD value of AALRT wheel profile is listed in Table 3.1(using equation 3.7) for AALRT maximum and minimum curves. Since RRD is dependence on Minimum Curve radius of track line. There for required minimum RRD is 0.099 (for large curve of 5000), 9.9 and *16.5* for minimum curves of 50m and 30m respectively.

In the optimization problem, the usual 21 mm flange height of the tram wheels is used and, as a result, the RRD values of designed wheels for top flange contact will be the same as, for example, "Target" and "AALRT_UIC60" lines at 6 mm of lateral displacement ( Figure 3.28).

Consequently, this is the first constraint on the target RRD function, point [$Y_{fh}$, $\Delta rfh$].

At the AALRT, a wheel flange width is measured at a level 10 mm below mean wheel circle. Let's name this point $F_w$ (Flange Width). The AALRT Wheel profile has the flange width of 21.21 mm. to obtain a profile with flange width equal to 21.21 mm, the corresponding point on the target RRD function must be at a certain point.

The AALRT profile has contact at point $F_w$ at a wheelset lateral displacement equal to 5 mm, and the corresponding RRD is equal to 21.21 mm. Therefore, during the design of the target RRD function (line "Target"), the point [$Y_{fw}$, $\Delta r_{fw}$] is placed at $Y_{fw}$ =5 mm and $\Delta r_{fw}$ =21.21mm. The "Target" and "AALRT wheel_UIC60" functions have a common point at 3.5 mm of lateral displacement (see Figure 3.28). This point serves to obtain the required wheel flange width, and is used as the second constraint of the target RRD function.

The new "AALRT Wheel profile" RRD function has four working areas corresponding to: tread contact, flange root contact, flange contact, and top of flange contact. (See Figure 3.28) The tread contact area is defined for 0– 2.5 mm of lateral displacement and corresponds to motion on a straight track. The flange root contact area starts from 2.5 mm to 5 mm. The RRD for that area rises from 1 mm to 13 mm, which satisfies the condition of passing curves with radius from 500 m up to 50 m, as shown in Table 3.1. The flange contact area starts after 5 mm, and continues until 6 mm of lateral displacement. The corresponding RRD rises from

13 mm up to 21 mm (top flange contact). The top of the flange contact area cannot be optimized; it is left without changes.

The target RRD function can be designed or smoother with the help of cubic spline approximation. But for this case optimization from S1002 profile is used.

After the design of target RRD function is defined, next the method of profile variation must be chosen. In this case, variation of the design points in Cartesian coordinates is chosen as the method for profile modification .This is done because only part of the profile will be varied during optimization.

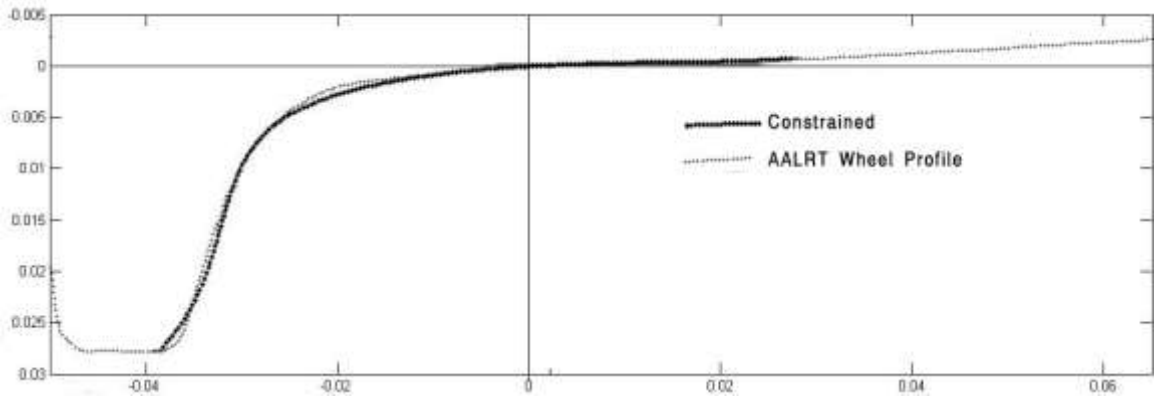


Figure 3.30 optimized wheel profile with moving and constrained points

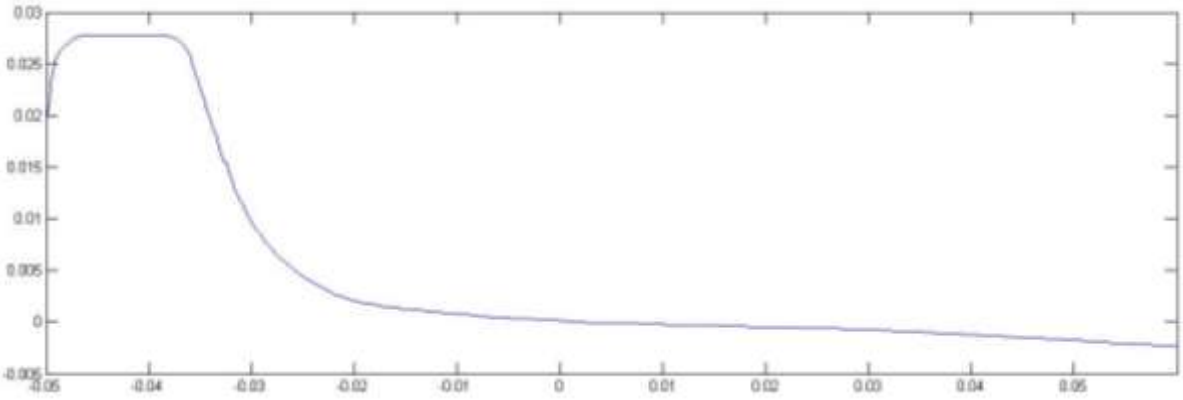

Figure 3.31 New optimized AALRT wheel profile (see x,y coordinates are in appendex Table 8)

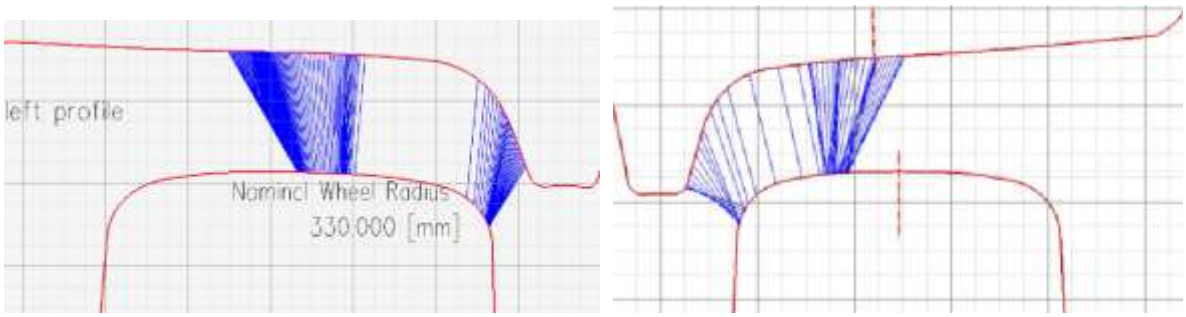


Figure 3.32 AALRT wheel profile and Optimized Wheel Profile Wheel Rail Contact (which has better wheel rail contact)

## 3.5. Wear law in rolling contact

Wear is the principal cause of rail replacement on almost all railways. But the analogous situation with wheels is different, in that they can be re-profiled by machining (turning) when worn. Re-profiling is undertaken either when the flange becomes too thin, or when tread wear has left the flange too high. Further, wheels are often machined when the profile has worn to a shape that causes the wheelset to have reduced steering ability.

In railway engineering practice, three main wear regimes for wheel/rail materials have been defined as a result of laboratory twin disc experiments (Bolton and Clayton [1984], Lewis et al. [2003]): mild, severe and catastrophic.

The regimes are described in terms of wear mechanism, as well as wear rate.

***Mild regime***: corrosive wear is most common and formed during absence of contact. Corrosive wear rate is very low under normal environmental conditions. However, some metallic wear can also be present. Mild wear is typical for the wheel tread and for the rail head contact.

***Severe wear*** occurs as slip and load in the contact are increased (to the levels experienced in a flange contact). Wear rate can increase tenfold comparing to mild regime. The wheel material wears out through a delamination process.

***Catastrophic regime*** as the contact conditions become more severe, these cracks alter direction from running parallel to the wear surface and turning up, to turning down into the material, causing larger chunks of material to break away. Lewis et al [2004].

- mild wear: $= 9.87 \cdot 10^{-14}$ $m^3/J$
- severe wear: $= 9.87 \cdot 10^{-13}$ $m^3/J = 10 \times$ mild wear

The actual values depend significantly upon the material hardness and other factors. The transition between mild and severe wear is said to be at 400 $W/mm^3$

Wheel wear is closely related to conditions of force and slip in the wheel/rail contact. Two basic types of wear models are described in the literature on wheel/rail interaction (Enblom and Berg [2005]):

1. Energy transfer models, which assume material loss to be a function of the energy dissipated in the contact patch.

2. Sliding models where material loss depends on combinations of sliding distance, normal force, and material hardness.

The wear of wheels and rails depends on the rate of dissipation of energy within the contact patch. It had been concluded that wheel wear rate could be related to the frictional energy expended through creepage in each wheel/rail contact.

This can be shown to be the sum of the products of the individual creep forces, and creepages in the longitudinal and lateral directions. In most cases, the contribution from the spin term is assumed to be small and is ignored. Wheel wear is estimated using the wear index W that reads:

$$W = Fx \cdot \xi + Fy \cdot \eta \qquad \text{Equation 9}$$

Where Fx is longitudinal creep force; $\xi$ is longitudinal creepage ; Fy is lateral creep force; and $\eta$ is lateral creepage.

In un-lubricated tests, McEwen and Harvey [1986] observe a mild wear regime (probably adhesive wear) if the wear number was less than 200N. A severe wear regime (probably delamination wear) was found for wear numbers greater than 400N. For wear numbers between 200N and 400N, either type of wear could occur.

## 3.6. Analysis of Addis Ababa Light Rail Train (AALRT)

### 3.6.1. AALRT Vehicle

Carboy mainly consists of 2 Mc and 1 Tp modules (Train formation: –Mc+Tp+Mc–)

- Mc module (Mc1 car and Mc2): motor car with driver's cab and motor bogie
- Tp module: trailer without driver's cab, with pantograph and trailer bogie installed

Such three modules are linked through articulation. Articulation device is provided between modules so that two cars are ready for double-heading operation

Articulation device can have relative movement. Its horizontal angle of rotation and longitudinal angle should be capable of negotiating minimum curve radius and vertical curve radius.

Motor bogie is fixed axle bogie. Trailer bogie is independently rotated wheelset bogie.

Damper systems are installed at both sides of lower articulation to cushion the vibration in longitudinal, vertical and lateral directions.

Main Parameters and main parts of the train that has an influence on the wheel rail interaction are described in APPENDEX 1.

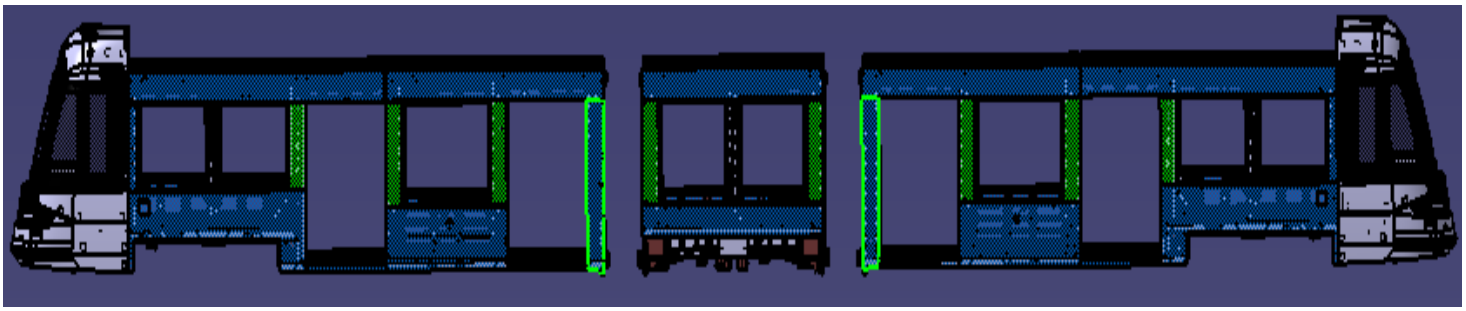

Figure 3.33 Carbody steel structure

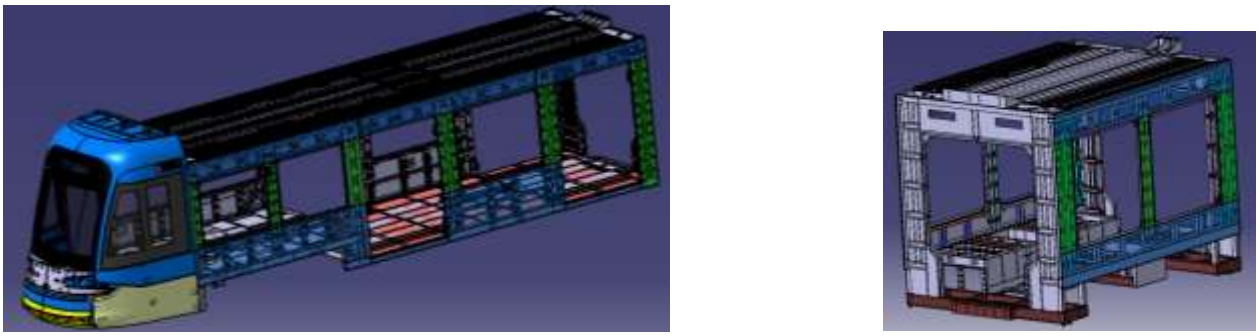

Figure 3.34 Mc module steel structure and T module steel structure

Figure 3.35 Real feature Addis Ababa LRT

[Source: South-north Line and East-west Line (Phase I) Light Rail EPC Project of Addis Ababa, Ethiopia, Technical Specifications of Vehicles, China Railway Group (CRECG) Project Manager Office for Light Rail Project of Ethiopia, July 2013]

### 3.6.2. AALRT Rail Line

Trams or Light rail trains of Addis Ababa has total length of main lines around 31.025km, where the East-west main line is around 16.998km long; the South-north main line is around 16.689km long. Both lines share the same section of around 2.662km.

**Sharp curve, Critical Track Line Selection of AALRT**


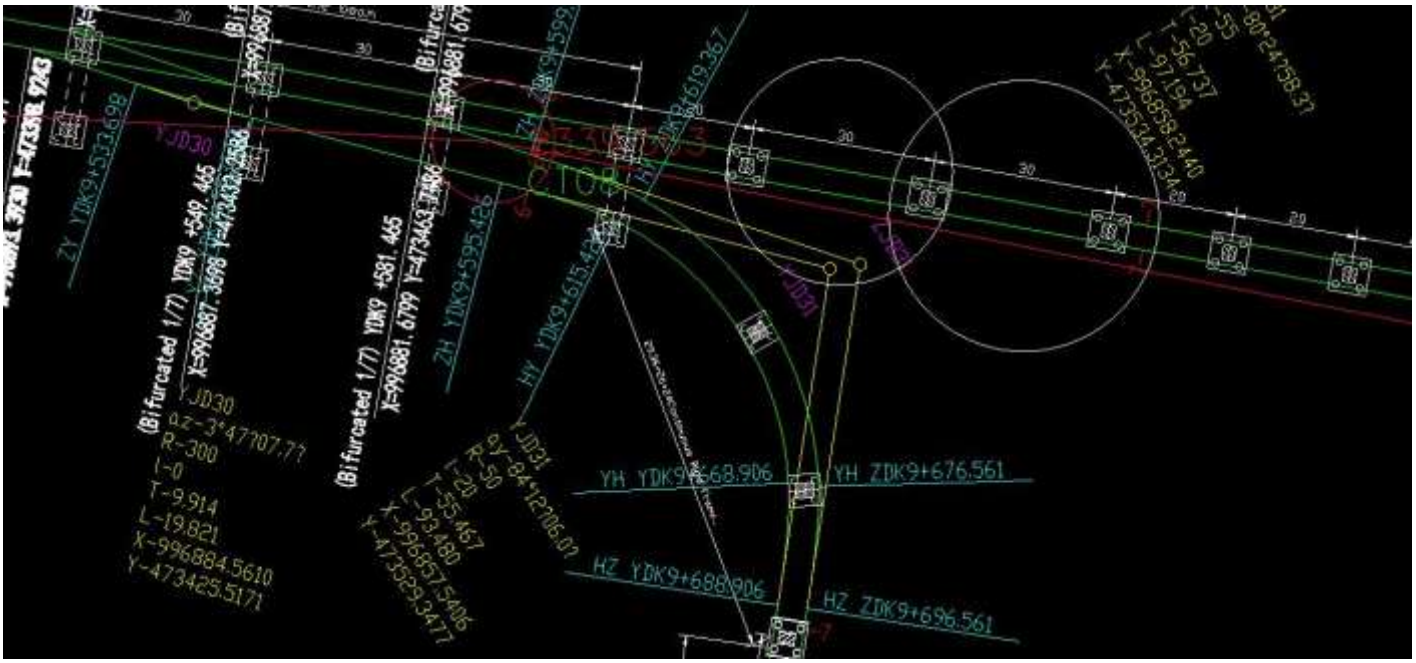


A: 20m length R50 Curve near EW16 stadium station (stadium to Kality junction)

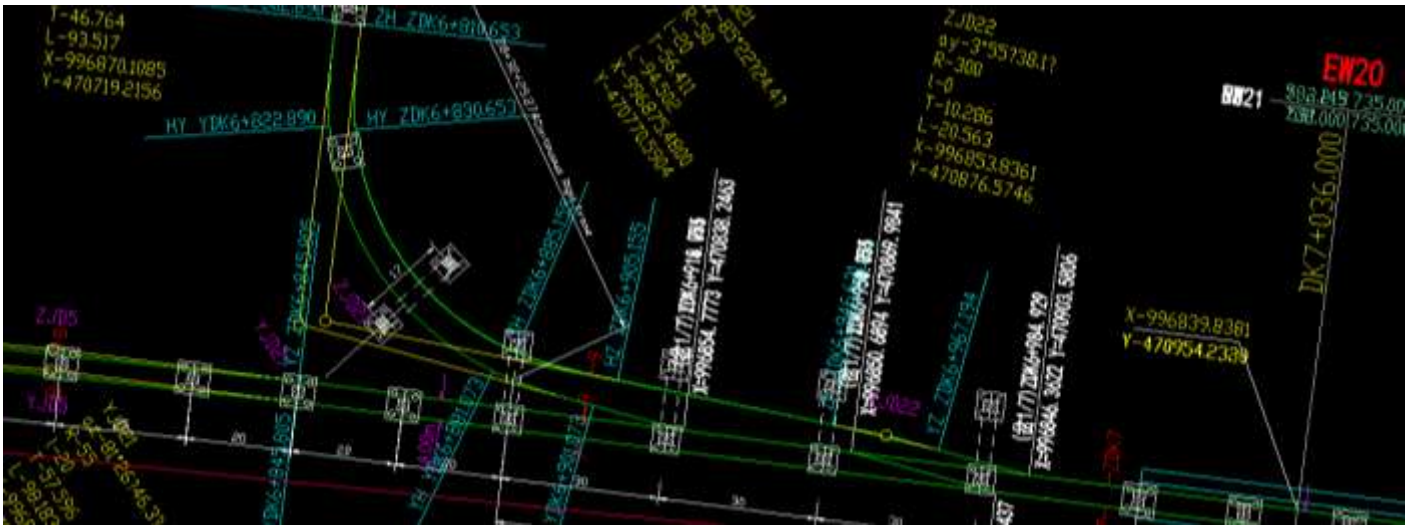


B: 20m length R50 Curve near EW20 Lideta station (lideta to Autobus tera junction)(AALRT design track line)


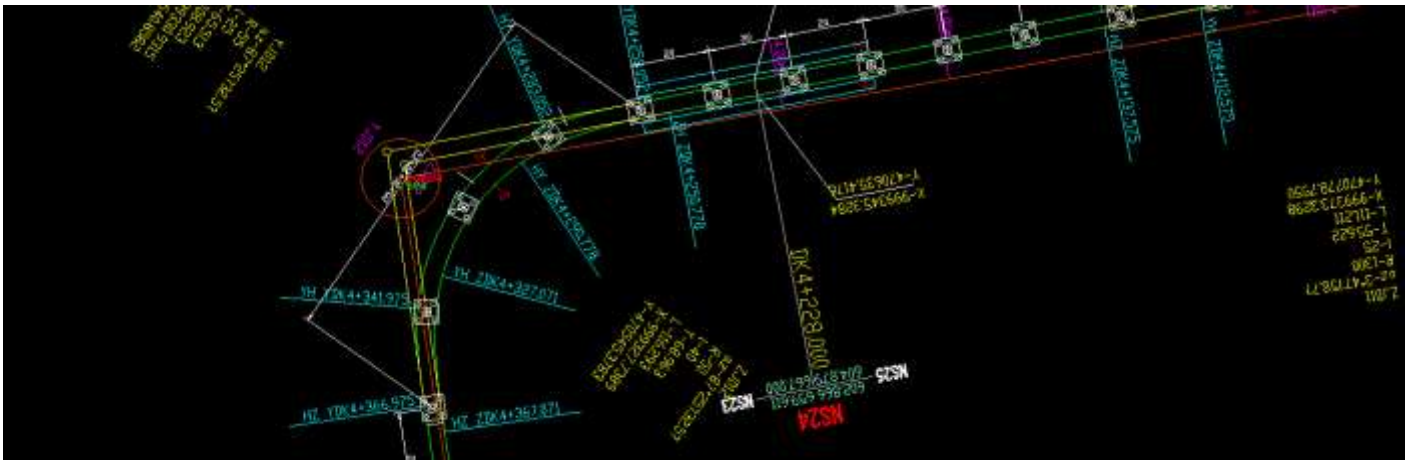


C: 40m length R50 Curve near station NS24 ‘Autobis tera’ station

Figure 3.36 Critical truck line selection of AALRT (a,b,c, small curve R50m )

## 3.7. Modeling Addis Ababa LRT in SIMPACK 8.94 Software Package

The large number of nonlinear components in a railway vehicle moving along a track creates a very complex mechanical system. In particular, interaction between wheel and rail is a very complex nonlinear element in the railway system. Wheel and rail geometries, involving both cross sectional profiles and geometry along the direction of movement, with varying shapes due to wear, have a significant effect on vehicle dynamic performance and operating safety.

Such modeling allows a designer to test a new vehicle design without having to build a prototype and tie up a track for testing, thereby increasing productivity through saving valuable time and manpower.

Computer modeling allows the user to test out various situations without spending the time, money, and use of equipment to test them on a track. Further, modelling can provide the means for derailment testing to enable prediction of when a given car might derail or overturn.

Modeling can predict at what speeds *derailment* will occur, or under what conditions it may be prevented. Stability analysis; one can model multiple suspensions and loading options and examine dynamic responses.

Modelling software can predict forces and accelerations at various positions throughout the vehicle to model ride characteristics, or to evaluate ideas for improving ride quality.

The modelling programs that have received wide acceptance in recent years include:

- SIMPACK,
- ADAMS/Rail,
- Universal Mechanism.
- VAMPIRE,
- NUCARS,
- MEDYNA,

All are developed specifically for rail dynamic modeling. Each program includes different solution methodology, wheel/rail models, analysis methods, and user interface.

The **SIMPACK** software package is a multi-body system mechanical design tool which assists engineers to model, simulate, analyze and design complex mechanical systems, such as vehicles, robots, machines and mechanisms.

The basic concept of SIMPACK is to create the equations of motion for mechanical and mechatronic systems and then from these equations, apply various different mathematical procedures to produce a solution (e.g. time integration).

The SIMPACK model is built up using the SIMPACK modeling elements. SIMPACK will then automatically generate the system equations from this model. The equations of motion

can be generated both symbolically and numerically (where the numeric form is the usual form).

The purpose of the software is to improve the design process involving multi-body systems. With the help of SIMPACK it is possible to reduce lead times and optimize the design process. More purposes that can be reached with SIMPACK are:

- Optimization of design parameters also in relation to the dynamic behavior
- Calculation of dynamically interacting forces within critical components
- Effect of varying design parameters
- Analyzing weak points of the mechanical design

## Vehicle Configuration

SIMPACK offers user interface for creating any type of virtual railway model. Starting with an automatically generated **wheelset,** or independent wheels, a user may build up, step-by-step, a complete vehicle. Multiple elements such as **wheelset, axle boxes**, **springs**, **data curves, Dampers** or even complete **bogies** can be called from databases.

SIMPACK models can be **fully parameterized**. Interdependencies of substitution variables may be assigned with user-defined formulas. Moreover, due to full compatibility between all SIMPACK modules, Wheel/Rail users can benefit from developments for other engineering disciplines.

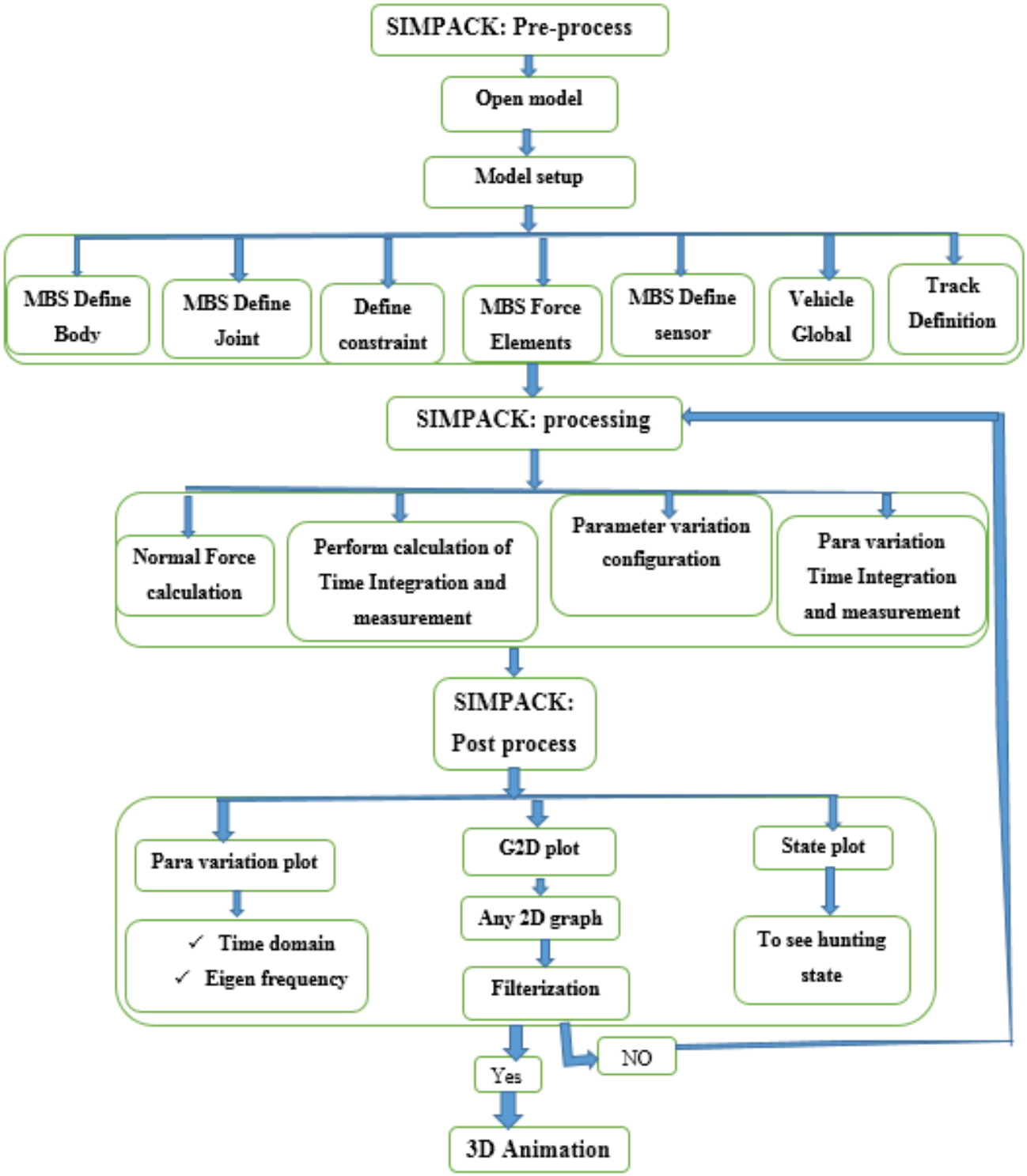


Figure 3.37 SIMPACK railway vehicle model Algorism (source: Simpack modeling software)

### 3.7.1. Description of the Addis Ababa Light Rail Train SIMPACK vehicle model

Almost all simulation has been done using real and related data's of AALRT and Main Characteristics of the model are:

- The model is composed of 28 bodies (3 car bodies,3 types of articulations(2 fixed articulation,1 flexible articulation,1 free articulation), 3 bogies, 6 wheelsets, 12 axle boxes) 96 degree of freedom
- The connecting elements between bodies are modeled in realistic way.
- The vehicle body and bogies are modeled using real data's of Addis Ababa Light Rail Train,
- The vehicle wheel profile is modeled specially for Addis Ababa Light Rail Train and it is optimized focusing on the need of wheel wear reduction.

The following pictures show steps of modeling AALRT starting from wheelset to car body.

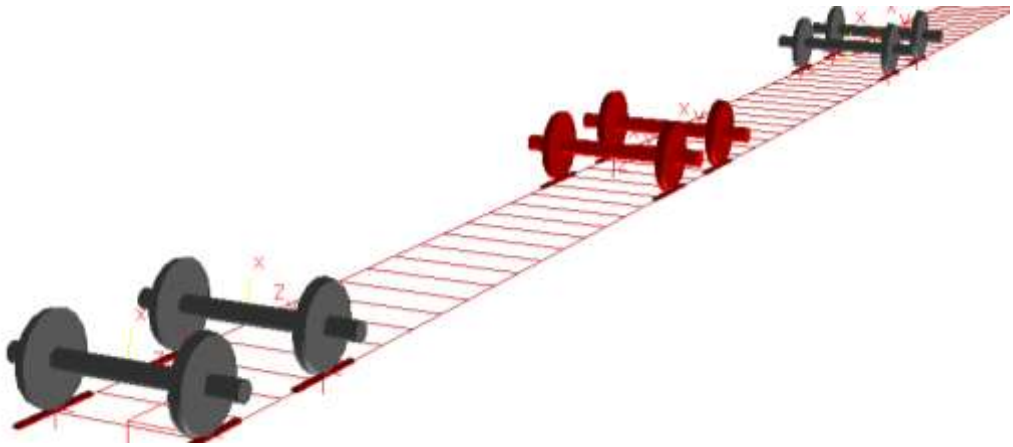

Figure 3.38 modeling Wheel set arrangement of AALRT

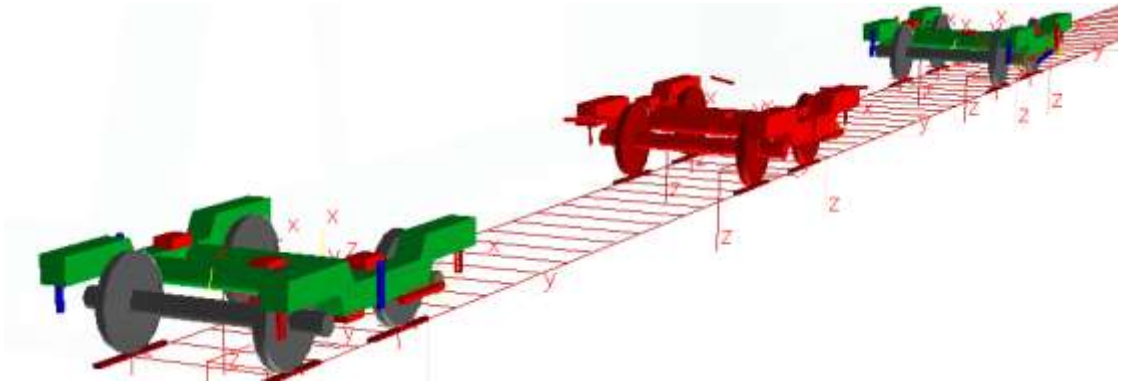

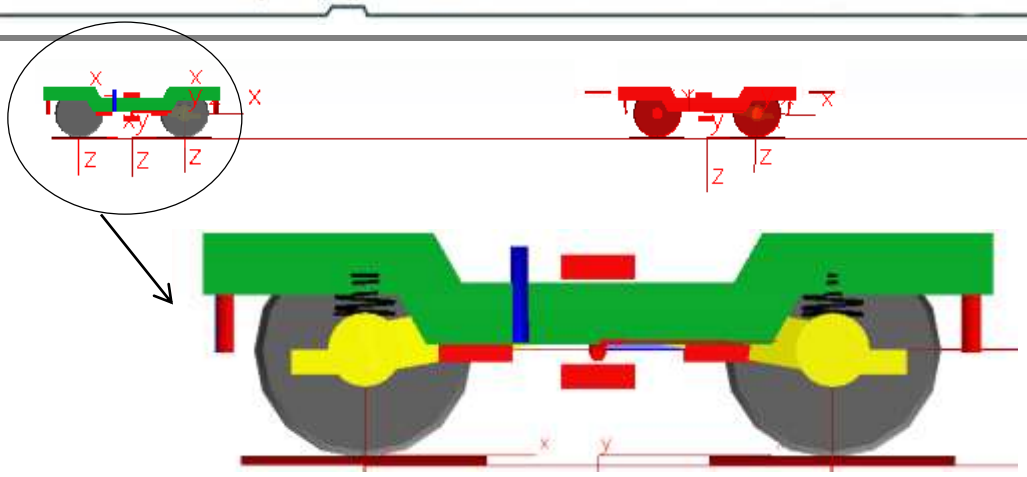

Figure 3.39 Modeled Bogie arrangement for AALRT

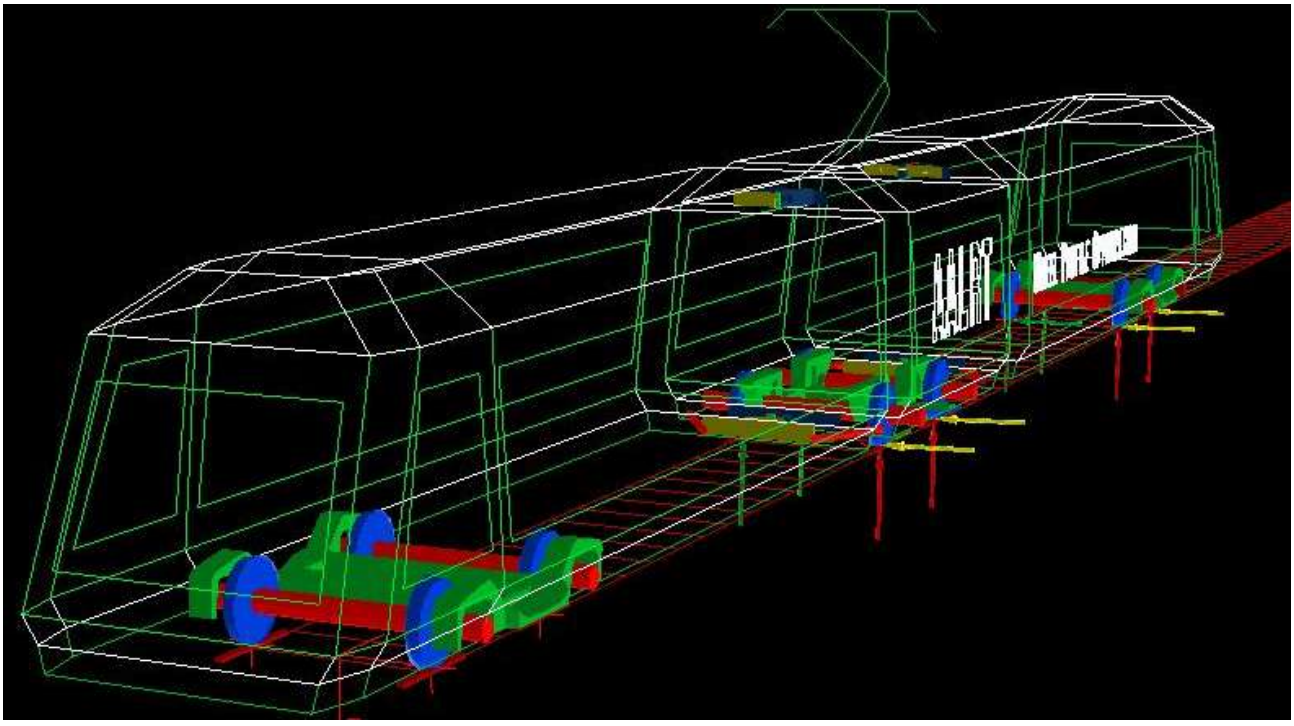


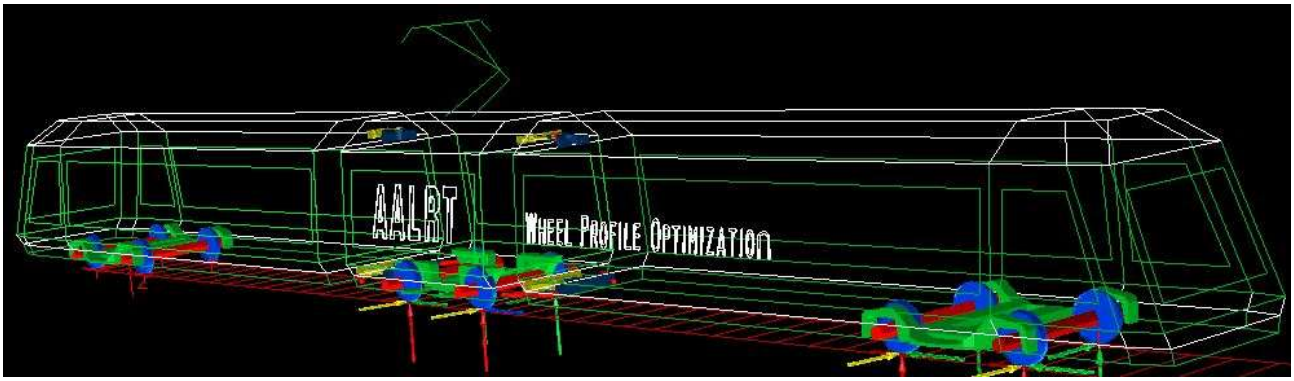

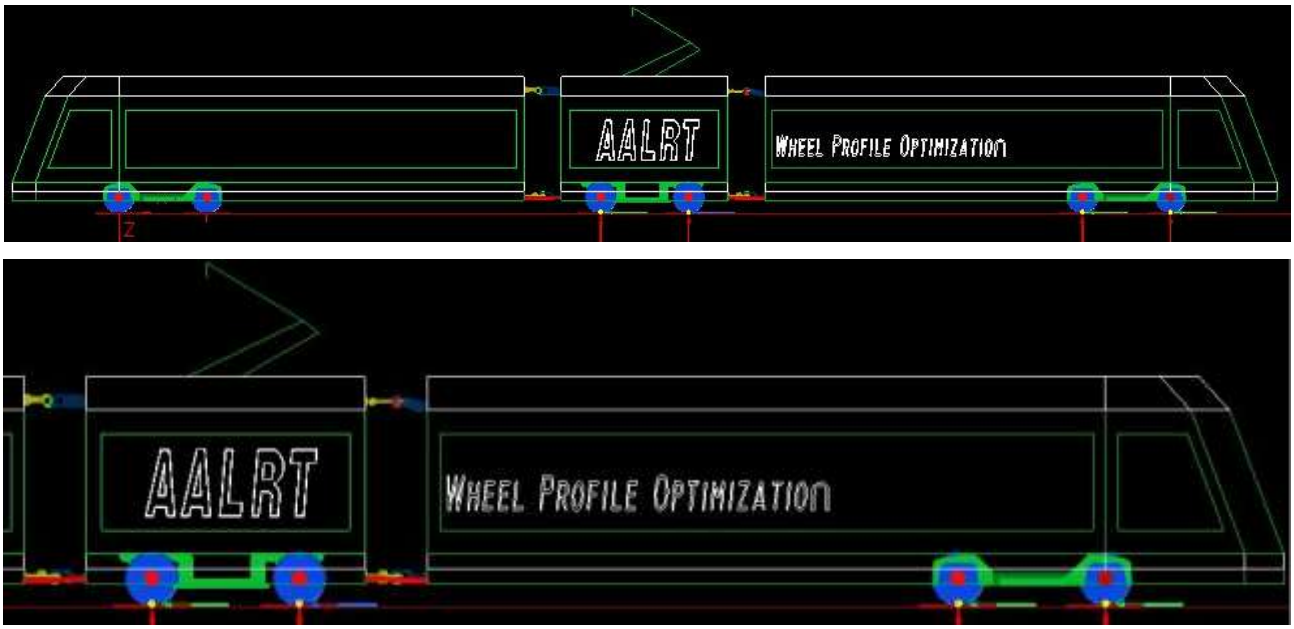


Figure 3.40 Modeled full train module of AALRT

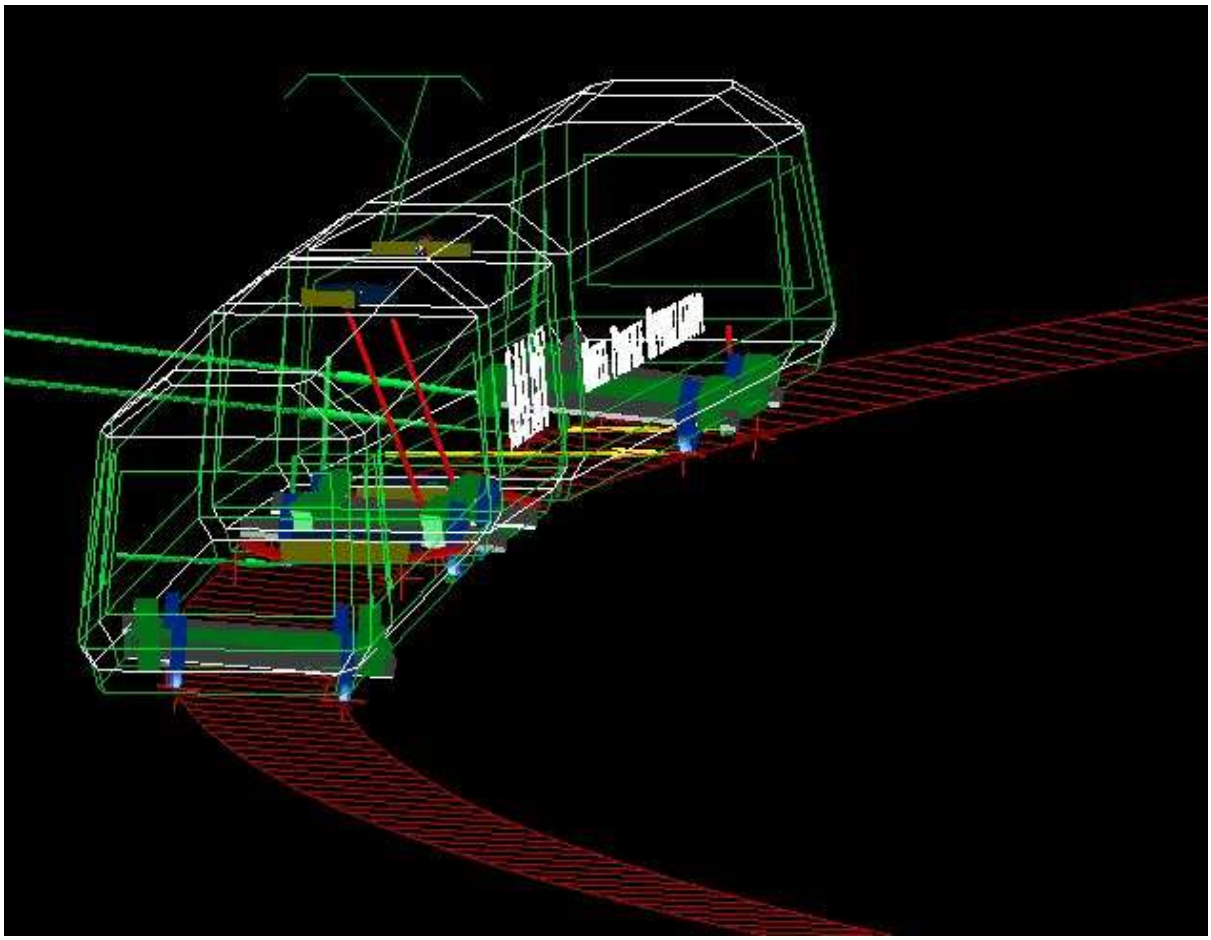

Figure 3.41 Model of AALRT negotiating sharp curve with radius of 50m

# CHAPTER FOUR

# RESULT AND DISCUSSION

Simulation is the representation of the behavior or characteristics of one system through the use of another system, especially a computer program designed for the purpose. In this paper Deterministic simulation type, Based on laws of physics and uses real world inputs, is used with SIMPACK Software. By changing variables in the simulation process, predictions of dynamic properties and failure state of railway passenger vehicle will be simulated. This simulation mainly focuses on straight and curved track under maximum load condition to see the effect of wheel profile optimization to reduce wear. The pre-condition of multi-body simulations and expected simulation output values according to the stated problem and objectives will be discussed.

## 4.1. RESULT

### 4.1.1.Assessment of Performance of Straight Track

#### 4.1.1.1. Non-linear stability under new wheel/rail profile

Non-linear stability of a railway vehicle is related to its initial states. At first, a 4mm lateral movement is applied to all wheelset, then let vehicle running with a high speed of 90 km/h on straight track. Hunting will occur and save this state of hunting as initial state of vehicle. The result lateral movement of the wheelsets is 2mm and the limit is 4mm so it is in good stable condition. The limit lateral wheel set load is 25kN for straight track and the result is under the limit.

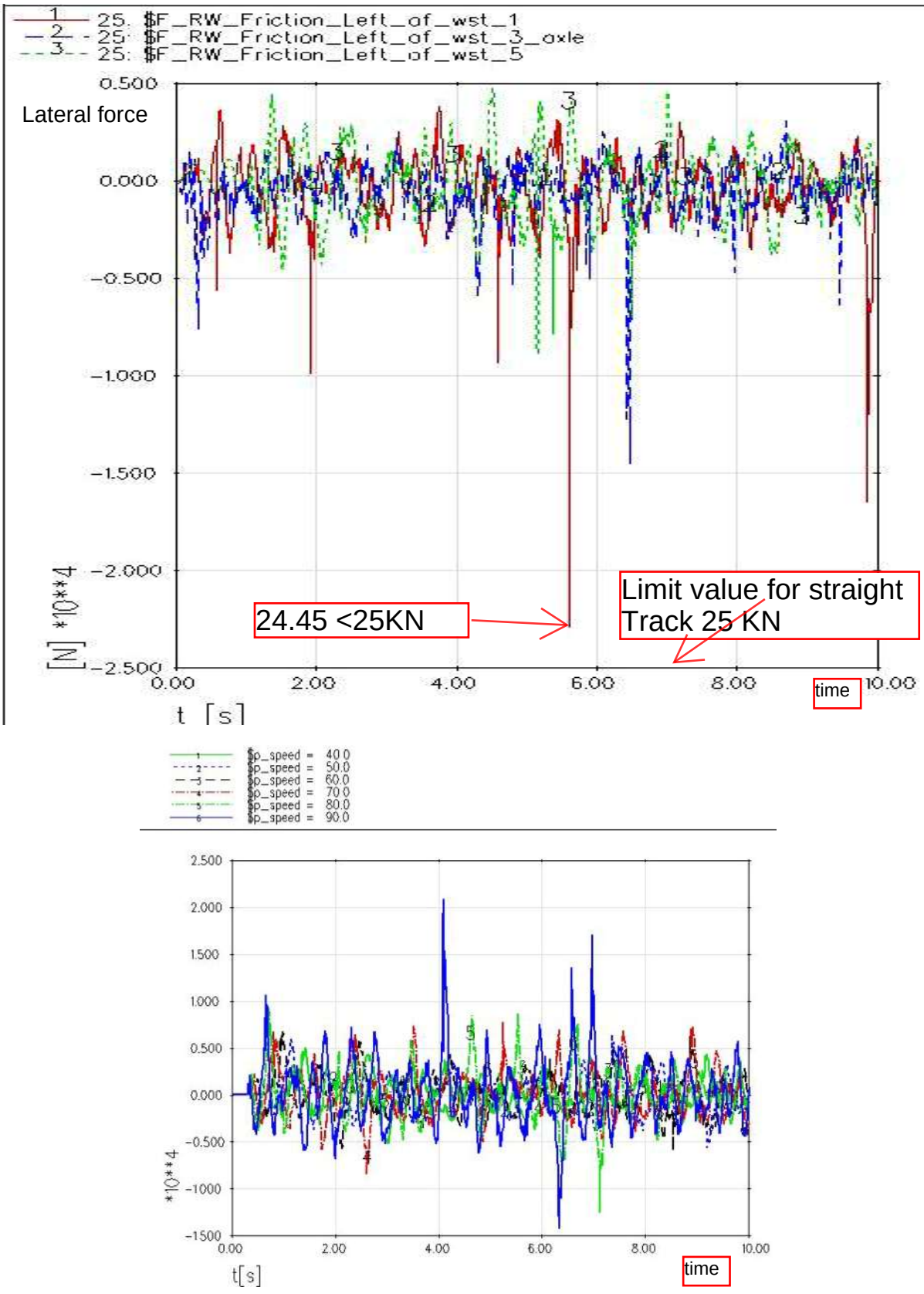


Figure 4.1: **a**. wheel set axle Lateral force of wst1, 3 and 5 **b**. Wheel set lateral force applied on track comparison with speed

#### 4.1.1.2. Wear Index

Wheel wear is estimated using the wear index W that reads: $W = Fx \cdot \xi + Fy$ Where Fx is longitudinal creep force; $\xi$ is longitudinal creepage ; Fy is lateral creep force; and $\eta$ is lateral creepage.

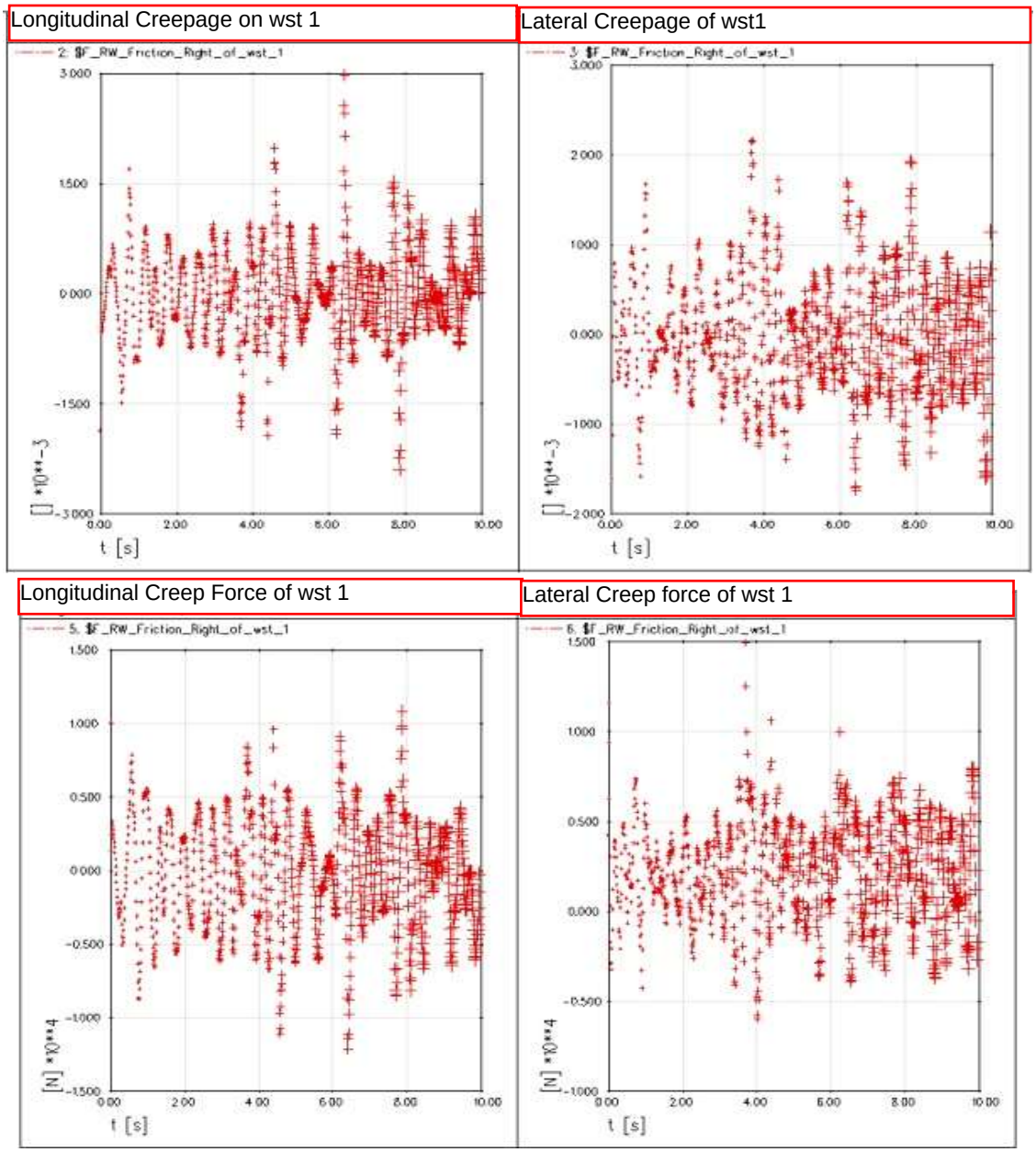


Figure 4.2. Longitudinal creepage, longitudinal creep force, Lateral creepage and Lateral creep force

The wear condition for AALRT on straight track, wear index for ***AALRT wheel profile*** is **78N** and Wear index for ***AALRT optimized wheel profile*** is **56N,** wear index for ***S1002 wheel profile*** is **48N**. See fig 4.3 and they are in good condition under the limit (<200N)

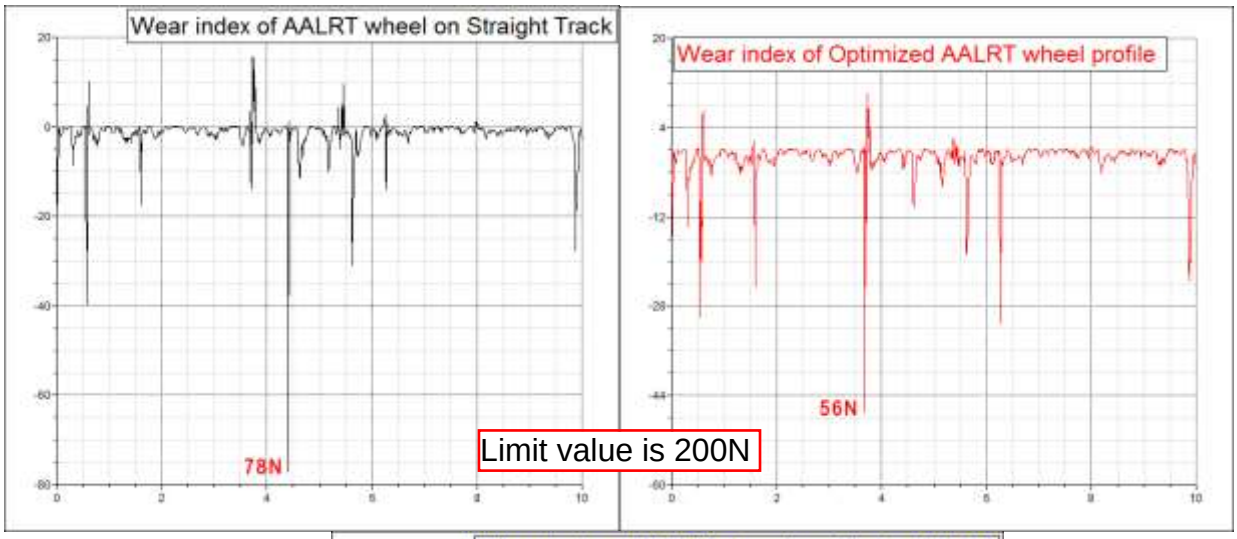


Limit value is 200N

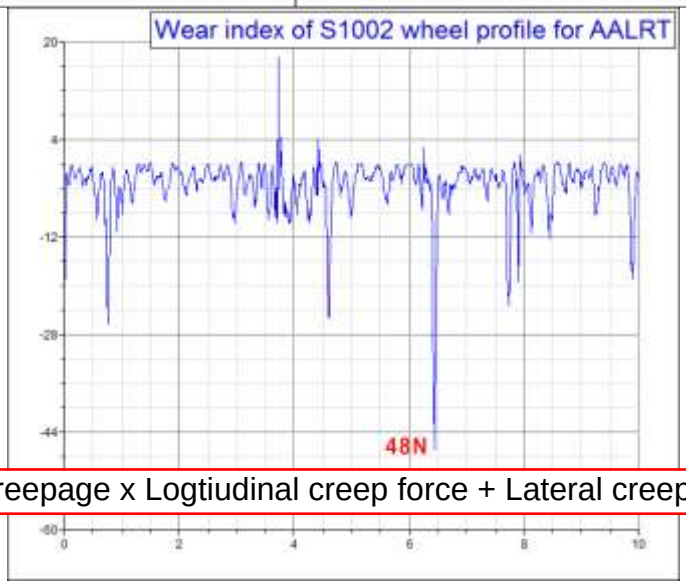


Wear index=Longitudinal creepage x Logtiudinal creep force + Lateral creepage x lateral creep force

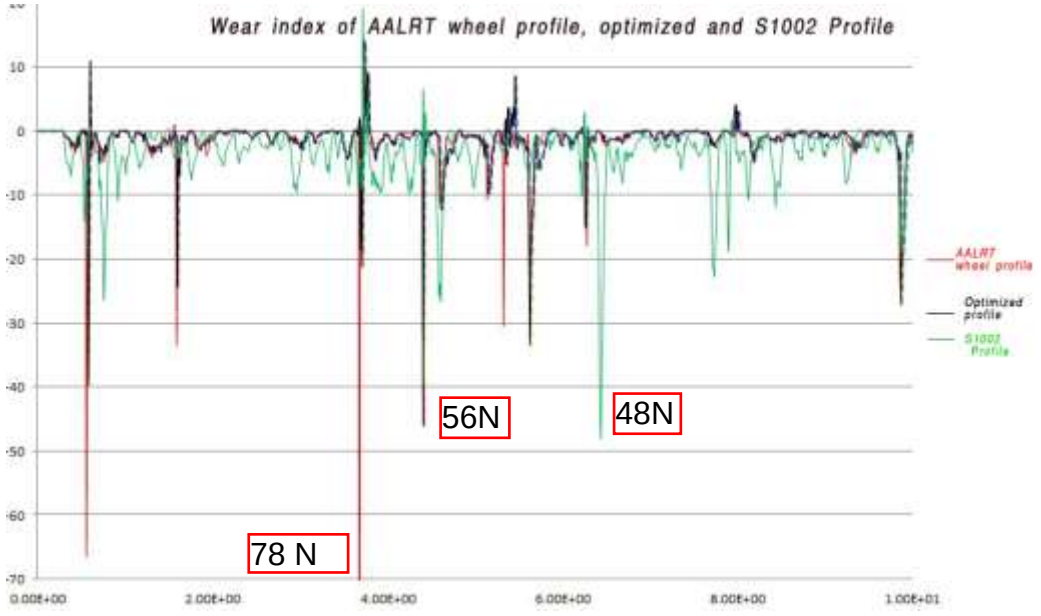


Figure 4.3 Wear index comparison on straight track

#### 4.1.1.3. Ride Comfort on straight

Track irregularities are necessary for this calculation. Because it is hard to give a real track irregularity, so track irregularities are given to the track. Checking points are located in three parts of carboy just above the bogie center. Lateral ride comfort according to ISO 2631 horizontal, Sparling ride index method is checked. And ride index is 2.45 < 4. See fig 4.4,4.5 and 4.6 which is in good comfort condition.

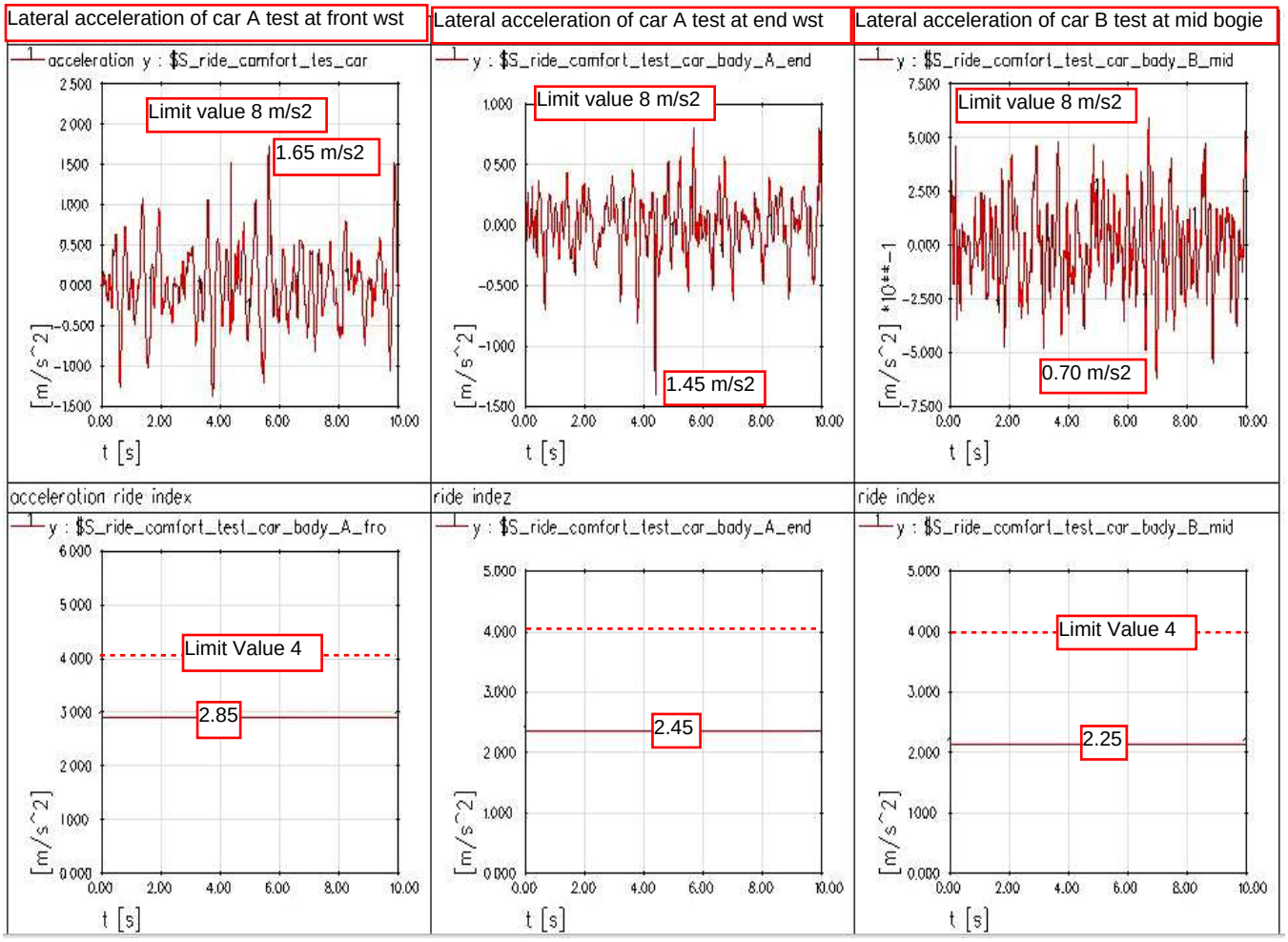


Figure 4.4 ride index on Car A and Car B

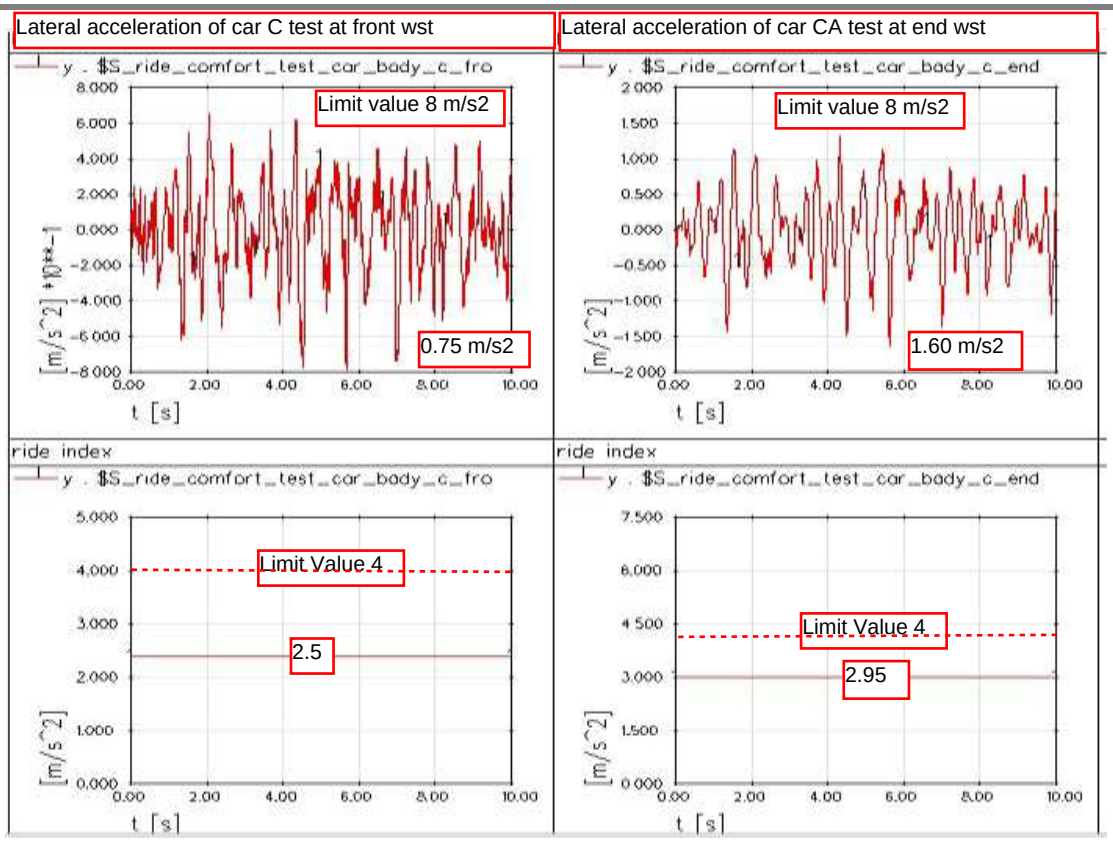


Figure 4.5 Ride index at car c

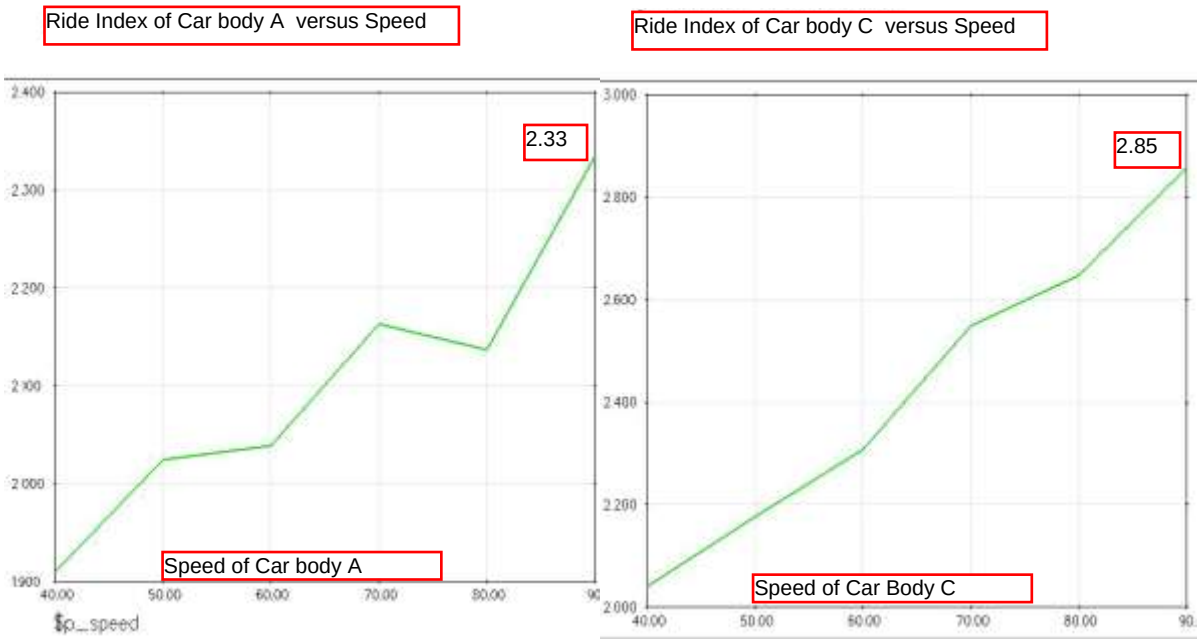


Figure 4.6 ride index vs. speed at binging of Car A and at the end of Car C

Under a speed of 50km/h the ride comfort is excellent, at a speed range from 50km/h to 70km/h, ride comfort is good, and above the speed of 70km/h the ride comfort is acceptable.

#### 4.1.1.4. Derailment Coefficient

The derailment coefficient of leading, high rail side wheel is checked. According to the specification of UIC518 the limitation value of derailment coefficient is 0.8. Obtained result is shown in Fig. 4-7. It shows that at all calculation cases this force never exceeds the limitation value.

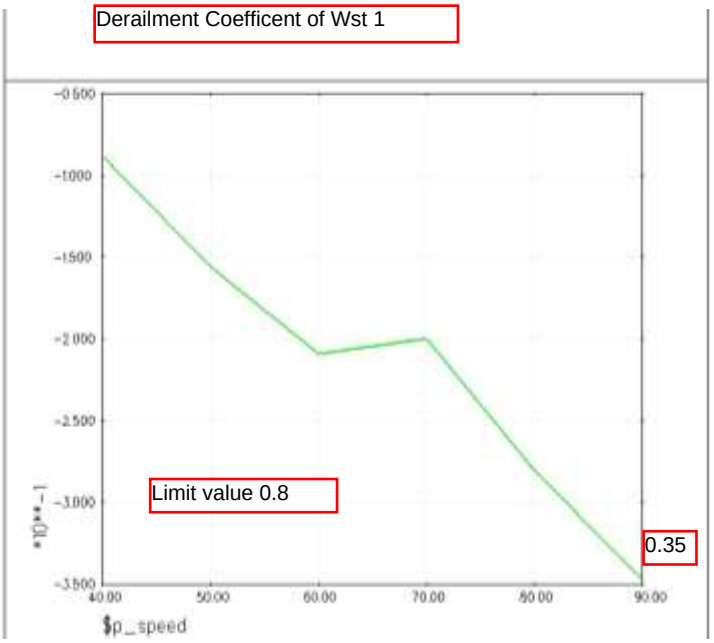


Figure 4.7 Derailment coefficient vs. speed

#### 4.1.1.5. Wheel Unloading

The wheel unloading of leading, low rail side wheel is checked**.** Which is in good condition and <0.6.

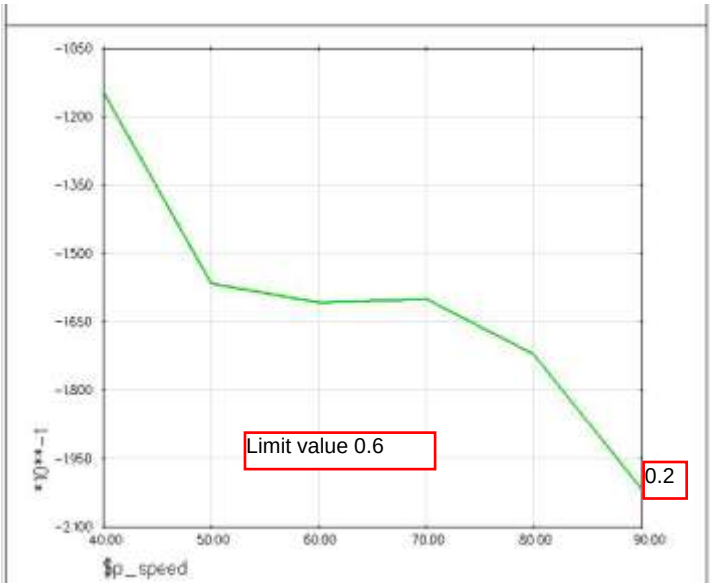


Figure 4.8 wheel unloading

## 4.1.2.Assessment of performance when Negotiating R150m Curve

### 4.1.2.1. Axle Lateral force

While negotiating a curve, the leading wheelset undertakes the maximum axle lateral force, so the result of axle lateral force for leading wheelset is given.

According to the specification of UIC518 clause, the limitation of axle lateral force is 42.5kN. Calculated result is shown in Fig. 4-9. It shows that at all calculation cases this force (34.5 kN) never exceeds the limitation value.

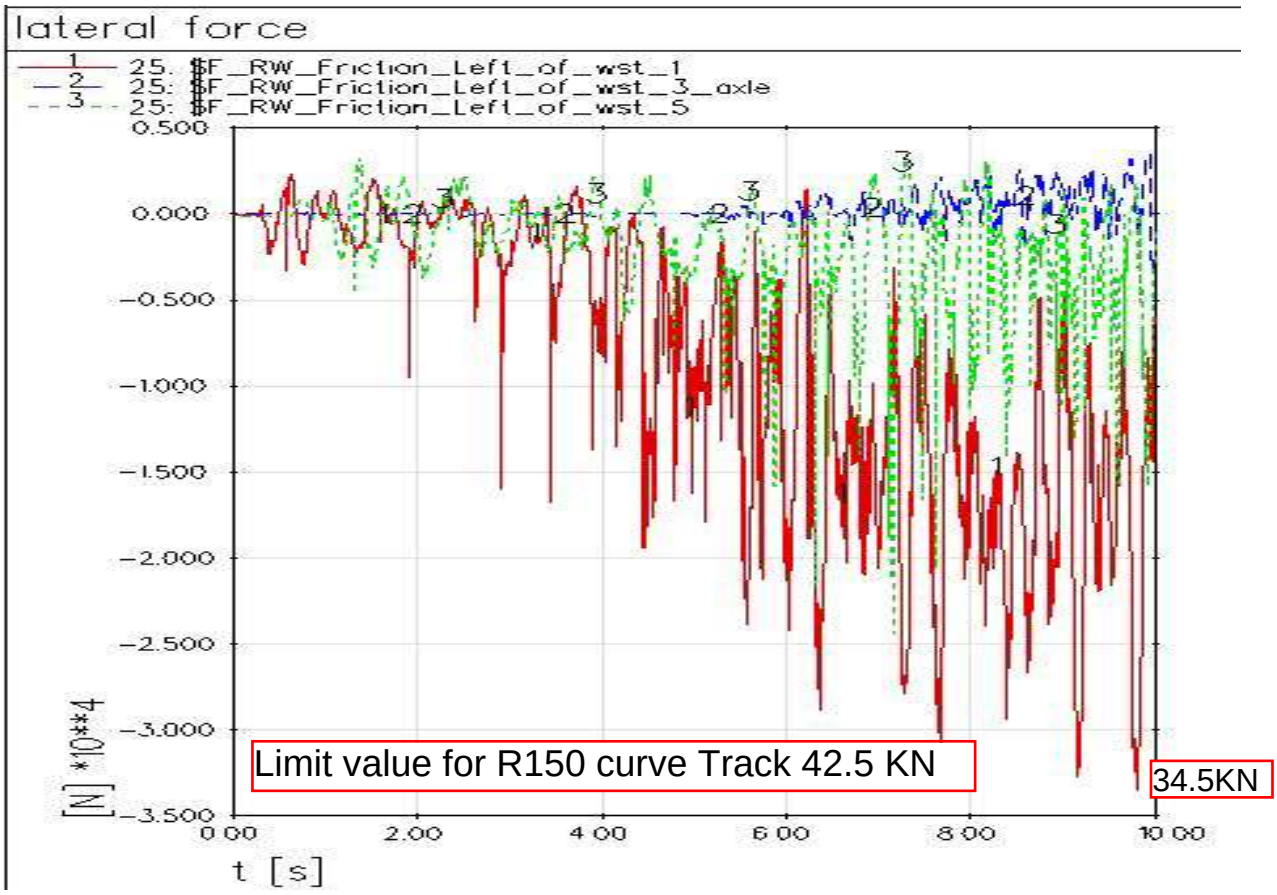


Figure 4.9 Lateral force of wst1, 3 and 5

### 4.1.2.2. Wear Index for R150m curve

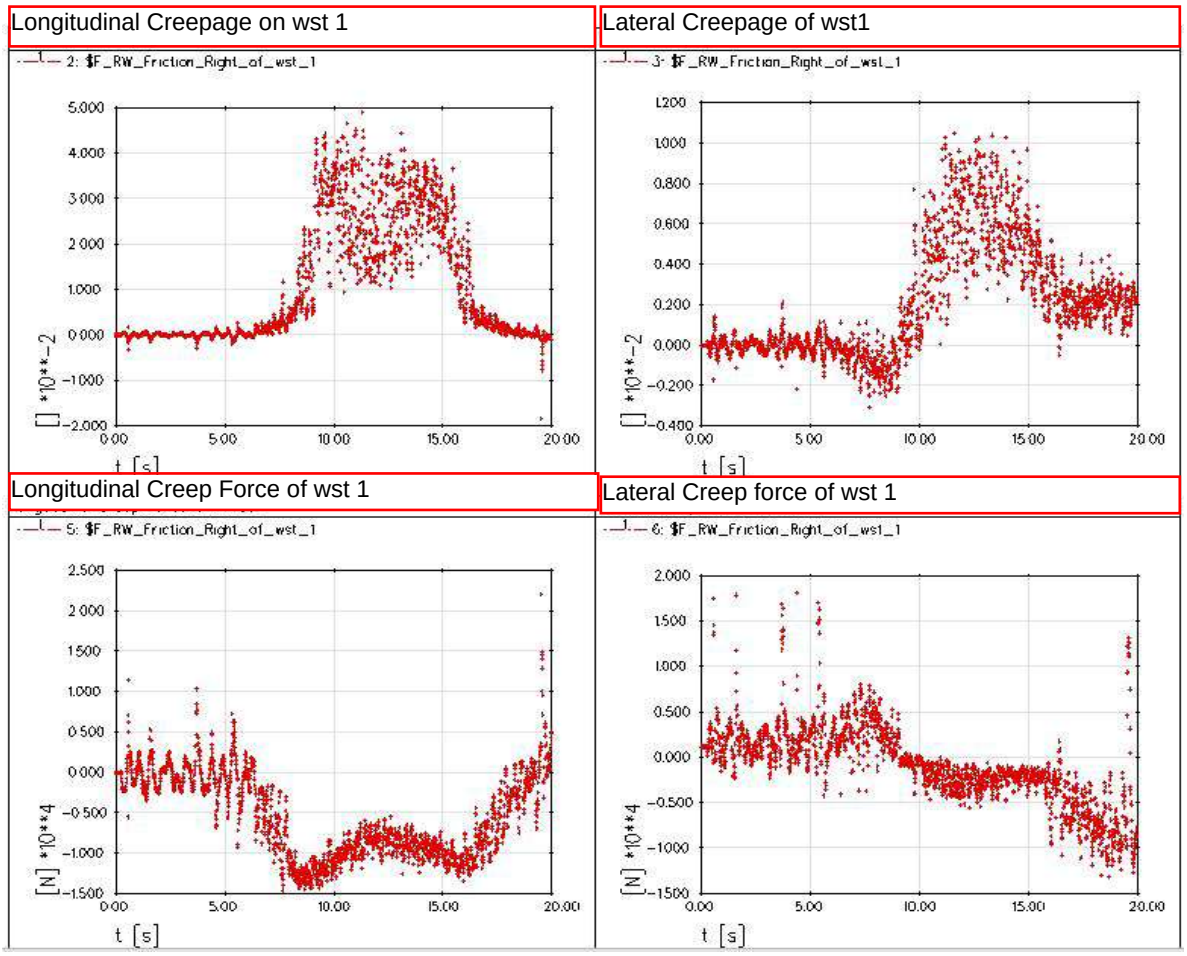


Figure 4.10 Lateral and longitudinal Creepage and creep forces

The wear condition for AALRT at R150m curve, wear index for ***AALRT wheel profile*** is 260 N which is in mild wear condition in transition Curve and **560N** which is in severe wear condition at the beginning of the curve.

Wear index for ***AALRT optimized wheel profile*** is **200N** which is at mild wear condition in transition Curve and **420N** which is in severe wear condition at the beginning of the curve. See fig 4.11

But ***S1002 wheel profile*** is at good condition for both Transition and R150m curve. The wear index is **150N**. See fig 4.12

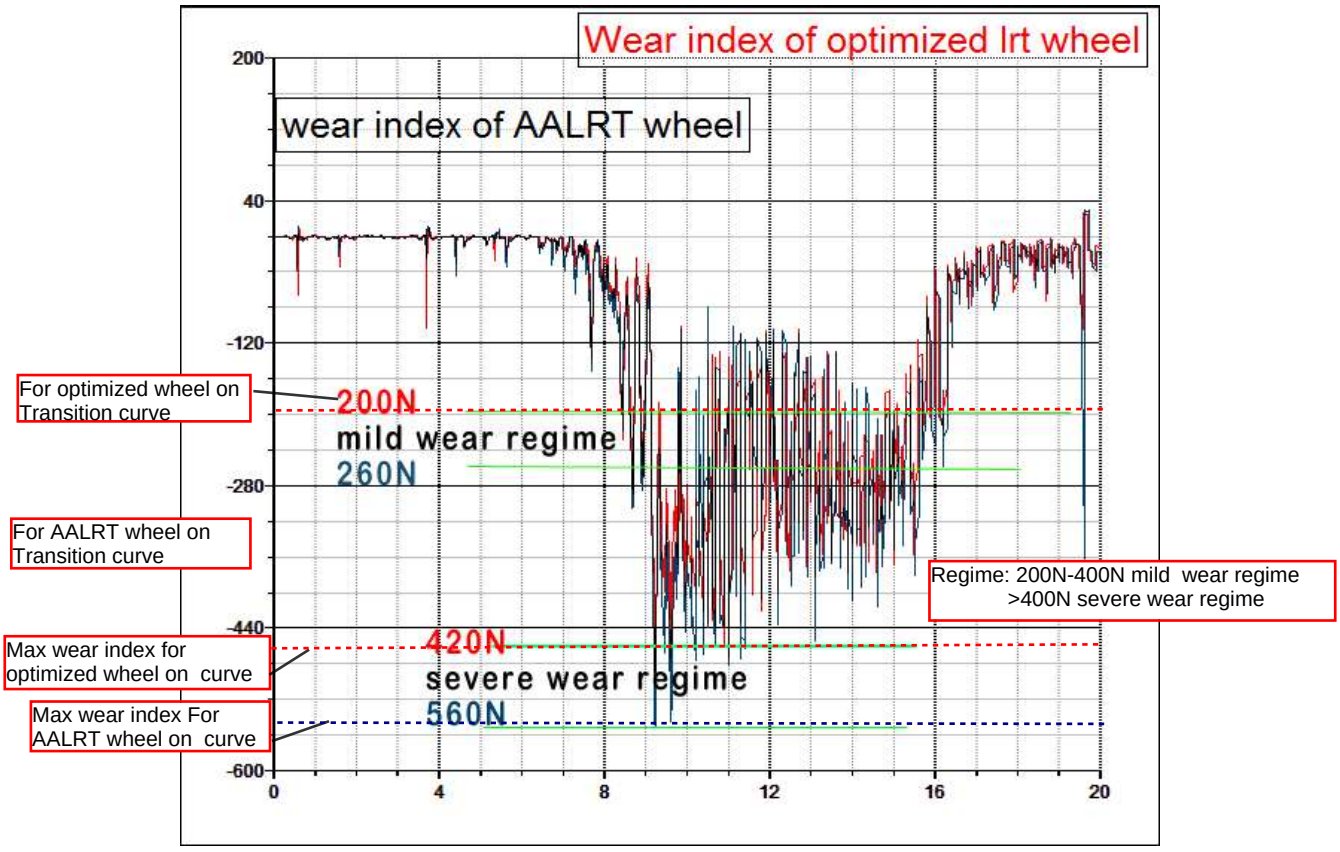


Figure 4.11Wear index comparison of AALRT wheel, optimized wheel

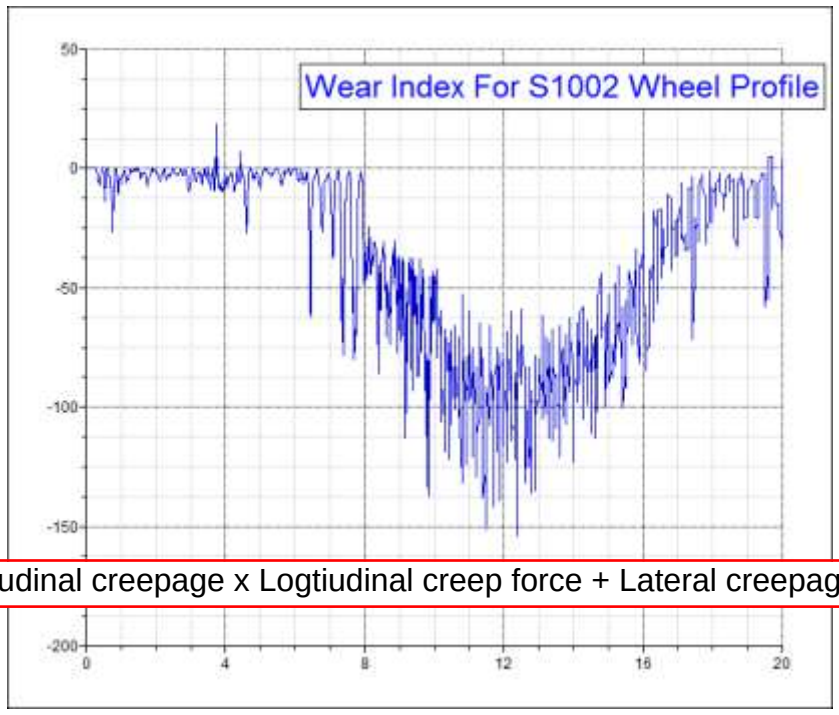


Wear index=Longitudinal creepage x Logtiudinal creep force + Lateral creepage x lateral creep force

Figure 4.12 S1002 wheel profile at R150 Curve for Addis Ababa Light rail Train condition

### 4.1.2.3. Ride Comfort on R150m Curve

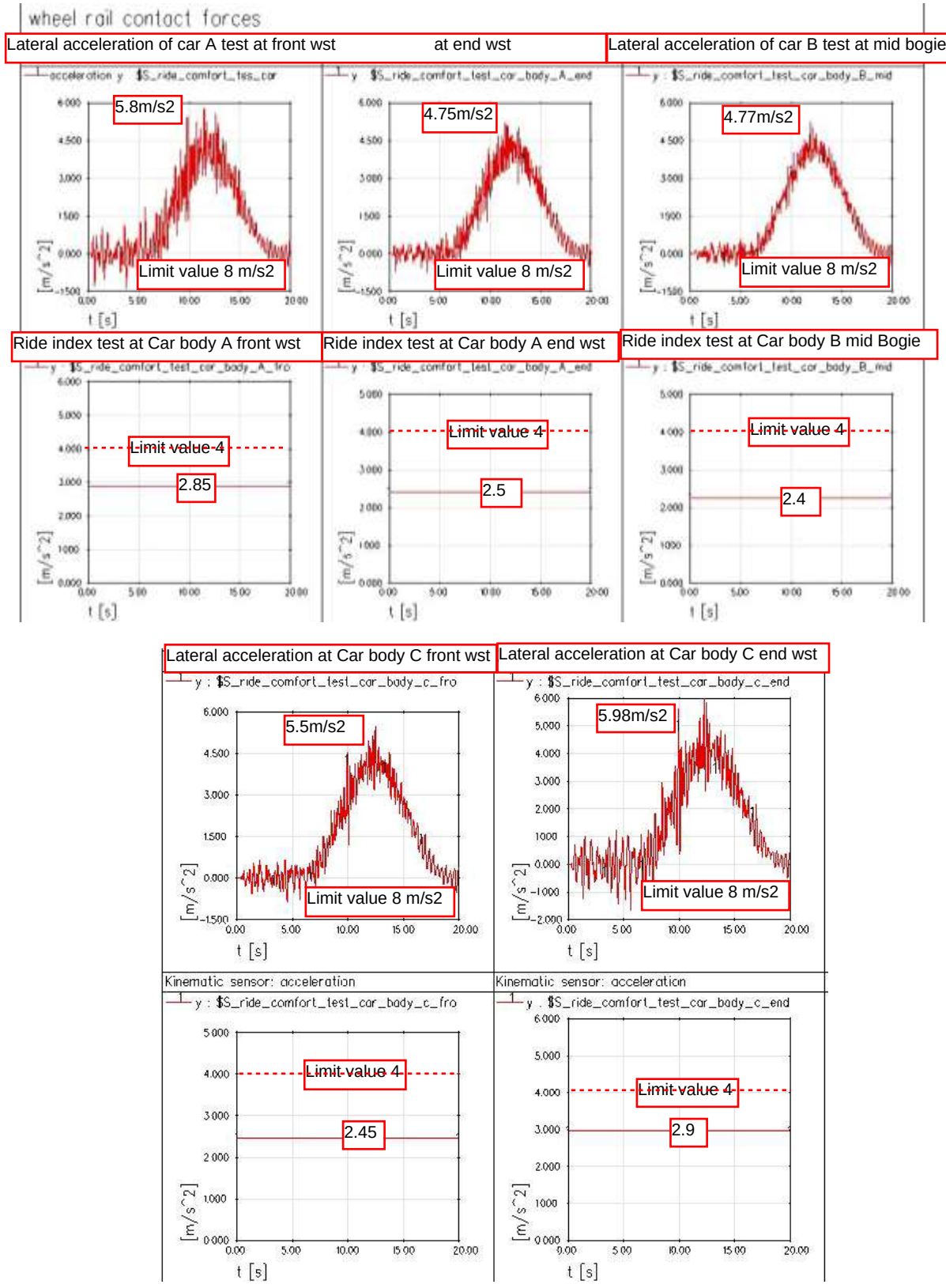


Figure 4.13 Ride index on Car body A, B, and C


Figure 4.14 Ride index at the front of car a and at the end of car c

Ride index 2.55, at a speed of 40km/h the ride comfort is excellent, at a speed range from 40km/h to 60km/h, ride comfort is good, and above the speed of 70km/h the ride comfort is acceptable.

#### 4.1.2.4. Derailment Coefficient for R150m Curve

The derailment coefficient of leading, high rail side wheel is checked. According to the specification of UIC518, the limitation value of derailment is 0.8. Obtained result is shown in Fig. 4-15. It is shown that while negotiating R150 curve or limitation value of derailment Y/Q is 1.2. The passing speed should be limited at a speed NOT exceed 80 km/h,

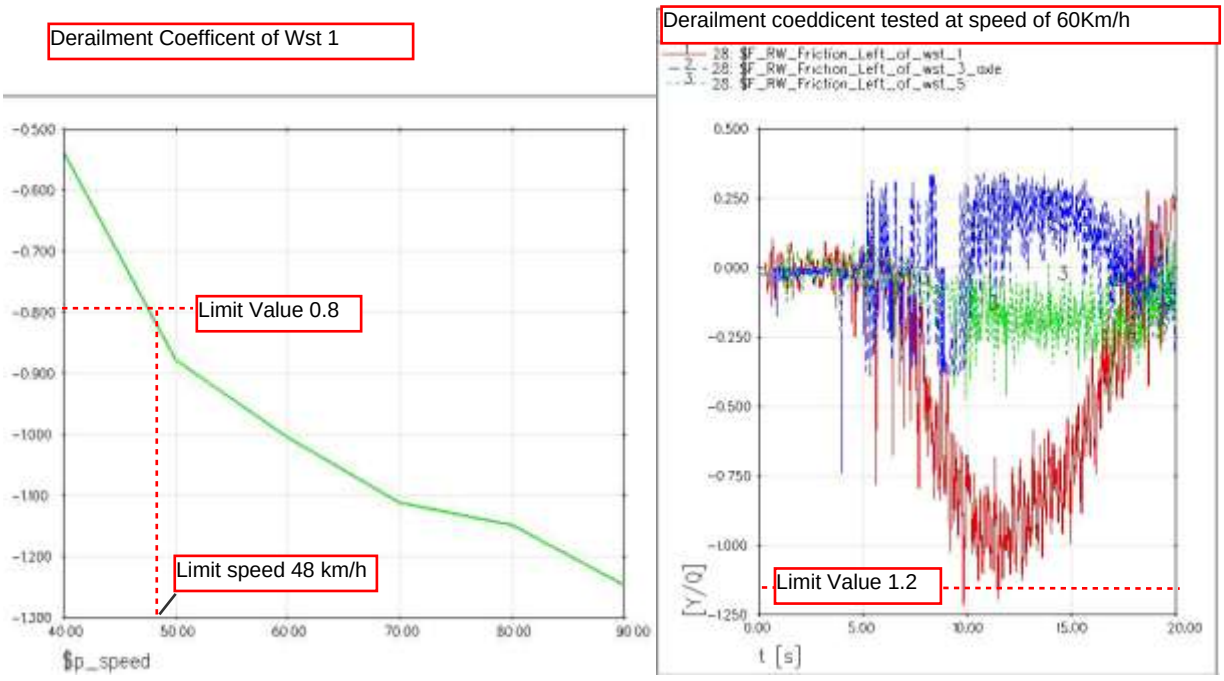


Figure 4.15 Derailment coefficient for R150m curve

#### 4.1.2.5. Wheel Unloading for R150m curve

The wheel unloading of leading, low rail side wheel is checked. Wheel unloading is specified in many specifications and the limitation value is 0.6. Leading and low rail side wheel undertakes the maximum wheel unloading; the result is shown in Fig. 4.26. It is shown that while negotiating R150 curve. This is under the limit value.

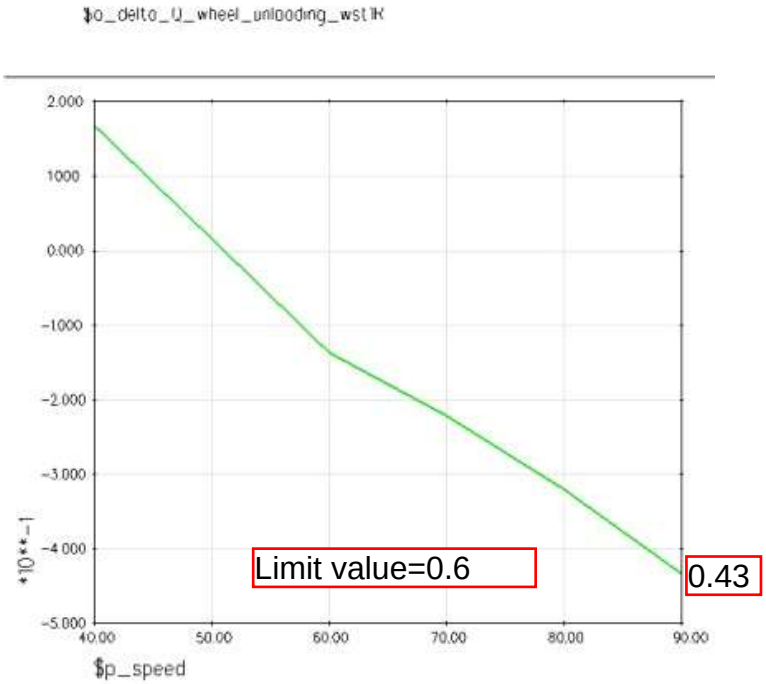


Figure 4.16 Wheel unloading at R150 curve

## 4.1.3.Assessment of performance When Negotiating Sharp Curve R50

### 4.1.3.1. Lateral Force of wheelset

Limitation value of axle lateral force is 65 kN for sharp curves and it is under limit.

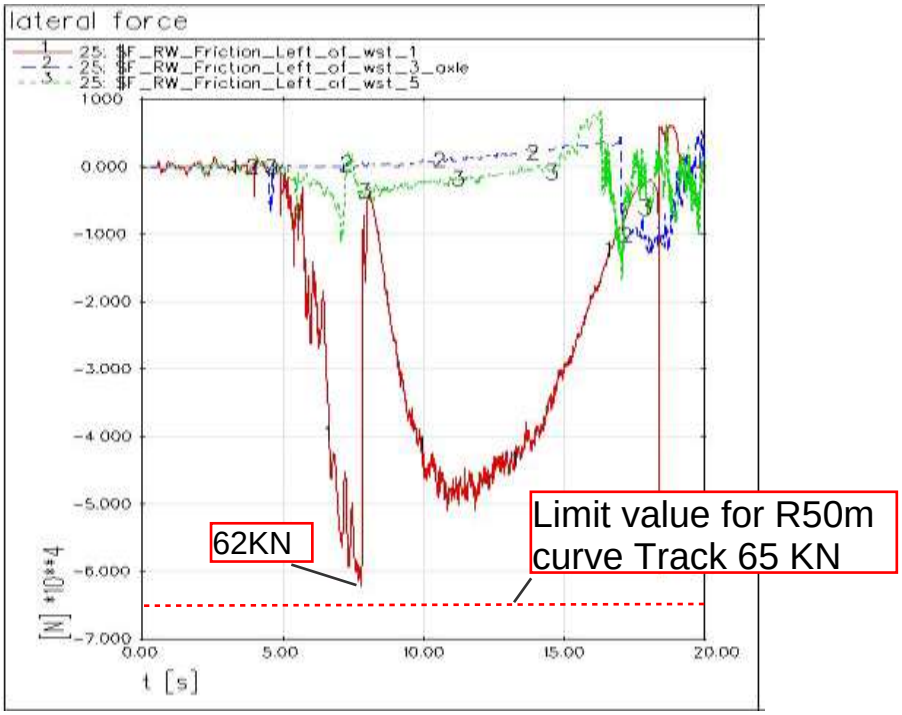


**Figure 4.17Wheelset Lateral force on wheelset 1,3, and 5**

### 4.1.3.2. Wear index for R50m Sharp Curve

Longitudinal Creepage on wst 1

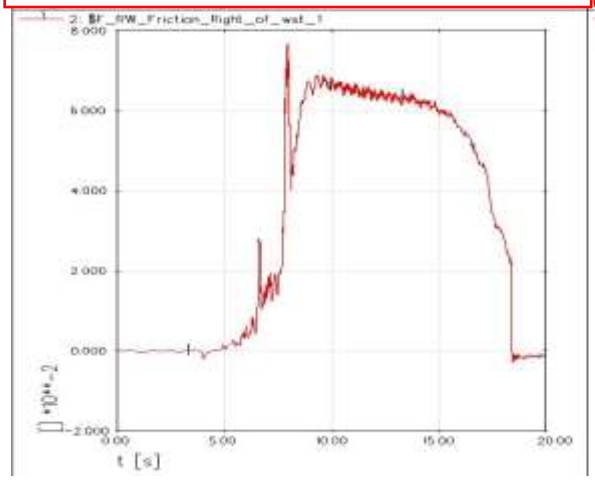


Lateral Creepage on wst 1

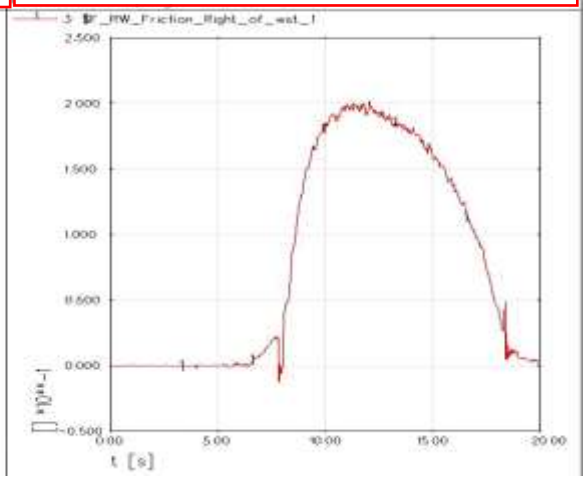


Longitudinal creep force on wst 1

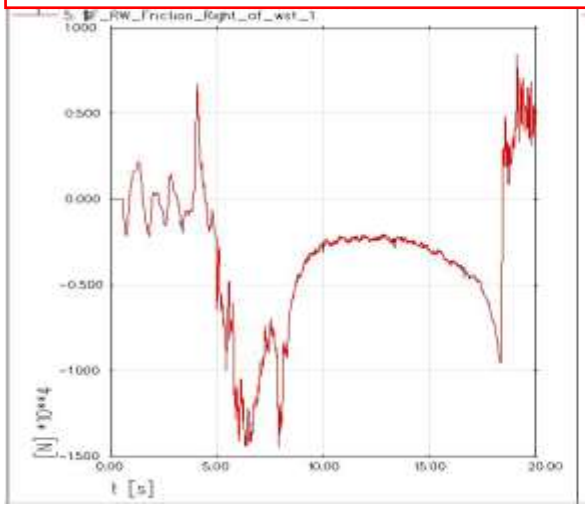


Lateral Creep force on wst 1

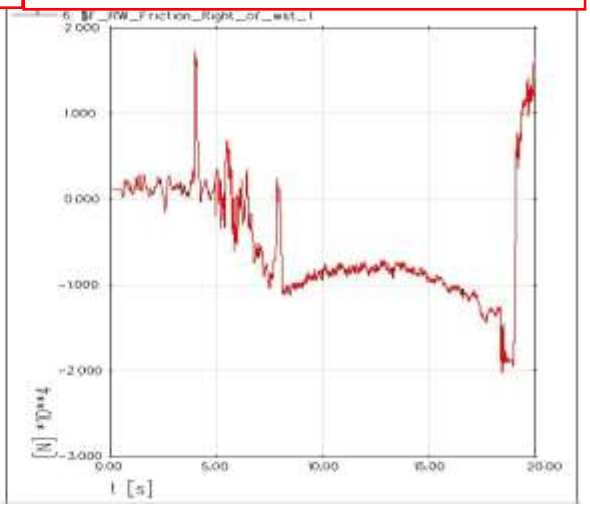


Figure 4.18 Longitudinal and Lateral Creepage ,creep forces


Wear index=Longitudinal creepage x Logtiudinal creep force + Lateral creepage x lateral creep force

Figure 4.19Wear index comparison for AALRT, Optimized and S1002 wheel profile

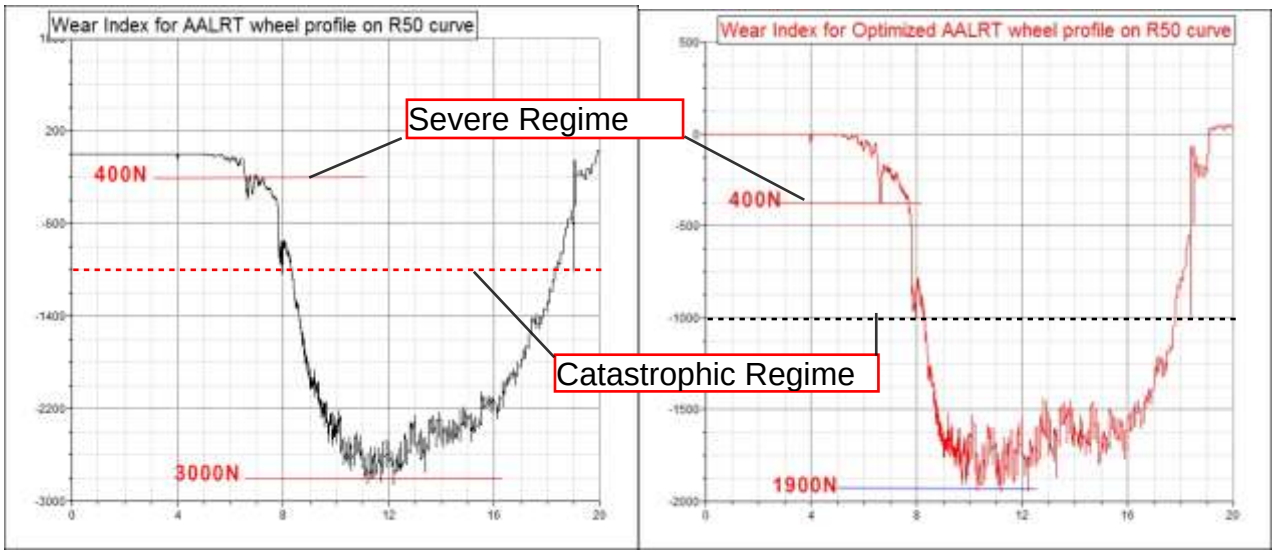


Figure 4.20 Wear index at R50 curve for AALRT wheel and Optimized Wheel profile

The wear condition for AALRT at R50m curve, wear index for ***AALRT wheel profile*** is **3000N** which is in catastrophic wear condition at the beginning of the curve and **400N** which is in mild wear condition in transition Curve.

Wear index for ***AALRT optimized wheel profile*** is **1900N** which is also in catastrophic wear condition (but better than AALRT wheel profile) at the beginning of the curve and **400N** which is at beginning of mild wear condition in transition Curve. See fig 4.20. This show wear index reduced in optimized wheel profile. Even if it's reduced, still the wear rate is severe and has to be minimized.

But ***S1002 wheel profile*** is at good condition for both Transition and R150m curve. The wear index is **150N**. See fig 4.20

### 4.1.3.3. Ride Comfort on R50m Curve

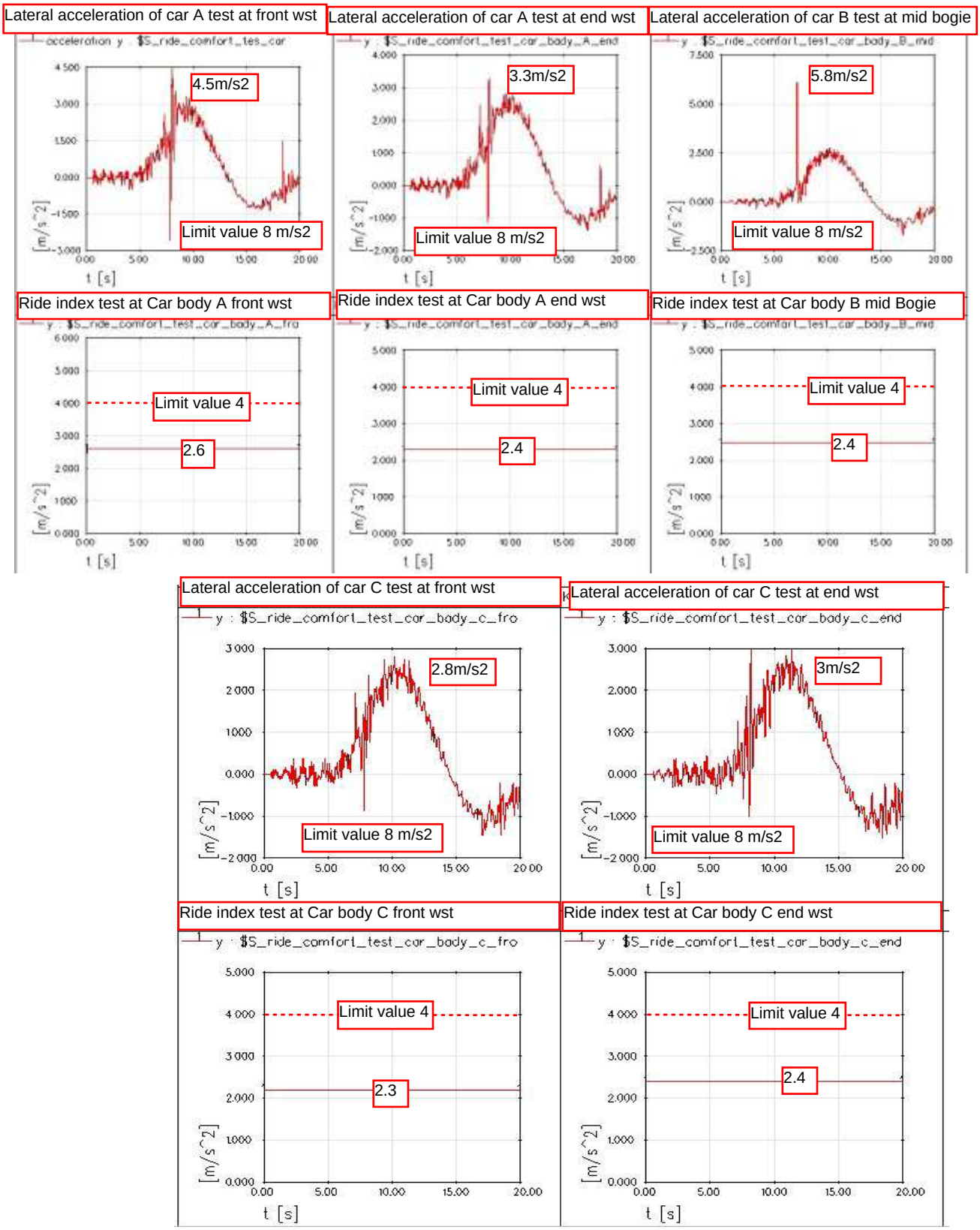


Figure 4.21 Rid index at different point of car body

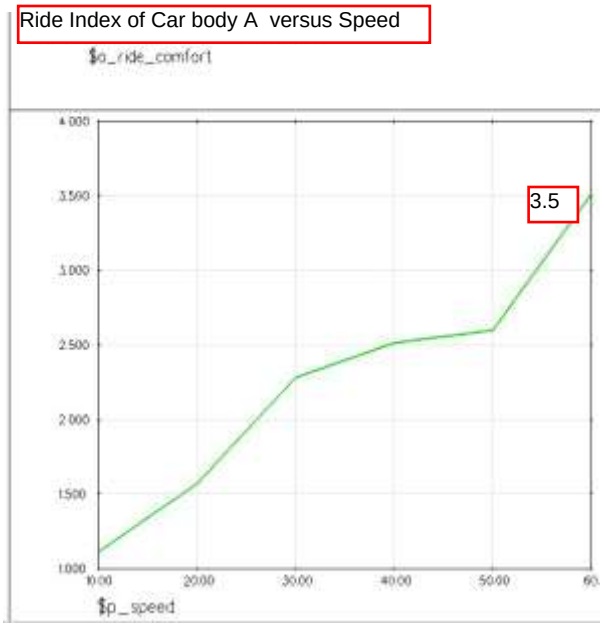


Figure 4.22 Ride index with speed

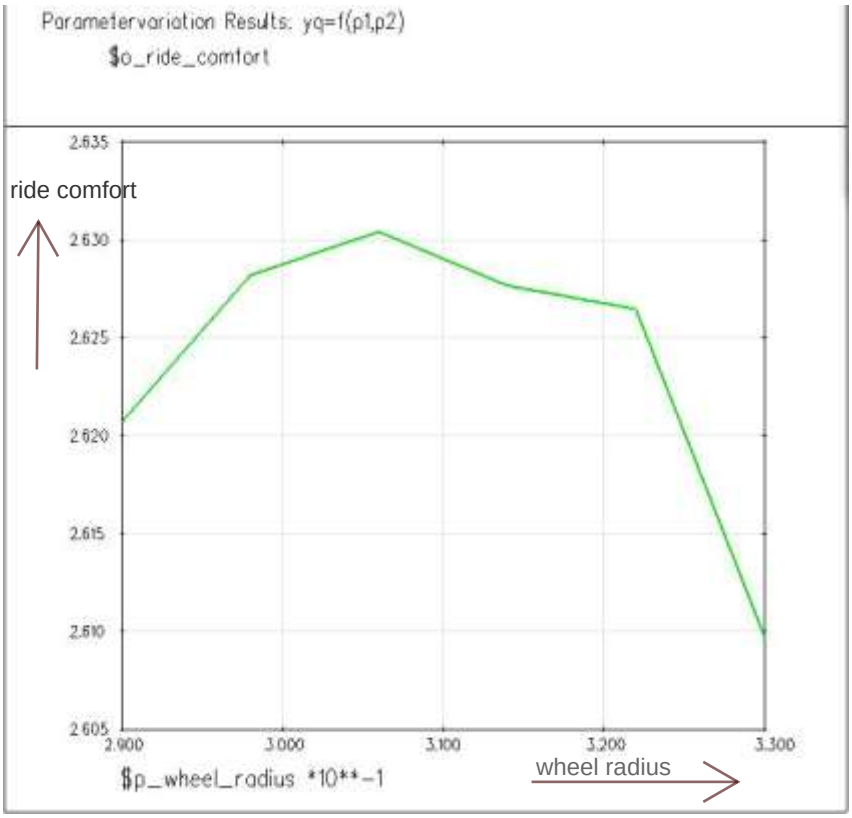


Figure 4.23 Effect of wheel radius on ride comfort

For Modeled AALRT vehicle, SIMPACK result shows when tested with wheel radius varied from 290 mm to 330 mm, radius 330mm has better and minimum ride comfort.

(In figure 4.23 X-axis shows wheel radius and Y-axis shows ride comfort)

### 4.1.3.4. Derailment coefficient

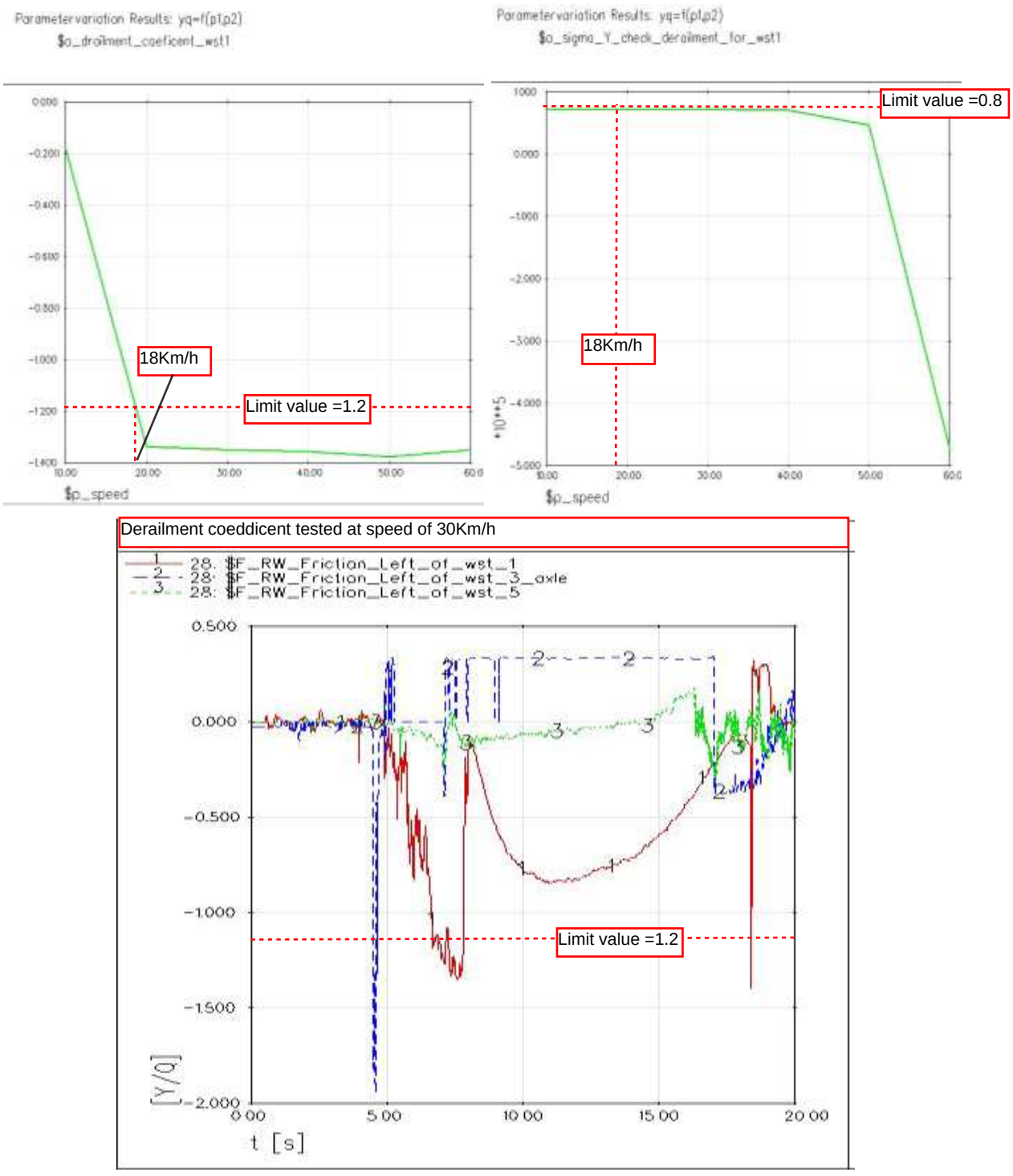


**Figure 4.24 Derailment coefficient on R50m sharp curve**

The derailment coefficient of leading, high rail side wheel is checked. According to the specification of UIC518, the limitation value of derailment is 0.8 or Y/Q is 1.2. Obtained result is shown in Fig. 4-24. It is shown that while negotiating R50 curve the passing speed should be limited at a speed NOT exceed 18 km/h, and should pass at constant speed.

#### 4.1.3.5. Wheel Unloading

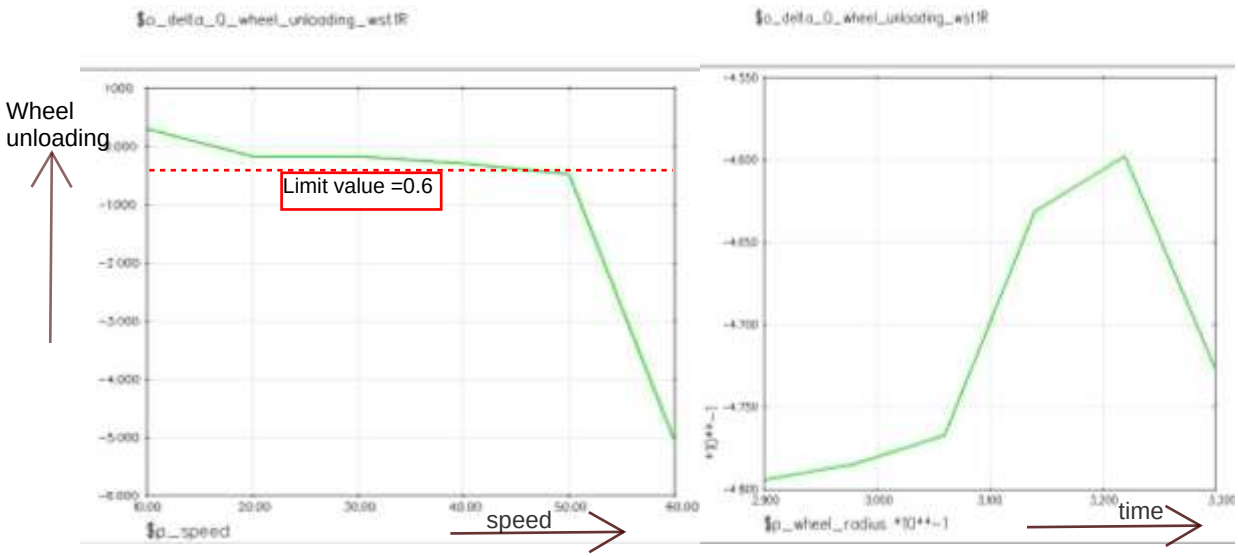


Figure 4.25 **a**.Wheel unloading for R50m Sharp curve **b**.effect of wheel radius on wheel unloading

The wheel unloading of leading, low rail side wheel is checked. Wheel unloading is specified in many specifications and the limitation value is 0.6. Leading and low rail side wheel undertakes the maximum wheel unloading; the result is shown in Fig. 4.25. It is shown that while negotiating R50 curve with 18 km/h wheel unloading is under the limit value.

## 4.2. DISCUSSION

Since each train vehicles has its own result when it runs on different rail line and there isn't any literature about wheel profile optimization on AALRT rail line, A comparison has been made only between railway standard values and results obtained from SIMPACK software for Vehicle track interaction Dynamic performance Analysis, in order to test the validity the developed optimized wheel profile and articulated three bogie vehicle. The selected contact model in SIMPACK is a single point contact model and the standard wheel profile S1002 and AALRT wheel profile was used in combination with the standard rail profile UIC60 with inclination 1:40. Finally Dynamic performance analysis is made on selected curve tracks and straight track for Optimized and AALRT wheel profile and the evaluation of the contact problem is selected to line evaluation to be in agreement with the procedure. Basic Simulation results presented in chapter 4 are summarized for validation in Table 2.

Table 2**:** Simulation result and validation criteria

| Value to be investigated | Assessment criteria | Standards | Criteria limits based on standards | Simulation results | | Status |
|---|---|---|---|---|---|---|
| | | | | Used AALRT wheel | Optimized wheel | |
| Leading wheel set Lateral shift forces in straight track (KN) | Maximum wheel rail force in lateral direction | UIC 518, EN 14643 | 25 | 16.3 | 12.5 | ✓ |
| Leading wheel set Lateral shift forces in large curved track(KN) | Maximum wheel rail force in lateral direction | UIC 518, EN 14643 | 42.5 | 37.8 | 34 | ✓ |
| Leading wheel set Lateral shift forces in large sharp curved track(KN) | Maximum wheel rail force in lateral direction | UIC 518, EN 14643 | 65 | 62.1 | 60 | ✓ |
| Wear Index In Straight track(N) | Maximum wheel rail force or wear | UIC 518, EN 14643 | <400 | ***78*** | ***56*** | ✓ |
| Wear Index In small curve R150m track (N) | Maximum wheel rail force or wear | UIC 518 | >400N | ***560*** | ***420*** | Sever condition |
| Wear Index In sharp curve R50m track(N) | Maximum wheel rail force or wear | UIC 518 | >400 N | ***3000*** | ***1900*** | Catastrophic condition |
| Horizontal ride index in straight track | Maximum value in lateral direction | ISO 2631 horizontal | 4 | 2.5 | 2.45 (for <90km/h) | ✓ |
| Horizontal ride index in small curves | Maximum value in vertical direction | ISO 2631 horizontal | 4 | 2.8 | 2.55 (for <75km/h) | ✓ |
| Horizontal ride index in small curves | Maximum value in vertical direction | ISO 2631 horizontal | 4 | 2.3 | <2.5 (for <18km/h) | ✓ |
| Derailment coefficient | Maximum Ratio of lateral to vertical forces | UIC 518 | Y/Q= 1.2 | 1.2 On R50m curve | 1.2 On R50m curve with 18km/h | ✓ |

As Mentioned in result section 4.1 and above table, basic Dynamic performance analysis is Valid to the standard. Even if The Wear index of optimized AALRT wheel profile is reduced, at curve track the wear rate is at catastrophic regime for both used AALRT wheel as well as new optimized AALRT wheel profile. This indicates it needs special attention for wheel rail contact in Curve negotiation.

# CHAPTER FIVE
# CONCLUSION RECOMMENDATION AND FUTURE WORK

## 5.1.CONCLUSION

Wheel profile optimization procedure for railway wheel profiles using RRD function and SIMPACK Software package has been presented. The procedure of Optimization is obtained by minimizing the difference between the target RRD (in this paper standard S1002 wheel profile RRD is taken as comparison and average RRD of new and worn AALRT wheel profile is taken as target RRD) and the RRD of the designed wheel profile. The presented procedure has been used for improvement of the wheel profile design for AALRT trains. The target RRD function has been obtained by modifying the RRD function of the existing wheel and rail profiles used in the AALRT network and the mostly used standard wheel profile S1002.

The results of the SIMPACK Dynamic performance Analysis of the optimized wheel profile in the AALRT network have shown that due to the application of the optimized wheel profile, the ***Wear index*** of AALRT Wheel Profile is ***Decreased*** or optimized by ***1100N***, ***120N*** and **22N** tested on **R50m**, **R150m** curve and **straight tracks** respectively when compared to used AALRT wheel profile.

As a conclusion wear of the wheels can significantly be reduced by optimizing wheel profile (by improving the wheel/rail contact).

## 5.2.RECOMMENDATION

Above Simulation results and practical observation of AALRT show that Excessive wear generally occur on curved tracks. The highest rate of wear occurs at ‘Stadium station’, ‘Lideta’ and ‘Autobis Tera’ Stations which have 50m radius curve. This will lead the transit early wheel wear and can cause early profiling which cause high cost and even derailment to the worst. Since changing constructed curve lines and rail geometry, using lubrication or re-profiling can cause high cost so the author tries to show optimizing wheel profile can reduce wheel wear and the transit should have to carefully study the wheel rail contact conditions and have to find an optimum wheel profile for existing rail. In addition to reduce this excessive wear the author recommends AALRT to negotiate sharp curves at constant speed, use friction modifiers or optimum Lubrications at Curves and restrain curve rails.

## 5.3. FUTURE WORK

Dynamic analysis and multi-body simulation for the development of advanced passenger railway vehicles is a complex research field that requires new ideas and innovative design solutions day to day. Especially Ethiopia starts a plan to connect regions with railway lines, so the study of railway dynamics will help to face challenges in operation, modify and mange her own vehicle types and tack lines for better operation. In this paper the author tries to find the solution for fat wheel wear challenges that Addis Ababa Light Rail Train faces. Through this process the author face limitations from different reasons. For better result the following points can be included in the future work.

- Under flour Lath machine is used for measurement of wheel profiles, but it's not easy, flexible and can't measure profiles as much as possible. So other wheel profile measuring devices like miniprof, shall be used in the future work
- The rail vehicle model used in the simulation study comprises a rigid car body, i.e. car body flexibility was not considered in the current study but it does influence rail vehicle dynamics and it is another engineering problem which needs to be solved
- Effect of wind, traction and braking were not considered in the current study but they do influence rail vehicle dynamics so incorporating traction and braking in rail vehicle dynamics analysis results in better simulation results.
- All wheel profiles were considered identical from left to right on a given axle and from axle to axle and all wheels remains in contact with the rails as well as no wheel flats was considered but in practice all wheel profiles are not identical, there are wheel lifts and wheel flats which influence ride dynamics; hence, consideration of such things will give better result.
- All the vehicle data's like mass of the vehicle, inertia ,mass of bogie, inertia of bogie and other sub variables have great influence on the result of dynamic performance analysis. Using exact information of vehicle one can check the performance of AALRT in different perspectives and it can be a research area

# REFERENCE


1. W. Partington. Wheel impact load monitoring. *Proc. Instn. Civ. Engrs Transp.*, 100: 243–245, Nov. 1993
2. Mikael Palo, *Condition monitoring of railway vehicles*, A study on wheel *condition for heavy haul rolling stock*, ISSN: 1402-1757, Universitets tryckeriet, Luleå 2012
3. I.Y. Shevtsov, V.L. Markine, C. Esveld, ‘’*Optimal Design Of Wheel Profile For Railway Vehicles’’,* Presented At The 6th International Conference On Contact Mechanics And Wear Of Rail/Wheel Systems (Cm2003) In Gothenburg, Sweden June 10–13, 2003
4. R. Verardi, C. Ariaudo, N. Kuka,ALSTOM Transport, *WEAR ANALYSIIS OF TIILTIING TRAIINS USIING “SIIMPACK RAIIL WEAR” MODULE*, SIMPACK User Meeting 2011 Salzburg – 18 & 19 May 2011
5. Design and optimisation of wheel–rail profiles for adhesion improvement B. Liu, T.X. Mei & S. Bruni
6. **Source:http://lists10.com/wp-content/uploads/2014/07/awash-trainderailment.jpg**
7. Kalousek J.J. (2002) Keynote address: light to heavy, snail to rocket, Wear 253, Issue 1-2, 2002, Elsevier, pp. 1-8
8. Magel E.E., (1999) Optimizing wheel, rail profiles, Railway track and structures, July 1999
9. Xinggao Shu, Wheel Profiles Design and Maintenance Guidelines for Rail Transit Operation, Transportation Technology Center, Inc. A subsidiary of the Association of American Railroads Pueblo, CO Contractor’s Final Report for TCRP Project D-07/Task 20,Submitted September 2014
10. I.Y. Shevtsov, ‘Wheel/Rail Interface Optimization’, Section of Road and Railway Engineering Faculty of Civil Engineering and Geosciences Delft University of Technology, ISBN 978-90-8570-303-7, The Netherlands, 2008
11. Dukkipati, R.V.(2000) Vehicle Dynamics, Boca Raton: CRC Press, ISBN 0-8493 0976-X.
12. Esveld, C. (2001) Modern Railway Track, (Second Edition), Zaltbommel: MRT-Productions, ISBN 90- 8004-324-3-3. (www.esveld.com)
13. Kalker, J.J. (1990) Three-Dimensional Elastic Bodies in Rolling Contact, Dordrecht: Kluwer Academic Publishers, ISBN 0-7923-0712-7.

14. Markine, V.L. (1999) Optimization of the Dynamic Behaviour of Mechanical Systems, PhD Thesis, TU Delft: Shaker Publishing BV, ISBN 90-423-0069-8.
15. Shevtsov, I.Y., Markine, V.L. & Esveld, C. (2002) One procedure for optimal design of wheel profile, Proceedings of the IQPC conference on Achieving Best Practice in Wheel/Rail Interface Management, Amsterdam, The Netherlands, January 31 - February 1, 2002.
16. Shevtsov, I.Y., Markine, V.L., Esveld, C. (2005) optimal design of wheel profile for railway vehicles. Wear 258 (2005), pp. 1022–1030. ISSN 0043-1648
17. Barthelemy J-FM, Haftka RT (1993) Approximation concept for optimum structural design—a review. Struct Optim 5:129–144
18. Persson I, Iwnicki SD (2004) Optimisation of railway profiles using a genetic algorithm. Veh Syst Dyn 41:517–527 (Suppl). ISBN 90- 265-1972-9
19. Shen G, Ayasse JB, Choller H, Pratt I (2003) A unique design method for wheel profiles by considering the contact angle function. Proc Inst Mech Eng F J Rail Rapid Transit 217:25–30
20. Smith RE, Kalousek J (1990) A design methodology for wheel and rail profiles for use on steered railway vehicles. Proceedings of the third international conference on contact mechanics and wear of rail/wheel systems, Cambridge, U.K., 22–26 July 1990. ISBN 0444-88774-1; also in Wear (1991), volume 144, pp 329–342
21. Wickens AH (1965) The dynamic stability of railway vehicle wheelsets and bogies having profiled wheels. Int J Solids Struct 1:319–341
22. Toropov, V.V. 1989. Simulation Approach to Structural Optimization, Structural Optimization 1: 37-46.
23. J. Auciello, E. Meli, S. Falomi, M. Malvezzi, Dynamic simulation of railway vehicles: wheel/rail contact analysis, Vehicle System Dynamics 47 (2009) 867–899.
24. EN 15313: Railway applications—in-service wheelset operation requirements— in-service and off-vehicle wheelset maintenance, 2010.
25. Rail transport in Ethiopia. Wikipedia, the free Encyclopedia. http://en.wikipedia.org/wiki/Rail_transport_in_Ethiopia. [Accessed 30 Aug 2017].

# APPENDEX 1

**Table 3: Data collected on Bogie wheel diameter and flange thickness of Addis Ababa Kality-Minilik route Trains**

| CAR ID | | A axle 1 | | A axle 2 | | B axle 3 | | B axle 4 | | C axle 5 | | C axle 6 | | |
|---|---|---|---|---|---|---|---|---|---|---|---|---|---|---|
| | | L | R | L | R | L | R | L | R | L | R | L | R | |
| 209 | diameter | 651.23 | 650.8 | 650.9 | 650.9 | 648.58 | 648.7 | 648.61 | 648.5 | 659.59 | 659.4 | 654.3 | 654.08 | 56447 |
| | flange thickness | 17.3 | 17.3 | 17.69 | 17.62 | 20.03 | 20.02 | 18.99 | 19.08 | 17.27 | 17.34 | 16.85 | 17.01 | |
| 216 | diameter | 649.82 | 650.6 | 650.3 | 650.2 | 660.32 | 660.3 | 660.35 | 660.3 | 660.01 | 659.8 | 648.8 | 648.18 | 35096 |
| | flange thickness | 19.16 | 19.17 | 17.81 | 18.20 | 17.95 | 18.13 | 18.46 | 18.50 | 19.90 | 20.49 | 18.35 | 18.58 | |
| 107 | diameter | 659.32 | 659.56 | 659.5 | 659.5 | 650.09 | 649.78 | 650.13 | 650.08 | 659.37 | 659.73 | 659.44 | 65.51 | 57419 |
| | flange thickness | 20.31 | 19.92 | 19.65 | 19.25 | 18.87 | 18.68 | 17.86 | 18.03 | 19.51 | 19.28 | 20.31 | 20.08 | |
| 212 | diameter | 641.14 | 641.17 | 638.4 | 638.3 | 653.41 | 653.03 | 653.38 | 653.65 | 653.58 | 653.52 | 653.15 | 653.14 | 44026 |
| | flange thickness | 19.70 | 19.86 | 18.40 | 18.41 | 18.60 | 18.42 | 19.53 | 19.51 | 18.36 | 18.36 | 18.07 | 18.14 | |
| 217 | diameter | 652.20 | 652.04 | 655.8 | 655.5 | 641.14 | 641.08 | 641.03 | 640.98 | 659.94 | 659.23 | 659.70 | 659.65 | 35568 |
| | flange thickness | 17.61 | 17.13 | 18.22 | 18.27 | 19.86 | 19.55 | 17.15 | 17.02 | 18.89 | 18.32 | 16.36 | 17.52 | |
| 211 | diameter | 660.01 | 659.87 | 659.7 | 659.9 | 639.99 | 640.00 | 635.18 | 634.89 | 660.14 | 659.93 | 660.03 | 659.91 | 26848 |
| | flange thickness | 19.42 | 19.11 | 18.32 | 17.89 | 18.31 | 18.87 | 18.74 | 19.52 | 19.35 | 19.19 | 17.03 | 19.46 | |
| 115 | diameter | 659.49 | 659.7 | 659.7 | 659.8 | 636.3 | 635.4 | 635.7 | 635.3 | 659.7 | 659.9 | 659.4 | 659.6 | |
| | flange thickness | 19.75 | 20.62 | 20.3 | 20.39 | 20.79 | 20.0 | 19.4 | 19.3 | 20.6 | 20.7 | 19.9 | 20.45 | |
| 206 | diameter | 649.4 | 649.2 | 648.2 | 648.1 | 639.31 | 639.04 | 638.0 | 637.63 | 653.6 | 653.16 | 653.4 | 653.2 | 53109 |
| | flange thickness | 19.38 | 18.97 | 18.57 | 18.1 | 18.8 | 18.56 | 17.9 | 17.68 | 18.01 | 17.9 | 17.9 | 17.61 | |
| 119 | diameter | 659.9 | 660.0 | 660.1 | 659.9 | 656.4 | 656.8 | 660.3 | 660.8 | 660.1 | 660.1 | 660.0 | 660.1 | |
| | flange thickness | 21.0 | 20.24 | 20.8 | 20.8 | 19.71 | 19.7 | 19.5 | 10.18 | 20.6 | 20.8 | 208 | 21.1 | |
| 104 | diameter | 660.5 | 660.6 | 660.6 | 660.5 | 651.3 | 649.9 | 651.2 | 651.4 | 660.6 | 660.5 | 660.3 | 660.5 | |
| | flange thickness | 23.13 | 23.3 | 23.3 | 23.0 | 19.75 | 19.58 | 20.1 | 20.2 | 23.34 | 23.19 | 23.2 | 23.4 | |

# APPENDEX 2

**Table 4: Mileage and re-profiling data of AALRT**

| mealage | vehicle No. | wheelset No. | pre-measurement | | | | | post-measurement | | | | | total re-profiled wheelset | remark |
|---|---|---|---|---|---|---|---|---|---|---|---|---|---|---|
| | | | Ø difference | diameter | | flange thickness | | Ø difference | diameter | | flange thickness | | | |
| | | | | left | right | left | right | | left | right | left | right | | |
| 45540 | 115 | 1 | 0.17 | 659.66 | 659.49 | 20.62 | 19.75 | - | - | - | - | - | | wheel flange thickness |
| | | 2 | 0.18 | 659.83 | 659.65 | 20.39 | 20.28 | - | - | - | - | - | | |
| | | 3 | 0.41 | 659.89 | 660.3 | 19.2 | 15.13 | 0.92 | **635.37** | **636.3** | 20 | 20.79 | 35 | |
| | | 4 | 0.32 | 659.94 | 660.26 | 19.77 | 14.08 | 0.37 | **635.29** | **635.66** | 19.25 | 19.38 | 36 | |
| | | 5 | 0.22 | 659.87 | 659.65 | 20.71 | 20.59 | - | - | - | - | - | | |
| | | 6 | 0.18 | 659.6 | 659.41 | 20.45 | 19.91 | - | - | - | - | - | | |
| 54471 | 218 | 1 | 0.3 | 659.29 | 659.59 | 13.7 | 16.65 | 0.24 | **642.86** | **643.11** | 17.65 | 17.59 | 39 | wheel flange thickness |
| | | 2 | 0.15 | 659.29 | 659.44 | 14.16 | 13.86 | 0.32 | **643.27** | **642.96** | 17.58 | 17.67 | 40 | |
| | | 3 | 0.01 | 660.19 | 660.21 | 17.08 | 16.14 | 0.24 | **636.55** | **636.79** | 19.55 | 19.72 | 41 | |
| | | 4 | 0.16 | 660.08 | 659.92 | 14.11 | 12.83 | 0.32 | **637.96** | **638.28** | 17.69 | 17.78 | 42 | |
| | | 5 | 0.53 | 659.12 | 659.65 | 18.38 | 18.06 | 0.03 | **647.98** | **647.95** | 21.11 | 20.85 | 43 | |
| | | 6 | 0.41 | 658.94 | 659.34 | 16.02 | 15.26 | 0.22 | **648.16** | **647.94** | 17.83 | 17.78 | 44 | |
| 47312 | 215 | 1 | 0.44 | 659.56 | 660 | 17.07 | 17.93 | 0.31 | **640.76** | **641.07** | 20.97 | 21.08 | 45 | wheel flange thickness |
| | | 2 | 0.06 | 659.79 | 659.73 | 15.46 | 13.46 | 0.1 | **642.02** | **642.12** | 17.44 | 17.55 | 46 | |
| | | 3 | 0.09 | 660.33 | 660.41 | 18.05 | 16.75 | 0.3 | **645.14** | **645.44** | 19.71 | 19.94 | 47 | |
| | | 4 | 0.18 | 660.1 | 660.28 | 17.09 | 15.45 | 0.21 | **644.17** | **644.38** | 18.82 | 18.81 | 48 | |
| | | 5 | 0.02 | 659.79 | 659.81 | 16.54 | 16.65 | - | - | - | - | - | | |
| | | 6 | 0.17 | 659.79 | 659.62 | 16.17 | 16.03 | - | - | - | - | - | | |
| 43452 | 208 | 1 | 0.07 | 659.43 | 659.5 | 16.34 | 17.53 | 0.29 | **637.93** | **638.21** | 20.11 | 20.24 | 51 | wheel flange thickness |
| | | 2 | 0.22 | 659.56 | 659.78 | 13.45 | 18.34 | 0.19 | **635.4** | **635.21** | 17.41 | 17.75 | 52 | |
| | | 3 | 0.15 | 660.14 | 660.29 | 17.05 | 15.44 | 0.1 | **640.15** | **640.05** | 18.58 | 18.78 | 53 | |
| | | 4 | 0.06 | 660.19 | 660.12 | 17.28 | 14.47 | 0.23 | **639.02** | **638.79** | 18.3 | 18.3 | 54 | |
| | | 5 | 0.12 | 659.67 | 659.56 | 18.68 | 16.96 | 0.19 | **645.95** | **645.76** | 19.68 | 19.82 | 55 | |
| | | 6 | 0.2 | 659.36 | 659.55 | 17.09 | 15.99 | 0.07 | **645.78** | **645.86** | 18.86 | 18.9 | 56 | |
| 51662 | 210 | 1 | 0.32 | 659.02 | 659.34 | 16.12 | 16.36 | 0.29 | **642.73** | **642.44** | 18.99 | 18.99 | 59 | wheel flange thickness |
| | | 2 | 0.24 | 659.44 | 659.2 | 16.3 | 14.39 | 0.61 | **642.23** | **641.63** | 17.75 | 18.09 | 60 | |
| | | 3 | 0.23 | 660.06 | 660.3 | 15.52 | 14.21 | 0.39 | **640.74** | **641.13** | 17.39 | 17.46 | 61 | |
| | | 4 | 0.21 | 650.68 | 650.89 | 17.51 | 17.45 | 0.05 | **642.57** | **642.52** | 18.1 | 18.44 | 62 | |
| | | 5 | 0.2 | 659.25 | 659.45 | 16.4 | 16.93 | 0.15 | **646.23** | **646.37** | 18.02 | 18.11 | 63 | |
| | | 6 | 0 | 659.15 | 659.16 | 16.38 | 14.98 | 0.41 | **645.96** | **645.55** | 17.27 | 17.58 | 64 | |
| 40415 | 108 | 1 | 0.42 | 659.94 | 659.52 | 20.44 | 20.4 | - | - | - | - | - | | |
| | | 2 | 0.03 | 659.67 | 659.64 | 19.94 | 19.66 | - | - | - | - | - | | |
| | | 3 | 0.21 | 660.49 | 660.28 | 18.59 | 17.81 | 0.65 | **654.65** | **655.3** | 18.52 | 18.82 | 65 | |
| | | 4 | 0.13 | 660.15 | 660.28 | 17.9 | 16.94 | 0.23 | **654.01** | **654.54** | 18.54 | 18.87 | 66 | |
| | | 5 | 0.38 | 659.94 | 659.56 | 19.64 | 19.67 | - | - | - | - | - | | |
| | | 6 | 0.37 | 659.9 | 659.53 | 20.05 | 20.08 | - | - | - | - | - | | |
| 45551 | 111 | 1 | 0.44 | 659.16 | 658.73 | 18.52 | 18.79 | - | - | - | - | - | | |

| | | | | | | | | | | | | | | |
|---|---|---|---|---|---|---|---|---|---|---|---|---|---|---|
| | | 2 | 0.19 | **658.93** | **658.74** | 18.05 | 18.59 | - | - | - | - | - | | wheel flange thickness |
| | | 3 | 0.53 | 659.83 | 660.36 | 17.14 | 13.11 | 0.31 | **636.12** | **636.43** | 17.94 | 17.76 | 67 | |
| | | 4 | 0.56 | 659.73 | 660.29 | 17.26 | 13.04 | 0.51 | **635.31** | **635.82** | 17.23 | 16.99 | 68 | |
| | | 5 | 0.09 | 659.88 | 659.79 | 19.68 | 20.34 | - | - | - | - | - | | |
| | | 6 | 0.12 | 659.79 | 659.67 | 21.11 | 19.99 | - | - | - | - | - | | |
| 54807 | 110 | 1 | 0.22 | 659.34 | 659.12 | 18.71 | 19.11 | - | - | - | - | - | | wheel flange thickness |
| | | 2 | 0.23 | 659.41 | 659.18 | 18.86 | 18.64 | - | - | - | - | - | | |
| | | 3 | 0.31 | 659.99 | 660.31 | 17.13 | 14.58 | 1.1 | **637.47** | **636.36** | 18.33 | 18.75 | 69 | |
| | | 4 | 0.58 | 659.8 | 660.37 | 17.02 | 13.09 | 0.22 | **636.5** | **636.28** | 18.24 | 18.07 | 70 | |
| | | 5 | 0.5 | 659.79 | 659.29 | 19.71 | 18.67 | - | - | - | - | - | | |
| | | 6 | 0.25 | 659.19 | 658.95 | 18.97 | 18.06 | - | - | - | - | - | | |
| 61474 | 219 | 1 | 0.42 | 658.83 | 659.26 | 13.78 | 15.73 | 0.22 | **632.77** | **633** | 18.46 | 18.34 | 71 | wheel thread scratch & wheel flange thickness |
| | | 2 | 0.11 | 659.02 | 658.91 | 14.12 | 12.97 | 0.27 | **631.54** | **631.8** | 17.84 | 17.87 | 72 | |
| | | 3 | 0.26 | 659.88 | 660.15 | 14.94 | 14.18 | 0.96 | **630.83** | **630.91** | 18.84 | 18.42 | 73 | |
| | | 4 | 0.12 | 659.95 | 659.83 | 14.97 | 13.22 | 0.75 | **631.27** | **631.42** | 18.3 | 17.86 | 74 | |
| | | 5 | 0.52 | 659.04 | 659.56 | 15.01 | 13.23 | 0.13 | **634.26** | **634.4** | 17.92 | 17.96 | 75 | |
| | | 6 | 0.43 | 658.92 | 659.36 | 13.68 | 12.55 | 0.19 | **633.38** | **633.19** | 17.94 | 18.11 | 76 | |
| 76430 | 109 | 1 | 0.11 | 658.81 | 658.7 | 18.71 | 18.59 | - | - | - | - | - | | wheel flange thickness |
| | | 2 | 0.05 | 658.86 | 658.81 | 19.16 | 18.28 | - | - | - | - | - | | |
| | | 3 | 0.49 | 660.35 | 659.86 | 12.45 | 17.42 | 0.65 | **629.45** | **628.8** | 17.88 | 18 | 77 | |
| | | 4 | 0.31 | 660.17 | 659.86 | 13.68 | 16.42 | 0.27 | **629.68** | **629.41** | 19.6 | 19.49 | 78 | |
| | | 5 | 0.19 | 659.16 | 658.97 | 18.65 | 18.27 | - | - | - | - | - | | |
| | | 6 | 0.09 | 658.89 | 658.8 | 19.18 | 18.24 | - | - | - | - | - | | |
| 78624 | 218 | 1 | 0.26 | 641.85 | 642.11 | 13.65 | 13.97 | 0.12 | **618.12** | **618** | 18.08 | 18.17 | 79 | wheel flange thickness |
| | | 2 | 0.12 | 642.28 | 642.16 | 14.71 | 14.09 | 0.06 | **616.53** | **616.59** | 20.35 | 19.53 | 80 | |
| | | 3 | 0.16 | 612.41 | 612.25 | 19.62 | 19.74 | 0.16 | **612.41** | **612.25** | 19.62 | 19.74 | 81 | |
| | | 4 | 0.32 | 637.64 | 637.96 | 13.25 | 13.07 | 0.18 | **609.91** | **609.73** | 17.89 | 18.05 | 82 | |
| | | 5 | 0.04 | 626.7 | 626.74 | 20.9 | 20.87 | 0.04 | **626.7** | **626.74** | 20.9 | 20.87 | 83 | |
| | | 6 | 0.13 | 647.16 | 647.03 | 14.81 | 14.29 | 0.11 | **626.16** | **626.05** | 17.99 | 17.93 | 84 | |
| 66522 | 216 | 1 | 0.15 | 648.92 | 649.07 | 16.52 | 16.1 | 0.3 | **623.18** | **623.48** | 20 | 20.09 | 85 | wheel flange thickness |
| | | 2 | 0.07 | 645.61 | 645.54 | 15.96 | 15.02 | 0 | **622.13** | **622.13** | 18.46 | 18.4 | 86 | |
| | | 3 | 0.07 | 660.03 | 659.96 | 17.86 | 16.84 | - | - | - | - | - | | |
| | | 4 | 0.15 | 659.99 | 659.84 | 18.15 | 17.53 | - | - | - | - | - | | |
| | | 5 | 0.08 | 647.3 | 647.22 | 18.47 | 16.75 | 0.05 | **627.07** | **627.02** | 19.69 | 19.12 | 87 | |
| | | 6 | 0.06 | 647.24 | 647.3 | 16.6 | 14.75 | 0.01 | **625** | **624.99** | 18.38 | 18.36 | 88 | |

# APPENDEX 3

## Main parameters of AALRT rail lines and Vehicle

- Track gauge: 1435mm
- Minimum radius of horizontal curve: Mainlines between sections 50m and Yard line 30m
- Minimum radius of vertical curve: 1000m
- Maximum gradient: 55%
- Type of rails for main lines and depot: 50kg/m; Maximum super elevation: 120mm

  Inclination at rail bottom: 1/40
- The vehicles adopt right-side running rules.
- Length of MC car 11340mm; Length of T car 3600mm, Max. width of car body : 2650mm and Car body height (to rail top) : 3025mm
- Height of vehicle floor from top of rail (exit and entry areas, new wheels and empty load) ≤350 mm
- Wheelbase: unpowered bogie 1800 mm; powered bogie 1900 mm
- Bogie base 10400 mm
- Wheel diameter (new wheel) =660 mm (Max. wear) ≤ 580 mm
- Weights of vehicles: Axle load: ≤11（1+3%）t

**Table 5: Total Car body weight at empty, normal and overload condition**

| Loads | Carbody weight | Passenger weight | Total weight |
|---|---|---|---|
| Empty vehicle (t) ($AW_1$) | 44 | 0 | 44 |
| Seatingcapacity (t) ($AW_2$) | 44 | 15.24 | 59.24 |
| Overload capacity (t) ($AW_3$) | 44 | 19.02 | 63.02 |

Note: Take 60kg as average weight of each passenger.

- Maximum operation speed : 70km/h
- Maximum test speed : 80km/h

- Suspension: Primary rubber spring ; Secondary steel spring
- Damping: Secondary lateral oil damper + secondary vertical oil damper

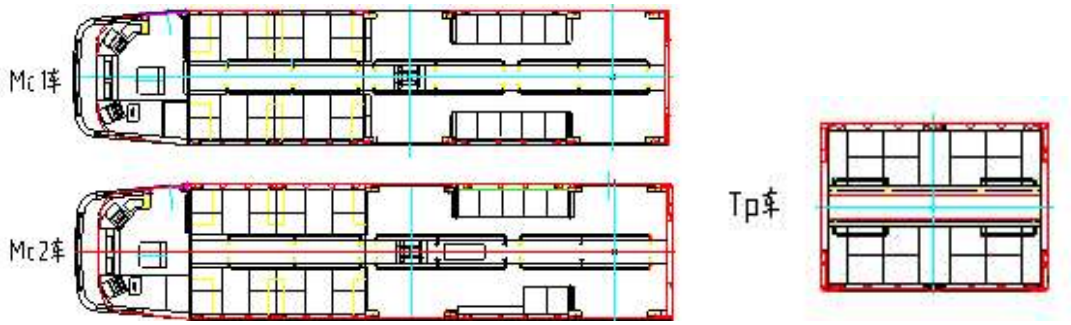


Figure 1. AALRT motor car and trailer car body module

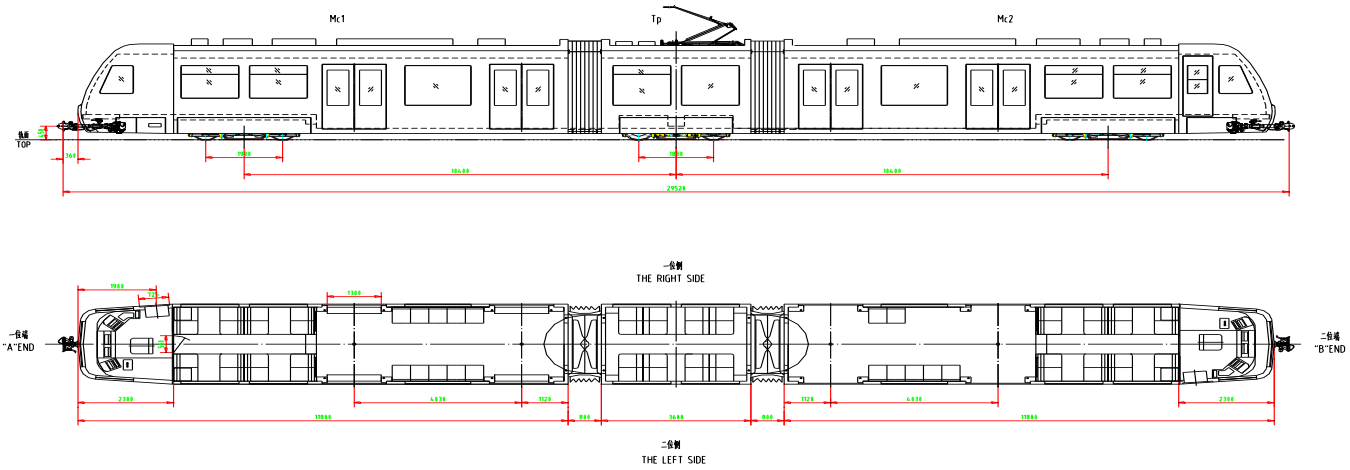


Figure 2. Overall layout of Ethiopia 70% low-floor coupler system which comprised of hinge device,

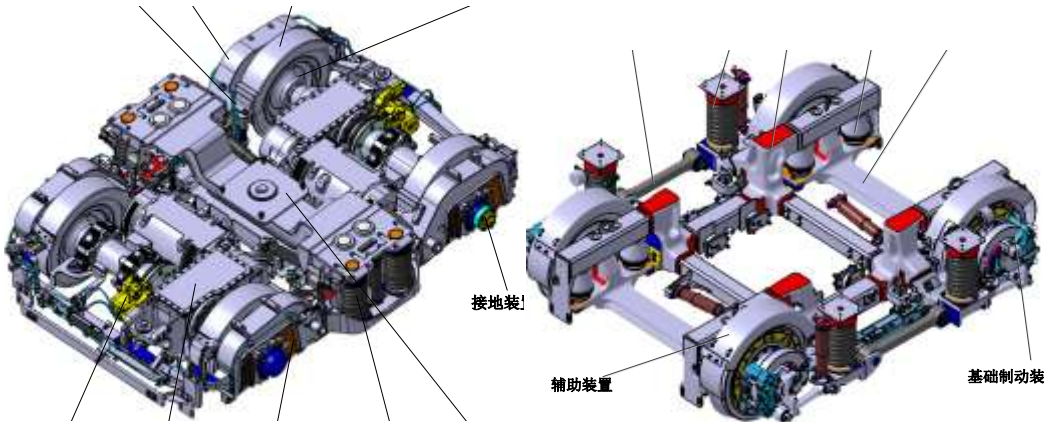


Figure 3. a) Designed structure of power bogie and b) designed structure of trailer bogie of AALRT

Figure 4. Resilient Wheel profile used in AALRT

Figure 5. a) free hinge b) elastic hinge and c) fixed Hinge (Articulation)

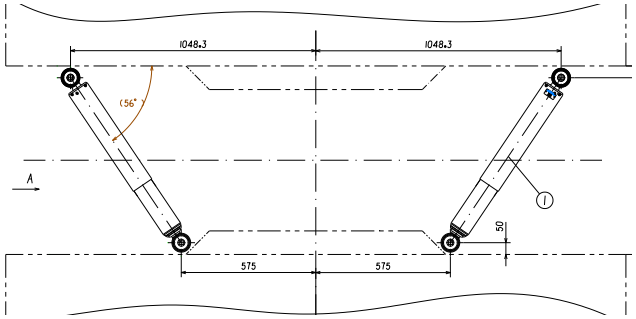


**Figure 6 : shock absorber**

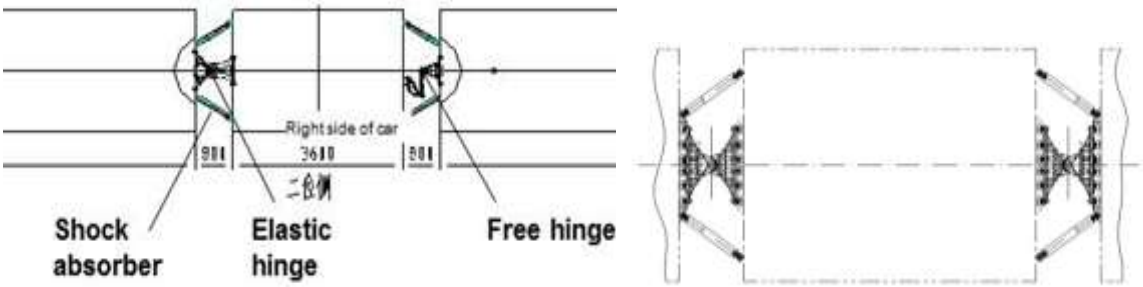


Figure 7. a) Upper Articulation configuration and b) Lower articulation configuration

## Input parameters

Table 6: Input parameters of dynamic modeling for vehicle simulation.

| Parameters | Trailer car（Tc） | Driving car（M） |
|---|---|---|
| Mass of wheelset（kg） | 1360 | 1587 |
| Inertia of wheelset x/y/z（$kgm^2$） | 410/50/410 | 440/56/440 |
| Mass of Bogie（kg） | 4680 | 7200 |
| Mass of fram and mounted parts（kg） | 1960 | 4026 |
| Inertia of frame（$kgm^2$） | 660/835/1410 | 1286/1629/2743 |
| Mass of carbody:AW0 /AW2 /AW3（kg） | 44890/59240/63020 | |
| Inetrtia of carbody x/y/z（$kgm^2$）,AW0 | 3.69e4 / 6.84e5 / 6.76e5 | 3.52e4 / 6.53e5 / 6.45e5 |
| Axle load: AW0/AW2/AW3（t） | 8.96/12.57 / 13.56 | 9.75 / 13.86 / 14.98 |
| Diameter of wheel（mm） | 660 | |
| Wheel /Rail profile | S1002(EN13715) /UIC60,(R330) | |
| Base of wheelset（mm） | 2200 | |
| Base between wheel inside planes（mm） | 1380±2 | |
| Base of bogie（mm） | 12600 | |
| Height of carbody gravity center above Top Of Rail mm） | 1428/1664(AW0/AW3，with bogie)；1791/1948（AW0/AW3，without bogie） | |
| Height of frame gravity center abvoe Top Of Rail（mm） | 510 | |
| Distance between left and right primary spring（mm） | 1930 | |
| Distance of left and right secondary vertical damper（mm） | 1860 | |

| | |
|---|---|
| Height of seconadary lateray damper,TOR（mm） | 485 |
| Stiffness of per coned primary rubber metal spring（N/m） AW3, x/y/z | 9.0e6/6.8e6/1.4e6 |
| Damping of primary vertical damper（N/m/s） | No damper, but 2000Ns/m is consider as coned element |
| Dapming of secondary vertical（N/m/s）,per side of bogie | 30000 |
| Damping of secondary lateral（N/m/s）, per bogie | 5000/0.1；7000/0.3 |
| Stiffness of ARB（Nm/rad） | Without anti-roll bar |
| Longitudinal stiffness of center pivort（N/m） | >7.0e6 ( take 7.0e6 for simulation) |
| Clearance of carbody lateral: free + elastic（mm） | 10+15 |
| Stiffness of elastic stop（N/m） | 5.0e6 |

# APPENDEX 4

**Table 7: AALRT RAIL LINE CURVES**

| STATION NO | Length | Curve R | COMMENT |
|---|---|---|---|
| NS6 | | | END |
| | 55 | 150 | small |
| | 60 | 150 | small |
| NS7 | | | |
| | 80 | 230 | |
| NS8 | | | |
| NS9 | | | |
| | 60 | 350 | |
| NS10 | | | |
| | 60 | 350 | |
| | 80 | 460 | |
| NS11 | | | |
| | 0 | 2000 | |
| | 35 | 300 | |
| | 30 | 350 | |
| | 80 | 350 | |
| | 60 | 1000 | |
| | 60 | 500 | |
| | 40 | 240 | |
| | 30 | 1000 | |
| | 25 | 1300 | |
| NS12 | | | |
| | 80 | 240 | |
| | 60 | 290 | |
| NS13 | | | |
| | 60 | 350 | |
| | 80 | 290 | |
| NS14 | | | |
| NS15 | | | |
| | 25 | 1000 | |
| | 45 | 650 | |
| | 30 | 1000 | |
| | 25 | 1300 | |

| | | | |
|---|---|---|---|
| | 0 | 2000 | |
| | 0 | 200 | |
| | 20 | 50 | sharp |
| EW16 | STADIUM | | |
| | 40 | 250 | |
| | 25 | 1300 | |
| EW17 | 0 | 2000 | |
| | 0 | 2000 | |
| | 0 | 5000 | large |
| | 65 | 200 | |
| EW18 | | | |
| | 60 | 200 | |
| | 85 | 600 | |
| EW19 | | | |
| EW20 | | | |
| | 20 | 50 | sharp |
| NS21 | | | |
| | 40 | 100 | small |
| | 55 | 100 | small |
| NS22 | | | |
| | 25 | 1200 | |
| | 0 | 2000 | |
| | 25 | 1300 | |
| NS23 | 0 | 2000 | |
| | 40 | 50 | sharp |
| NS24 | | | |
| | 60 | 300 | |
| NS25 | | | |
| | 90 | 400 | |
| NS26 | 20 | 800 | |
| | 80 | 400 | |
| | 60 | 305 | |
| | 40 | 65 | small |
| NS27 | 15 | 300 | |
| | 20 | 1400 | |

# APPENDEX 5

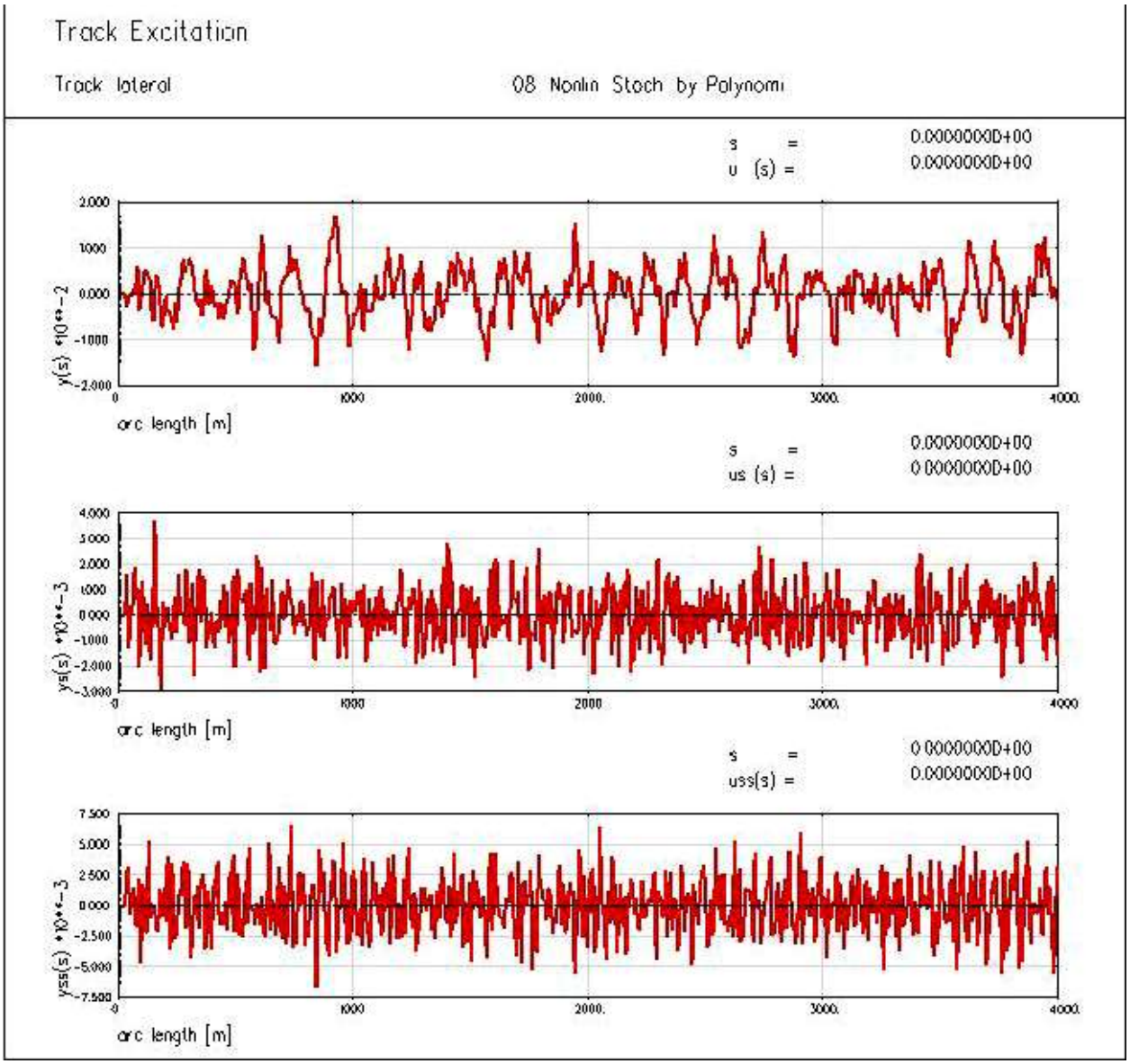


Figure 8. Lateral Track excitation at frequency of 60HZ

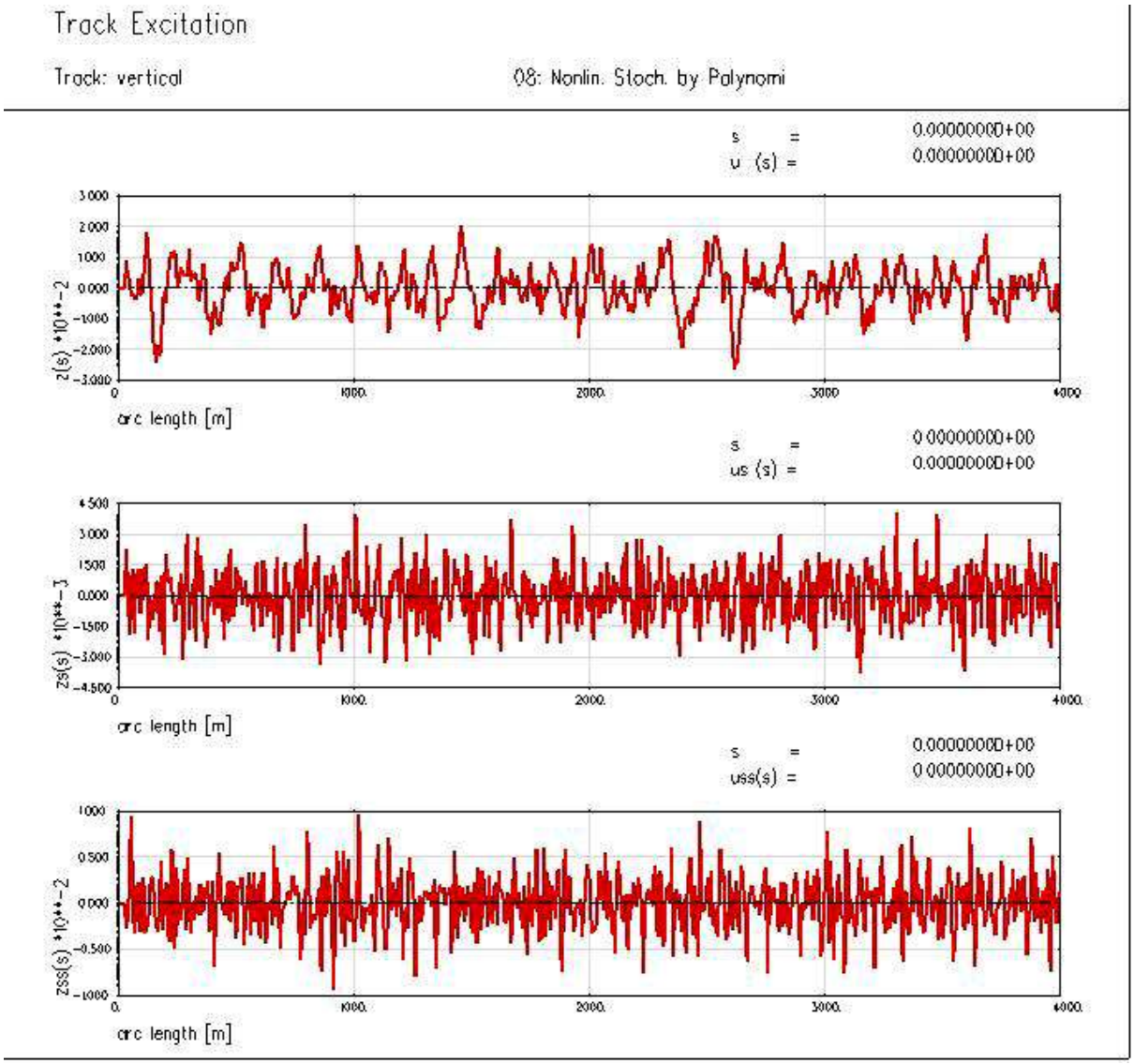


Figure 9. Vertical Track excitation

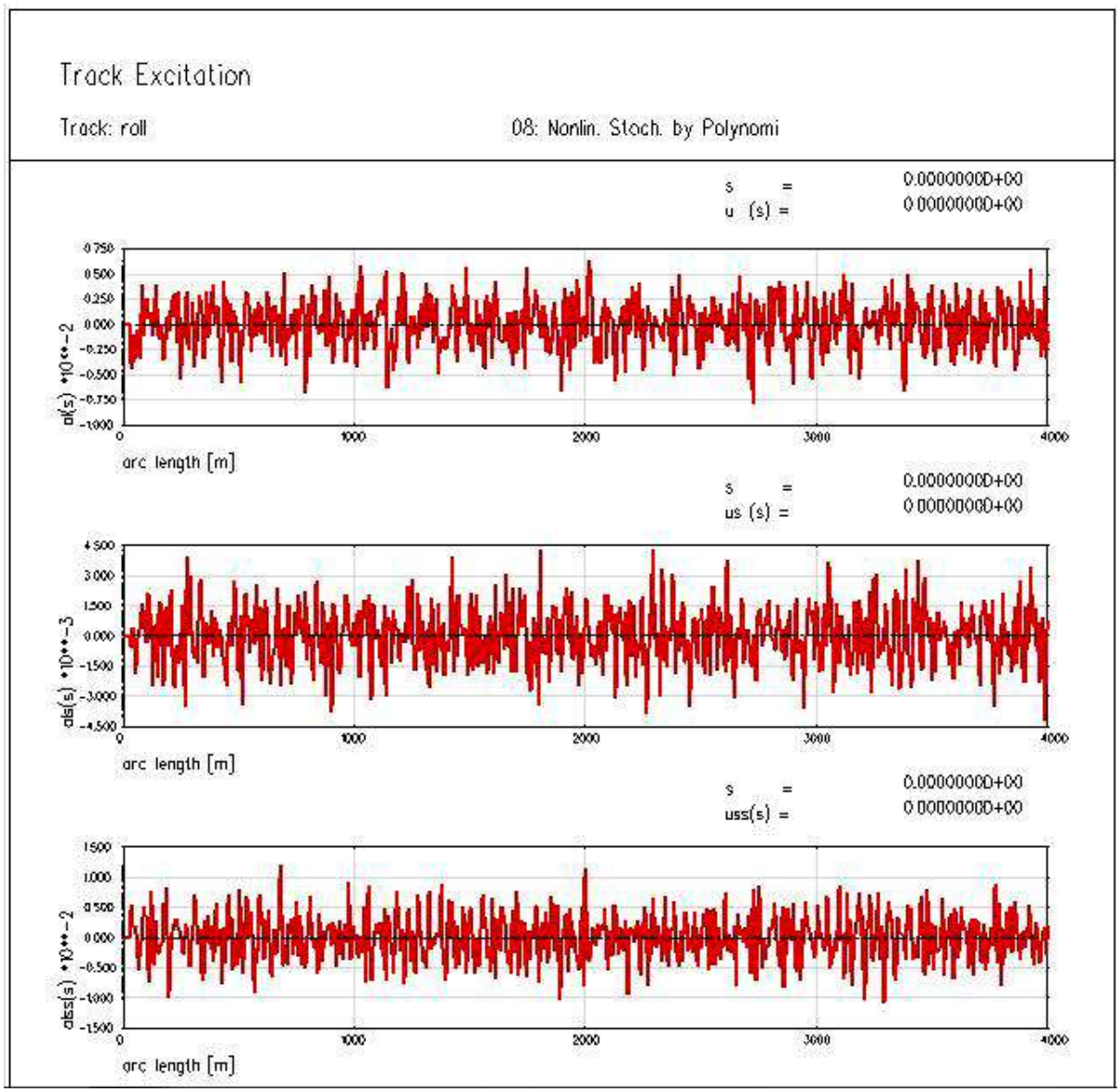


Figure 10. Roll Track excitation

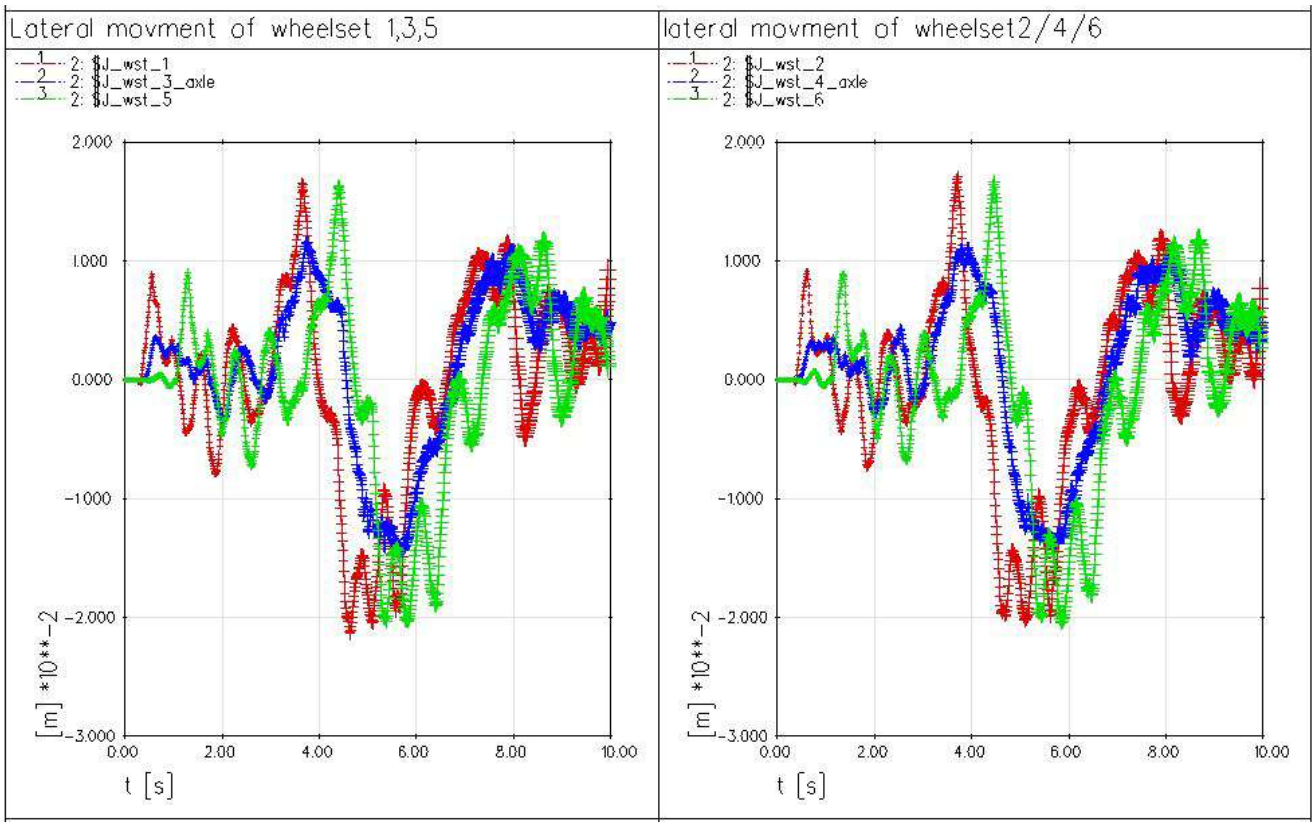


Figure 11. Lateral movement of wheel sets on Straight Track

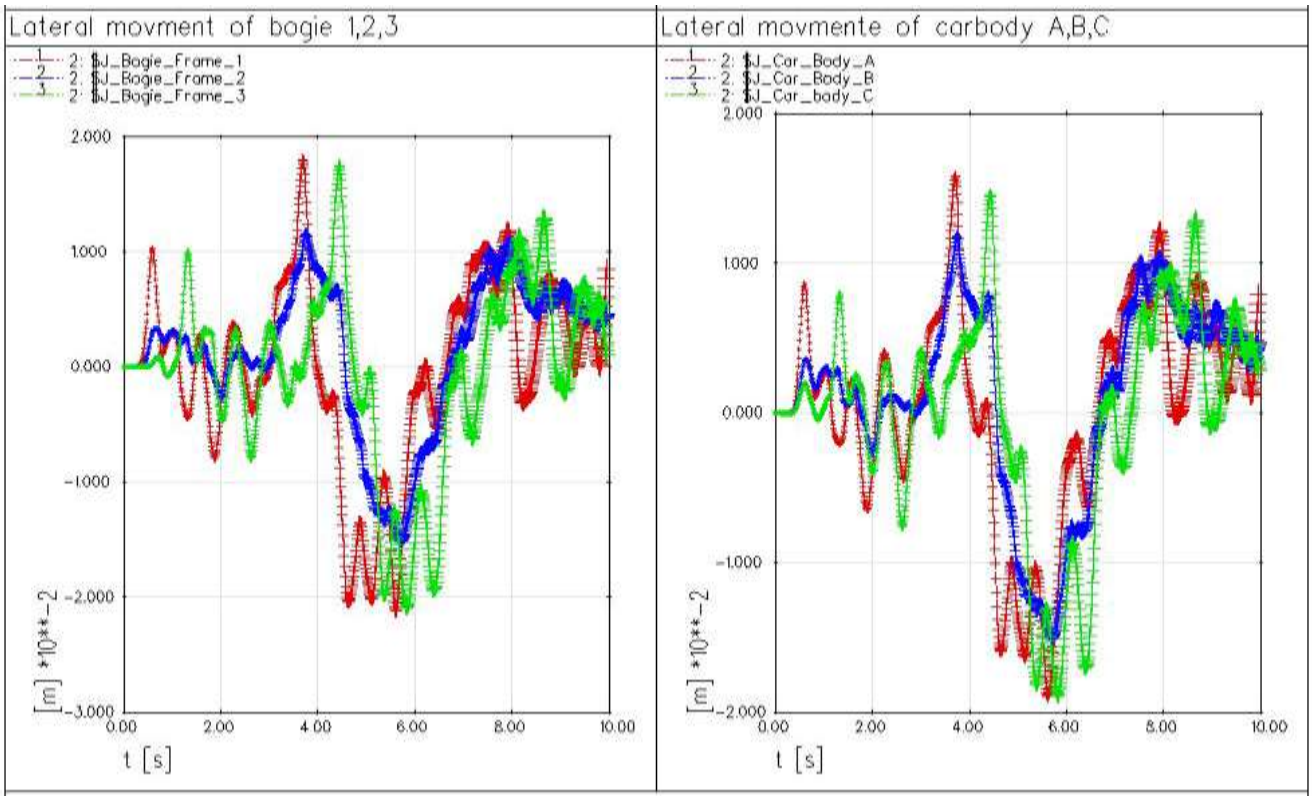


Figure 12. Lateral Movement of Bogie and Car body on Straight Track

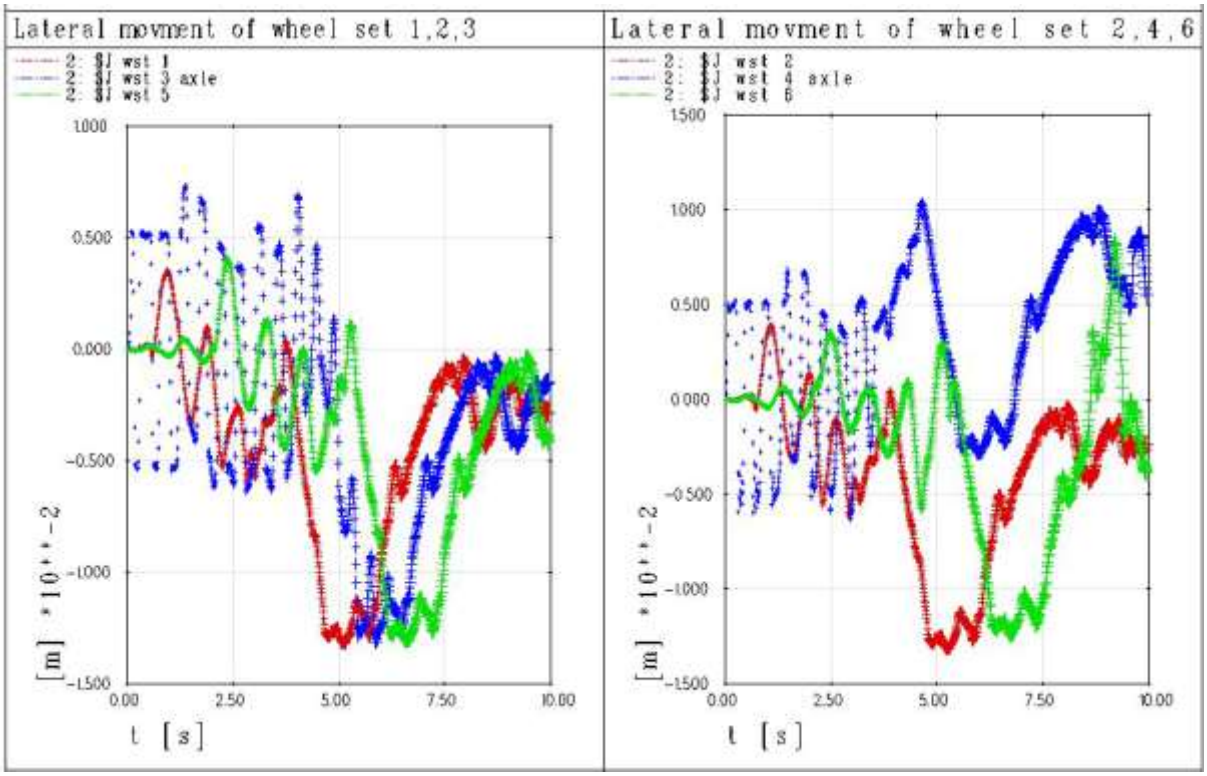


Figure 13. Lateral movement of wheel sets on R150m curve track

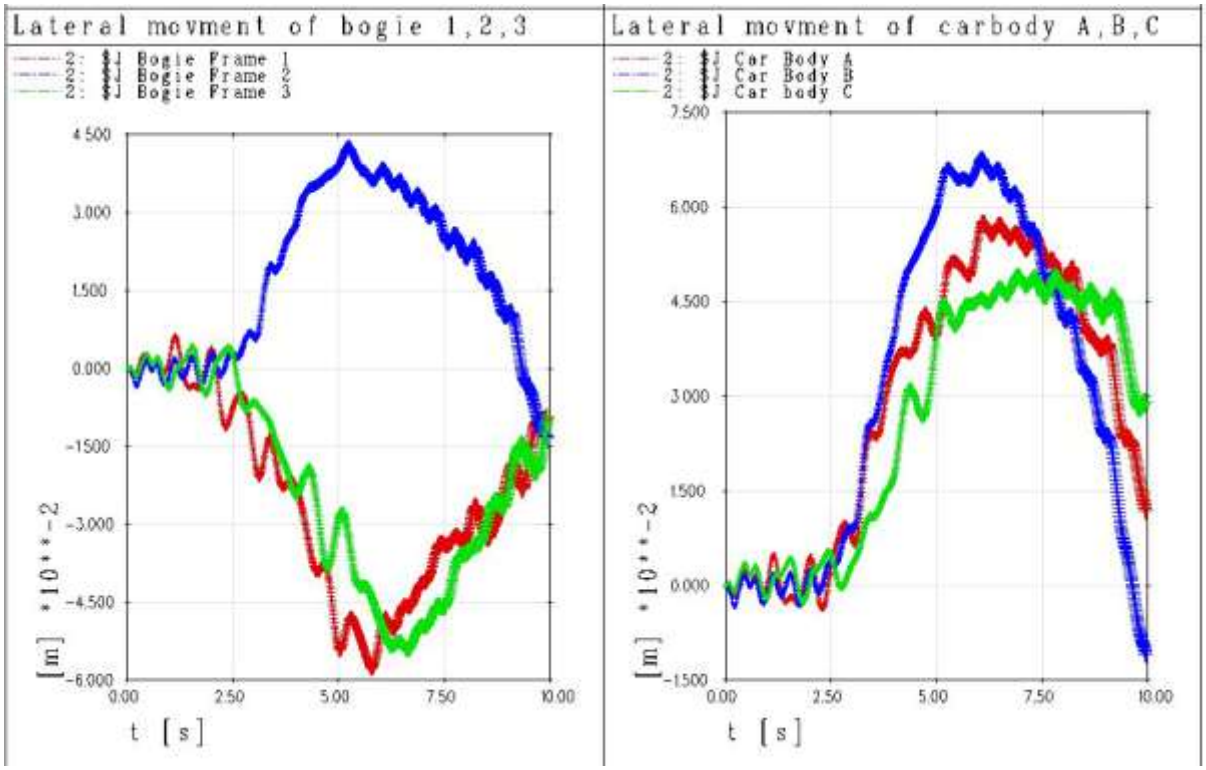


Figure 14. Lateral movement of bogie and car bodies on R150m curve

At curve the lateral movement becomes higher and unstable. Articulation helps to negotiate the curve without derailment.

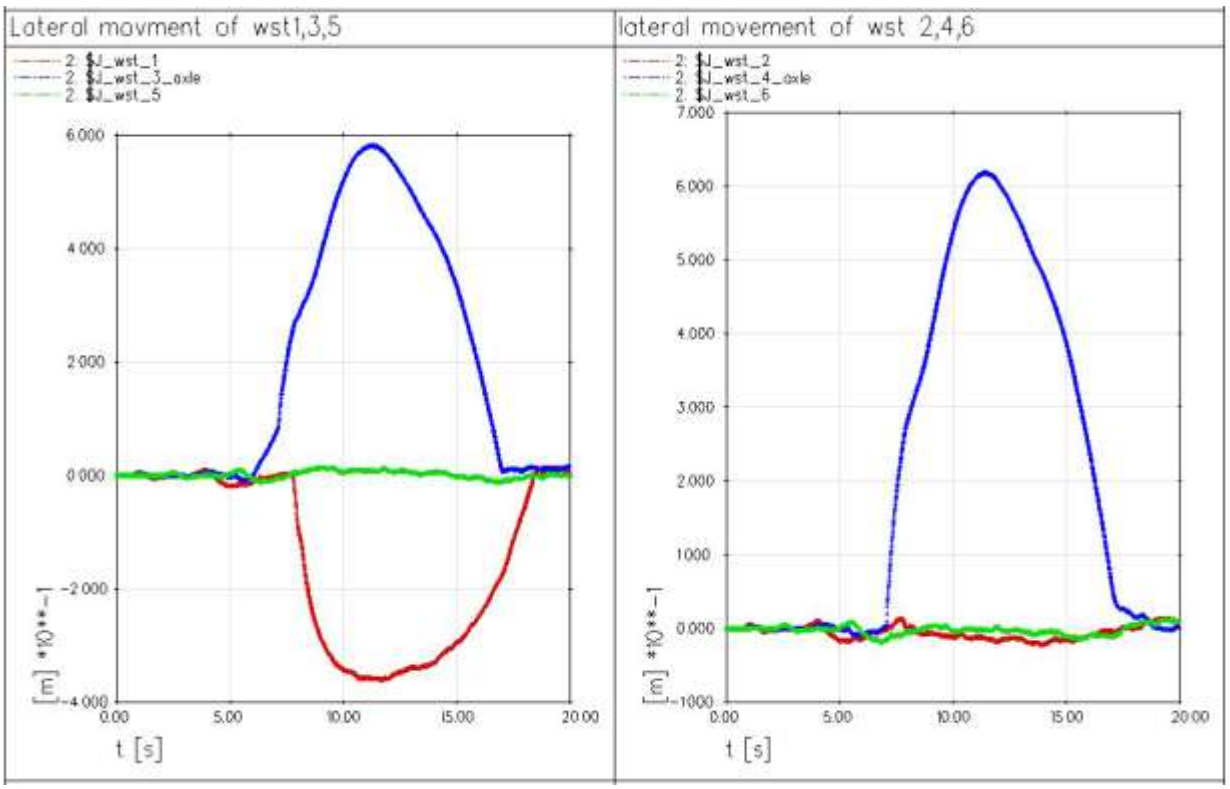


Figure 15. Lateral movement of wheel-sets on R50m sharp curve

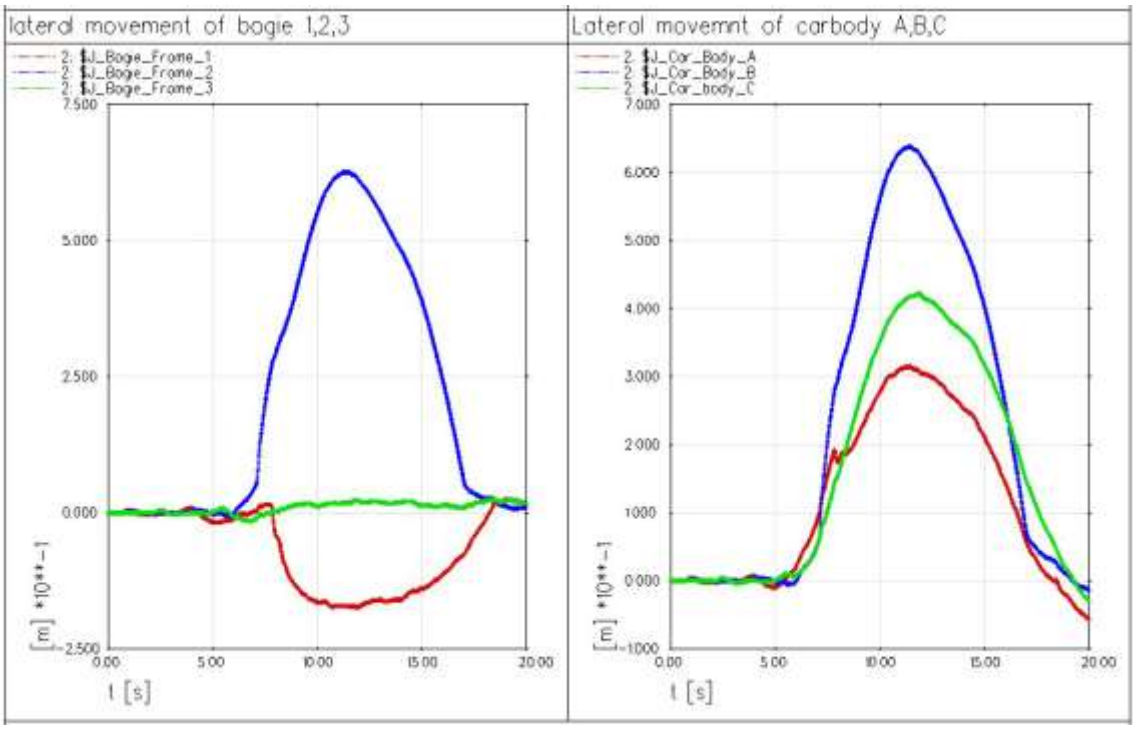


Figure 16. Lateral movement of bogie and carboy on R50m sharp curve

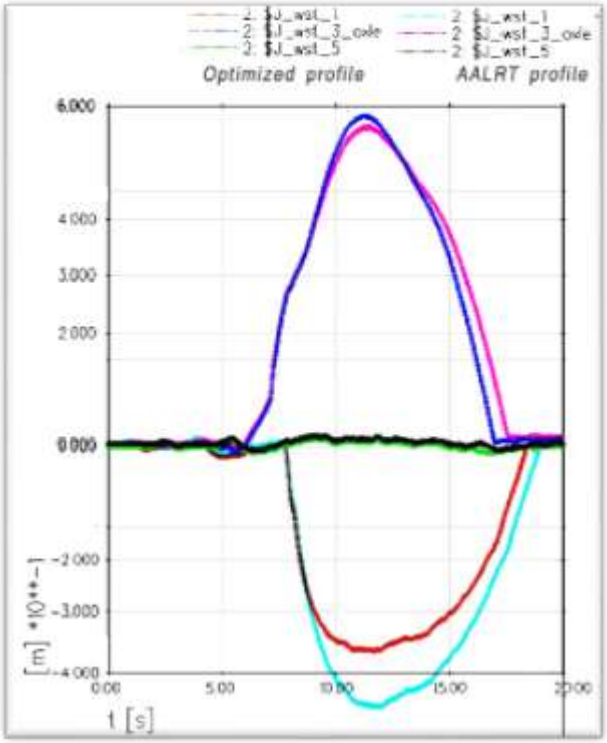


Figure 17. Lateral movement of used AALRT wheel profile and optimized wheel profile on R50m curve

At curve the lateral movement becomes higher and unstable. Articulation and RRD function helps to negotiate the curve without derailment.

# APPENDEX 6

**Table 8: Optimized Wheel profile Cartesian coordinate**

| X | Y | -0.0424774 | 0.0262831 | -0.0373984 | 0.0113366 | -0.027579 | 0.00238483 |
|---|---|---|---|---|---|---|---|
| -0.0546106 | 0.0277117 | -0.0423081 | 0.0258012 | -0.0371727 | 0.0108724 | -0.027184 | 0.00222703 |
| -0.054272 | 0.027957 | -0.0421953 | 0.0254147 | -0.036947 | 0.0104162 | -0.0267889 | 0.00210468 |
| -0.053877 | 0.0281746 | -0.0420824 | 0.025021 | -0.0367212 | 0.0100121 | -0.0263375 | 0.00198773 |
| -0.0534819 | 0.0283123 | -0.0419131 | 0.0244774 | -0.0364955 | 0.00965899 | -0.025886 | 0.00187869 |
| -0.0530869 | 0.0284623 | -0.0417438 | 0.0239176 | -0.0362698 | 0.00931938 | -0.0254345 | 0.00181784 |
| -0.0526354 | 0.0285319 | -0.0415745 | 0.0233985 | -0.0359876 | 0.00891239 | -0.0249831 | 0.00175188 |
| -0.052184 | 0.0285249 | -0.0414052 | 0.0229343 | -0.0357054 | 0.0085074 | -0.024588 | 0.00165162 |
| -0.0517325 | 0.0284767 | -0.0412359 | 0.0224498 | -0.0354233 | 0.00811003 | -0.0241366 | 0.00158398 |
| -0.051281 | 0.0284691 | -0.041123 | 0.0220807 | -0.0351411 | 0.0077549 | -0.0236851 | 0.00152885 |
| -0.0508296 | 0.0284713 | -0.0409537 | 0.0215328 | -0.0348589 | 0.0074203 | -0.0232336 | 0.00147128 |
| -0.0503781 | 0.0284713 | -0.0408409 | 0.0211541 | -0.0345767 | 0.00711369 | -0.0227822 | 0.00141346 |
| -0.0499266 | 0.0284692 | -0.0406716 | 0.0206217 | -0.0342946 | 0.00678554 | -0.0223307 | 0.00135374 |
| -0.0494752 | 0.0284769 | -0.0405023 | 0.0201031 | -0.0340124 | 0.0064858 | -0.0218792 | 0.0013038 |
| -0.0490237 | 0.0285232 | -0.040333 | 0.0195943 | -0.0337302 | 0.0062059 | -0.0214278 | 0.00129234 |
| -0.0485722 | 0.0285308 | -0.0401637 | 0.0191157 | -0.0333916 | 0.00591122 | -0.0209763 | 0.00124037 |
| -0.0481208 | 0.0285288 | -0.0399944 | 0.0186082 | -0.033053 | 0.00562477 | -0.0205248 | 0.00118834 |
| -0.0476693 | 0.0285287 | -0.0398251 | 0.0180894 | -0.0327144 | 0.00533456 | -0.0200734 | 0.00117688 |
| -0.0472178 | 0.0285288 | -0.0396558 | 0.0175587 | -0.0323758 | 0.00505462 | -0.0196219 | 0.00112701 |
| -0.0467664 | 0.0285288 | -0.0394865 | 0.0169954 | -0.0320372 | 0.00480702 | -0.0191704 | 0.00106736 |
| -0.0463149 | 0.0285287 | -0.0393172 | 0.0164757 | -0.0316986 | 0.00453533 | -0.018719 | 0.00100957 |
| -0.0458634 | 0.0285286 | -0.0391479 | 0.015998 | -0.03136 | 0.00429425 | -0.0182675 | 0.000949899 |
| -0.045412 | 0.0285335 | -0.0389786 | 0.0155053 | -0.0310214 | 0.00406787 | -0.017816 | 0.000899951 |
| -0.0449605 | 0.028522 | -0.0388093 | 0.0150111 | -0.0306264 | 0.00384275 | -0.0173646 | 0.000888494 |
| -0.0445655 | 0.0284131 | -0.0386964 | 0.0146125 | -0.0302314 | 0.0036531 | -0.0169131 | 0.000836524 |
| -0.0441704 | 0.0282466 | -0.0385835 | 0.0141807 | -0.0298928 | 0.00343242 | -0.0164616 | 0.000784556 |
| -0.0437754 | 0.0280659 | -0.0384142 | 0.0136305 | -0.0295542 | 0.00320896 | -0.0160102 | 0.000773052 |
| -0.0434368 | 0.0278365 | -0.0382449 | 0.0131325 | -0.0291591 | 0.00302478 | -0.0155587 | 0.000721149 |
| -0.0431546 | 0.0275505 | -0.0380756 | 0.0127206 | -0.0287641 | 0.00285563 | -0.0151072 | 0.000669109 |
| -0.0428725 | 0.027139 | -0.0378499 | 0.0122551 | -0.0283691 | 0.00268079 | -0.0146558 | 0.000657708 |
| -0.0426467 | 0.0266861 | -0.0376242 | 0.0117983 | -0.027974 | 0.002516 | -0.0142043 | 0.000607854 |

| | |
|---|---|
| -0.0137528 | 0.000546112 |
| -0.0133014 | 0.00049398 |
| -0.0128499 | 0.000488342 |
| -0.0123984 | 0.000492421 |
| -0.011947 | 0.000486737 |
| -0.0114955 | 0.000434705 |
| -0.011044 | 0.000372979 |
| -0.0105926 | 0.000320903 |
| -0.0101411 | 0.000315321 |
| -0.00968962 | 0.000319412 |
| -0.00923815 | 0.000311627 |
| -0.00878668 | 0.000265209 |
| -0.00833521 | 0.0002575 |
| -0.00788375 | 0.000261663 |
| -0.00743228 | 0.000255933 |
| -0.00698081 | 0.000201841 |
| -0.00652935 | 0.000149884 |
| -0.00607788 | 0.000138498 |
| -0.00562641 | 8.65E-05 |
| -0.00517494 | 3.25E-05 |
| -0.00472348 | 2.87E-05 |
| -0.00427201 | 2.31E-05 |
| -0.00382054 | -2.10836E-05 |
| -0.00336907 | -3.66011E-05 |
| -0.00291761 | -8.08362E-05 |
| -0.00246614 | -8.84903E-05 |
| -0.00201467 | -0.000086498 |

| | |
|---|---|
| -0.00156321 | -8.64396E-05 |
| -0.00111174 | -8.65001E-05 |
| -0.000660271 | -8.65604E-05 |
| -0.000208804 | -8.64987E-05 |
| 0.000242664 | -8.45E-05 |
| 0.000694131 | -9.23E-05 |
| 0.0011456 | -0.000136556 |
| 0.00159707 | -0.000152024 |
| 0.00204853 | -0.000196319 |
| 0.0025 | -0.000203917 |
| 0.00295147 | -0.000199879 |
| 0.00340293 | -0.000207606 |
| 0.0038544 | -0.000253965 |
| 0.00430587 | -0.000261667 |
| 0.00475734 | -0.000259607 |
| 0.0052088 | -0.000259553 |
| 0.00566027 | -0.000259615 |
| 0.00611174 | -0.000259677 |
| 0.00656321 | -0.000259618 |
| 0.00701467 | -0.000257568 |
| 0.00746614 | -0.000265417 |
| 0.00791761 | -0.000311657 |
| 0.00836907 | -0.000317317 |
| 0.00882054 | -0.000323041 |
| 0.00927201 | -0.00036928 |
| 0.00972348 | -0.000377116 |
| 0.0101749 | -0.000374998 |

| | |
|---|---|
| 0.0106264 | -0.000372898 |
| 0.0110779 | -0.000380748 |
| 0.0115293 | -0.000427036 |
| 0.0119808 | -0.000434737 |
| 0.0124323 | -0.000432745 |
| 0.0128837 | -0.000432636 |
| 0.0133352 | -0.000430656 |
| 0.0137867 | -0.000438436 |
| 0.0142381 | -0.000484727 |
| 0.0146896 | -0.00049243 |
| 0.0151411 | -0.000490438 |
| 0.0155926 | -0.000490329 |
| 0.016044 | -0.000488349 |
| 0.0164955 | -0.000496126 |
| 0.016947 | -0.000542417 |
| 0.0173984 | -0.000550188 |
| 0.0178499 | -0.000548074 |
| 0.0183014 | -0.000545974 |
| 0.0187528 | -0.000553818 |
| 0.0192043 | -0.000600176 |
| 0.0196558 | -0.000607822 |
| 0.0201072 | -0.000603715 |
| 0.0205587 | -0.00061151 |
| 0.0210102 | -0.000657817 |
| 0.0214616 | -0.000663473 |
| 0.0219131 | -0.000669194 |
| 0.0223646 | -0.000715435 |

| | |
|---|---|
| 0.022816 | -0.000723269 |
| 0.0232675 | -0.000721145 |
| 0.023719 | -0.000719106 |
| 0.0241704 | -0.00072697 |
| 0.0246219 | -0.000771185 |
| 0.0250734 | -0.000784591 |
| 0.0255248 | -0.000836536 |
| 0.0259763 | -0.000890527 |
| 0.0264278 | -0.000896273 |
| 0.0268792 | -0.000894225 |
| 0.0273307 | -0.000894173 |
| 0.0277822 | -0.00089225 |
| 0.0282336 | -0.000900043 |
| 0.0286851 | -0.00094426 |
| 0.0291366 | -0.000957667 |
| 0.029588 | -0.00100961 |
| 0.0300395 | -0.00106367 |
| 0.030491 | -0.00106936 |
| 0.0309424 | -0.00106526 |
| 0.0313939 | -0.001073 |
| 0.0318454 | -0.00111739 |
| 0.0322968 | -0.0011328 |
| 0.0327483 | -0.00117507 |
| 0.0331998 | -0.00119043 |
| 0.0336512 | -0.0012327 |
| 0.0341027 | -0.00124818 |